PB-227 307

FEASIBILITY OF FLUX FORCE/CONDENSATION SCRUBBING FOR FINE PARTICLE COLLECTION

A.P.T., INCORPORATED

PREPARED FOR
ENVIRONMENTAL PROTECTION AGENCY

OCTOBER 1973

DISTRIBUTED BY:

NTIS
National Technical Information Service
U. S. DEPARTMENT OF COMMERCE

BIBLIOGRAPHIC DATA SHEET

1. Report No. EPA-650/2-73-036

2.

3. **PB 227 307**

4. Title and Subtitle
Feasibility of Flux Force/Condensation Scrubbing for Fine Particle Collection

5. Report Date
October 1973

6.

7. Author(s)
Seymour Calvert, Jhuda Goldshmid, David Leith, Nikhil Jhaveri

8. Performing Organization Rept. No.

9. Performing Organization Name and Address
A. P. T. , Inc.
P.O. Box 71
Riverside, California 92502

10. Project/Task/Work Unit No.
ROAP 21ADL

11. Contract/Grant No.
68-02-0256

12. Sponsoring Organization Name and Address
EPA, Office of Research and Development
NERC-RTP, Control Systems Laboratory
Research Triangle Park, North Carolina 27711

13. Type of Report & Period Covered
Final

14.

15. Supplementary Notes

16. Abstracts

The report gives results of a feasibility study of flux force/condensation (FF/C) scrubbing for fine particle (smaller than 2.0 micron diameter) control. FF/C scrubbing includes effects of diffusiophoresis, Stephan flow, thermophoresis, and particle growth due to condensation of water vapor; it is not restricted to a specific scrubber configuration. Experimental determination of sub-micron particle collection efficiency in a bench-scale, sieve-plate FF/C scrubber validated the mathematical model developed in the analytical phase. Process designs and cost estimates for applying FF/C scrubbing to two fine particle pollution sources demonstrated its technical and economic feasibility. FF/C scrubbing is an attractive control method for fine particles when high efficiency is required and when the gas is hot enough to evaporate the necessary water vapor. Further development of FF/C scrubbing is clearly warranted. (M)

17. Key Words and Document Analysis. 17a. Descriptors

Air Pollution
Condensing
Scrubbers
Fines
Mathematical Models

17b. Identifiers/Open-Ended Terms

Air Pollution Control
Flux Force/Condensation Scrubbing
Diffusiophoresis
Particle Growth
Thermophoresis
Stephan Flow

17c. COSATI Field/Group 13B, 7D, 14A

Reproduced by
NATIONAL TECHNICAL
INFORMATION SERVICE
U S Department of Commerce
Springfield VA 22151

18. Availability Statement
Unlimited

19. Security Class (This Report)
UNCLASSIFIED

20. Security Class (This Page)
UNCLASSIFIED

21. No. of Pages
~~158~~ 160

22. Price
$5.00/1.45

EPA-650/2-73-036

FEASIBILITY OF FLUX FORCE/CONDENSATION SCRUBBING FOR FINE PARTICULATE COLLECTION

by

Seymour Calvert, Jhuda Goldshmid,
David Leith, and Nikhil C. Jhaveri

A. P. T., Inc.
P. O. Box 71
Riverside, California 92502

Contract No. 68-02-0256
Program Element No. 1AB012
ROAP No. 21ADL

EPA Project Officer: Leslie E. Sparks

Control Systems Laboratory
National Environmental Research Center
Research Triangle Park, North Carolina 27711

Prepared for

OFFICE OF RESEARCH AND DEVELOPMENT
U. S. ENVIRONMENTAL PROTECTION AGENCY
WASHINGTON, D.C. 20460

October 1973

i a

This report has been reviewed by the Environmental Protection Agency and approved for publication. Approval does not signify that the contents necessarily reflect the views and policies of the Agency, nor does mention of trade names or commercial products constitute endorsement or recommendation for use.

FOREWORD

This report, "Feasibility Of Flux Force/Condensation Scrubbing For Fine Particle Collection", is the final report submitted to the Control Systems Laboratory for E.P.A. Contract No. 68-02-0256.

The principal objective of this experimental and theoretical program was to determine the feasibility of flux force/condensation (FF/C) scrubbing. The main activities under the scope of work were:

1. An extension of the existing theoretical treatment of FF/C scrubbing, starting with a review and analysis of past work and proceeding to engineering design methods suitable for evaluating practical systems.
2. An exploratory experimental study limited to the evaluation of key features of FF/C scrubbing.
3. Preliminary engineering and cost analyses of promising practical cases.
4. Recommendations for future development of FF/C scrubbing systems.

Dr. Leslie E. Sparks, of the Control Systems Laboratory, National Environmental Research Center, Environmental Protection Agency was the Project Officer for this program.

Dr. Seymour Calvert, of A.P.T., Inc., was the Project Director.

ABSTRACT

This report presents the results of a feasibility study of flux force/condensation (FF/C) scrubbing for fine particle control. FF/C scrubbing includes the effects of diffusiophoresis, Stephan flow, thermophoresis, and particle growth due to the condensation of water vapor, and is not restricted to any specific scrubber configuration. Fine particles are those smaller than 2.0 micrometer diameter.

The program purpose was to determine whether a development program to maximize FF/C effects is warranted and, if so, to detail the recommended program. The scope of analytical and experimental work was limited to the exploration of the most essential features.

Experimental determination of sub-micron particle collection efficiency in a bench-scale, sieve plate type FF/C scrubber validated the mathematical model which had been developed in the analytical phase of this program. Process designs and cost estimates for the application of FF/C scrubbing to two fine particle pollution sources demonstrated its technical and economic potential feasibility. It is concluded that FF/C scrubbing is an attractive control method for fine particles when high efficiency is required and when the gas is hot enough to evaporate the necessary water vapor. Further development of FF/C scrubbing is clearly warranted.

This report was submitted in fulfillment of Contract No. 68-02-0256 by A.P.T., Inc. under the sponsorship of the Environmental Protection Agency. Work was completed as of February 17, 1973.

CONTENTS

Page

Abstract iii

List of Tables v

List of Figures vi

Acknowledgements viii

Sections

Summary and Conclusions 1

Introduction 7

Engineering Design 22

Theoretical Background 27

Mathematical Model, Sprays 44

Mathematical Model, Plates 59

Mathematical Model, Impinging Jet 77

Mathematical Model, Liquid Sheets 81

Experimental 92

Economic Feasibility 118

Future Research Recommendation 133

References 138

Glossary 144

TABLES

No.		Page
1	Selected References On FF/C Applications	15
2	Collection Efficiency Of Particles By Drops For $K_p = 1.1$ And $G_F = 0.1$ At Various Boundary Layer Thickness	54
3	Summary Of Plate Computations With Penetration Theory Predicted Coefficients	74
4	Results Of Computer Predictions Of Collection By Sheets	88
5	Experimental Conditions And Results	111
6	Transfer Coefficients Determined By Mickley's Method	116
7	P O.F. Control System Costs	126

FIGURES

No.		Page
1	Schematic Representation For FF/C Scrubbing On A Sieve Plate.	23
2	Critical Saturation Ratio For Homogeneous Nucleation Of Water (After Amelin (1967))	33
3	Critical Saturation Ratio For Water Upon A Plane Substrate Of Given Contact Angle - Water At 20°C (After Fletcher 1966).	34
4	Critical Saturation Ratio For Nucleation Of Water Droplets Upon A Particle Of Given Radius With $\cos\alpha$ At 20°C As Parameter - (After Fletcher 1966).	35
5	Equilibrium Supersaturation As A Function Of Droplet Radius With (im) As A Parameter (After Howell 1949).	35
6	Dimensionless Concentration Or Temperature Vs. Dimensionless Distance	40
7	Saturation Ratio Vs. Dimensionless Distance	43
8	Efficiency Of Single Drop Versus Inertia Parameter At $N_{Red} = 9.6$ With N_{FD} As Parameter	51
9	Efficiency Of A Single Drop, η, Versus N_{FD} As A Parameter ($N_{Red} = 9.6$)	52
10	Collection Efficiency For 0.5 μm Diameter Particles In A 1 Meter Spray Column	57
11	Computed Prediction Run #3 For Sieve Plate	71
12	Predictions Of Effect Of Water Vapor Concentration On Particle Radius	71
13	Computed Predictions Run #16	72
14	Computed Predictions Run #18	72
15	Computed Predictions Run #20	73

FIGURES

No.		Page
16	Computed Prediction For Sheets, Run #1	89
17	Computed Prediction For Sheets, Run #2	89
18	Computed Prediction For Sheets, Run #3	90
19	Computed Prediction For Sheets, Run #4	90
20	Experimental Apparatus	93
21	Operating Characteristics Of The Sieve-Plate	95
22	Particle Generator Assembly	97
23	Sampling System	100
24	Particle Penetration Vs. Water Vapor Condensed	113
25	Theoretical Vs. Experimental Penetration	115
26	Flow Scheme For B.O.F. Gas Cleaning	123
27	Flowsheet For FF/C Scrubber On Kraft Liquor Recovery Furnace	129

ACKNOWLEDGEMENTS

A.P.T., Inc. wishes to express its appreciation for excellent technical coordination and for very helpful assistance in support of our technical effort to Dr. Leslie Sparks, E.P.A., Project Officer, and Mr. Robert Lorentz, E.P.A.

SUMMARY AND CONCLUSIONS

Flux force and water vapor condensation effects have the potential to cause high efficiency collection of fine particles by scrubbers. These effects can result from the cooling of a hot, humid gas by contact with cold water. The temperature gradient causes thermophoresis, which drives the particles from the hot gas to the cold water and the water vapor concentration gradient causes diffusiophoresis, which also drives the particles toward the water surface. Condensation of water vapor on the particles will cause their mass to increase and the particles will then be easier to collect by inertial impaction.

The object of the research reported here was to determine the feasibility of using flux force/condensation (FF/C) effects for fine particle (i.e., particles with diameter smaller than 2 microns) collection and, if it appears feasible, to specify the nature of a development program which would be required to provide a proper basis for designing practical systems. The results of the study have established the feasibility of FF/C scrubbing and have indicated the crucial design questions. At the time of writing, development is continuing in order to extend and strengthen the base of engineering design knowledge.

At the beginning of this research it was known from the literature and previous experience that FF/C scrubbing "works". The phenomena of thermophoresis, diffusiophoresis and condensation on particles had been observed and there were reasonably accurate quantitative theories to describe each of them when it occured in a simple system. On an empirical level, there were reports of several scrubber systems which employed flux forces and/or condensation either as the result of deliberate planning or happenstance. Missing, however, was an integration of theory of flux force deposition and particle growth by condensation into an overall quantitative model which would account simultaneously for these phenomena. The model would also have to include heat and mass transfer, particle collection by other mechanisms, and the balances for energy, water vapor, and particles.

The first stage of the research was to put all of the pieces together for the prediction of particle collection in scrubbers of several representative types. Literature search and a review of theory led to the selection of the elements which were incorporated into the overall mathematical models. These models have been, and are still being, refined through a series of evolutionary steps and have reached the point for some scrubber types where they are quite comprehensive and appear to be capable of realistic and accurate representation of particle collection so far as the available experimental data show.

Models for plate scrubbers (as represented by sieve plates) and packed scrubbers have been developed to the point where they appear to do a good job of showing the simultaneous effects of heat and mass transfer for gas/particles and gas/liquid. diffusiophoresis, thermophoresis, Brownian diffusion, inertial impaction, and changes in particle concentration, humidity, and temperature as the gas flows through the scrubber.

The model for spray scrubbers required appreciable effort on the computation of particle trajectories for the combined effects of flux forces and inertial collection by liquid drops. The influence of flux forces on collection by drops was found to be defined by a new dimensionless parameter which is the ratio of flux force deposition velocity to the gas velocity and which we call the "flux deposition number". If the flux deposition number is greater than 0.1, particle collection efficiency will be good and if it is less than 0.01, efficiency will be poor. The model for collection from an impinging jet showed that negligible benefit is given by flux force deposition because of the very short contact time.

Theoretical analysis showed that, in general, the particle deposition velocity has to be on the order of 0.1 cm/sec or larger for appreciable collection efficiency to occur. Diffusiophoresis can produce deposition velocities this high under the heat and mass transfer conditions of a realistic scrubber, but thermophoresis generally cannot. If particle growth due to condensation occurs, inertial impaction of the resulting two or three micron diameter particles can give sufficiently high deposition velocities. Particle growth has the advantage that the high deposition velocity can persist after the heat and mass fluxes are dissipated, because once the particles are enlarged, they can be collected to an increasing degree at the cost of relatively little additional pressure drop.

Experiments were designed to explore the regions of FF/C scrubbing where the mathematical model was most dependent on the several relationships, coefficients, and assumptions which had been used. A test aerosol of condensed dibutyl phthalate smoke particles 0.7 µm diameter was scrubbed from humid air by a 10 cm diameter sieve plate. Particle size and concentration, gas and liquid flow rates, temperatures, and other significant parameters were measured.

Comparison of the experimental data with the model required that first the heat and mass transfer coefficients used in the model be computed from experimental measurements of heat and mass transfer. Predictions of particle collection efficiency based on the experimental transfer coefficients were then compared with the experimental efficiencies. The predictions were sufficiently close to the experimental data to validate the mathematical model as a basis for exploration of FF/C scrubbing potentiality. A number of details remain to be resolved by further effort despite the fact that the model will give a realistic prediction of flux force effects for the experimental system.

Economic Evaluation

The exploration of the economics of FF/C scrubbing was started as soon as an apparently realistic mathematical model was available. Two candidate processes (Basic oxygen furnace and a Kraft liquor recovery furnace) were selected for study on the basis of their meeting the criterion that the gas should ideally be hot enough to evaporate the necessary water.

This criterion develops from the fact that steam purchased at a cost of $1.32 or more per 1,000 Kg steam ($0.60 or more per thousand pounds) is expensive and its use must compete with high-energy scrubber (or electrostatic precipitators or fabric filters) on the basis of operating costs. For illustration, if 0.15 Kg steam were used per Kg of dry gas (this is a fairly low ratio for FF/C scrubbing), the steam cost would be about $0.24/1,000 m^3 dry gas ($0.20/1,000 Kg dry gas). Cooling water for this case might cost from about $0.01/1,000 m^3 to $0.12/1,000 m^3 dry gas, with $0.03/1,000 m^3 being a probable minimum for cooling tower water.

The FF/C steam and water costs may be compared with the power cost for a high-energy scrubber which is capable of 80% collection efficiency on 0.5 μm diameter particles of density 1.0 g/cm^3. A venturi scrubber would require a pressure drop of about 450 cm W.C., which would mean a power cost of \$0.24/1,000 m^3 of gas if electricity cost 1.0¢/K.W.H. One can see that at this performance level an FF/C system could purchase steam and be nearly competitive, and that it would become more attractive as efficiency requirement becomes more stringent. Generally, it would be advantageous to FF/C scrubbing if the gas were hot or moderately hot and humid so that steam need not be purchased.

A preliminary design and cost estimation for the use of a 99.9% efficient FF/C spray scrubber on a basic oxygen furnace of 250 ton/heat capacity resulted in a capital investment of about \$1,700,000 and annual operating costs of about \$790,000. Cost given by others for electrostatic precipitator, fabric filter, and high-energy wet scrubber systems ranged from about \$3,200,000 to \$6,000,000 for capital investment and from \$1,200,000 to \$2,400,000 for annual costs. Since the gas is very hot and must be cooled (usually by water sprays) before it can be cleaned by any means, this situation is very favorable to FF/C scrubbing. This design should be revised in the light of the additional understanding of FF/C scrubbers which has been acquired since the time when the estimate was made.

For another example of the possibilities for FF/C scrubbing, a system for up-grading an existing Kraft pulping liquor recovery furnace air pollution control installation was compared to two other alternatives. In each of the three revision alternatives the original 80% efficient venturi scrubber was replaced with a low efficiency venturi evaporator and a high efficiency particulate collector was added as a second stage.

If one added an electrostatic precipitator such that overall efficiency would be 99% the capital investment would be \$1,930,000 and the annual cost \$420,000. A venturi in series with the first such that overall efficiency would be 97% would require a \$710,000 investment and an annual cost of \$32,000. An FF/C system consisting of a condenser (tubular heat exchanger) and a spray scrubber capable of an overall 97% efficiency would require a $610,000 capital investment and an annual cost of $24,000.

At the level of precision of a preliminary estimate, there is no appreciable difference between adding a high efficiency venturi and adding an FF/C system. The FF/C system has the great advantage that if higher efficiency than 97% is required, as would be likely, it can be upgraded for relatively low cost. For example, the overall efficiency would be increased to 99% for an additional investment of $150,000 and an annual cost of about $40,000. This is possible because once the particle size has been increased by condensation, additional collection efficiency is much easier to obtain than it would be for the original particle size.

Conclusions

The results of the preliminary study show that FF/C scrubbing is capable of high particle collection efficiency on fine particles and that performance is "accountable" through the use of mathematical models. Experimental data served the purpose of verifying the general content and form of mathematical models and, while the efficiencies measured for one-plate scrubbers are not very high, the predictions for multi-plate scrubbers can now be viewed with more confidence.

Of the several particle collection mechanisms involved in FF/C scrubbers, diffusiophoresis and inertial impaction enhancement by particle growth are the two most important. Preliminary indications are that particle growth is the more important of the two.

Economic considerations define the most favorable area of application for FF/C scrubbing as those situations in which the enthalpy of vaporization is available from the gas to be cleaned, although for high efficiency collection of fine particles the purchase of steam can be justified. If an existing scrubber need be up-graded for the removal of sub-micron fume it could pay to introduce some steam, even if it had to be purchased. Another criterion is that the smaller the particles, the better FF/C scrubbing will look, because its efficiency is relatively unaffected by particle size. Cooling water costs can be significant although, depending on the system, charges as high as 4¢/m^3 (15¢/1,000 gallons) can be accomodated.

The most suitable types of scrubber for FF/C application appears to be multi-stage or continuous contact type. This kind of apparatus can be readily adapted to provide different conditions and geometry on different plates to accomodate changing flow rates and particle concentrations. From the pressure drop standpoint, there should be not much difference between this and other scrubber types for the same performance.

Development Required

The research which has been performed up to this point has established the feasibility of FF/C scrubbing and our ability to describe the process with engineering design equations. It has also shown that the specific details of heat and mass transfer, the nucleation of condensation, and other matters have very significant influence on FF/C mechanisms.

In order to resolve the areas of uncertainty mentioned above and to further refine the engineering design methods, a pilot plant development effort is necessary. The pilot plant scale is important because of the necessity for having realistic heat and mass transfer conditions. Some additional bench-scale work is also needed to provide a means for rapid scanning of a variety of conditions. The importance of particle properties and concentration also dictates that the effects of their variation be studied.

Next, there must be a pilot plant demonstration test under the actual conditions of the specific application in order to ensure the performance and economics of FF/C scrubbing. Ultimately, we will have to identify the specific characteristics which are of most significance and develop test methods for measuring them so that performance can be predicted and FF/C scrubbers designed without pilot plant testing.

INTRODUCTION

Preliminary theoretical predictions which were carried out as a part of the "Wet Scrubber System Study" and reported by A.P.T. in the "Scrubber Handbook" (1972), indicated that flux forces (i.e., forces due to temperature and composition gradients) and particle growth due to moisture condensation offered much promise as a means for separating fine particles from gases. In order to follow-up and evaluate that lead, Contract No. 68-02-0256 was established to determine the feasibility of flux force/condensation (FF/C) scrubbers. This report is the final report for that feasibility study.

The major efforts of the study were to make experimental and theoretical explorations of a key region in which flux forces would act to separate particles. It was anticipated that the experimental results would enable the validation of mathematical models which could be used with some confidence to predict the technical and economic potential of FF/C scrubbing. The object was to determine whether a development program to maximize such forces is warranted and if so, to detail the recommended program.

FF/C scrubbers were shown in the system study to have the potential for filling a gap in present day scrubber technology. Whereas scrubbers as commonly used will collect fine particles poorly unless high energy is expended in accelerating the gas, this is not the case for FF/C scrubbers. By applying forces other than inertia on the particles and/or by causing the particles to grow so that inertial deposition is more effective, the FF/C scrubber can give performance on fine particles which is nearly independent of the size of the particles entering the scrubber.

FF/C scrubbing involves those forces which result from temperature, composition, or electric fields in the gas phase. These include thermophoretic, diffusiophoretic, photophoretic and electrophoretic forces and the Stefan flow. The present study is limited only to thermophoresis and diffusiophoresis (which we define to include both diffusiophoretic and Stefan flow forces). Accordingly, we consider only those FF/C scrubbers where particle removal from the gas is aided by a temperature gradient, a vapor concentration gradient, vapor condensation, or combinations of the three. It is not necessary that all three forces act simultaneously, but in most actual cases they do.

For the case of air and water contacting it can readily be shown that the force resulting from the mass transfer of water vapor is the dominant force and a FF/C scrubber is distinguished by vapor condensing inside the scrubber.

Flux forces may stem from the difference in momentum imparted to the particle on opposite sides by the molecules colliding with it or desorbing from it. In the case of a temperature gradient, hotter (and thus faster) molecules colliding with the particle will impart a higher momentum to the particle than the cooler (slower) molecules. In a concentration gradient, which is accompanied by diffusion but not necessarily by net motion of the gas phase, the heavier molecules will again impart a higher momentum than the lighter molecules.

Another kind of flux force is due to Stefan flow which occurs when there is a net motion of the gas phase. The mass transfer can be brought about by evaporation, condensation or a chemical reaction. It was first suggested by Stefan in 1881 that near the surface of an evaporating or condensing body there must exist a hydrodynamic flow of the medium (directed away from the evaporating and towards the condensing surface).

It should be noted here that we refer to the combination of forces due to Stefan flow and to the differential bombardment caused by a gas composition, or molecular weight gradient, as diffusiophoretic force.

In case of condensation of vapor molecules which are heavier than air, then both forces act in the same direction; toward the condensing surface. If the condensing molecules are lighter than air (as in the case with water vapor), the Stefan flow force acts towards the condensing surface while the molecular weight gradient force acts away from it. The net force for the condensation of water from air or flue gas is toward the cold surface because of the overwhelming effect of Stefan flow.

Flux force effects on particles have been known for many years and the background is reviewed and discussed in depth by authors such as Waldman and Schmitt (1966), Goldsmith and May (1966), and Hidy and Brock (1970). The studies reported by these authors include both theoretical and experimental work. The experimental systems were designed so as to be readily definable and were much simpler than a scrubber in terms of the number of phenomena and unsteady conditions involved. For example, we find experimental studies of particle deposition from gas flowing between flat parallel surfaces under the influence of a constant heat or mass flux between the surfaces. Details of pertinent previous studies will be discussed later in this report.

PRACTICAL APPLICATIONS

Over a period of many years there have been numerous instances of the use of scrubbers in which FF/C effects occured. In most of the early pertinent literature, such as patents issued around the beginning of this century, there was no deliberate or conscious design to use FF/C but we can reasonably surmise from the descriptions given that FF/C effects were active. For example, U.S. patent no. 1,039,008 (1912) employed sprays to clean blast furnace top gas and we would expect that the hot gas first became saturated with water vapor and subsequently was de-humidified by further contact with spray water. Consequently, particle collection could have been enhanced by FF/C effects.

More recent literature reveals a growing awareness of the potentialities of FF/C scrubbing; often as a means of explaining anomalously high particle collection efficiency. Schauer (1951) reported high removal of DOP smoke when steam was introduced into a venturi scrubber. Lapple and Kamack (1955) reported that the addition of steam reduced dust loss at a given air pressure drop. Semrau et al. (1958) reported that the observed performance differences between particle collection by a pipeline scrubber and a venturi-cyclonic spray scrubber were probably due to differences in the scrubbing liquid temperature.

Description of other cases where particle collection was enhanced by steam addition can be found in articles by Demshin et al. (1965), Litvinov (1964) and many others. However, most of these authors observed the phenomena but did not study them in detail. Increased collection efficiency due to steam addition was usually attributed to two groups of phenomena: 1) Flux forces. 2) Particle growth. In most studies no attempt was made to isolate the various phenomena and determine relationships between operating conditions and particle collection efficiency that will permit the engineering design of a FF/C scrubber.

More detailed studies of the deliberate use of FF/C effects can be found in engineering articles after about 1965 and in the patent literature. These studies generally fall into one of four categories:

1. Studies of FF/C scrubbers, per se.
2. Studies in other fields such as meteorology and atomic reactor accidents where particle growth and phoretic forces were analyzed.
3. Attempts at analyzing the FF/C scrubber.
4. Patent literature.

Studies of Flux Force/Condensation Scrubbers

Rozen and Kostin (1967) studied the collection of fine oil mist (average particle diameter of 0.3 μm) in a perforated plate column. They built their column in such a way that the gas passed first through a plate with warm water where it became saturated with water vapor and then through a cold water plate where condensation took place. Four such plate pairs were in their column and collection efficiency was studied as a function of temperature of the plates.

Collection efficiency increased with the temperature difference between the hot and cold plates. The further downstream the plates were, the higher was the collection efficiency. Thus, for example, for a 50°C temperature difference collection efficiency for the first pair of hot and cold plates was 45%, for the second pair it rose to 57.4%, for the third pair of plates it reached 74%, and in the fourth pair collection efficiency came to 90%. They found that their results could be represented by an empirical equation relating the particle penetration, "Pt", with the mass of steam condensed per gram of inlet particles, "q".

$$Pt = 12.5\ q^{-0.56} \qquad (1)$$

While these results are encouraging, it is difficult if not impossible to extrapolate the Rozen and Kostin data to other installations mainly because of the lack of a theoretical analysis. Rozen and Kostin presented only their experimental results and attributed the high efficiencies to particle growth. Our theoretical analysis of their data showed that their experimental results could be due to flux forces as well as growth. There is also some uncertainty about their results at high temperatures because of the possibility of particle loss by evaporation of the oil.

Litvinov (1964 A), (1964 B), (1965), (1967) and (1972) did extensive experimental laboratory and industrial scrubber work on the effect of condensation on particle collection efficiency in venturi scrubbers followed by a cyclone or a tray column for mist elimination. In his 1967 paper he reported on the collection of fine carbon black dust (≈1 μm in diameter) and apatite dust in a venturi scrubber followed by a two stage tray column. In this paper he presented engineering data which permit the reproduction of his work. However, his analysis of the results is very limited and somewhat peculiar. He speculates that neither particle growth nor diffusiophoresis should have appreciable effect on the collection efficiency and he suggests that "condensation produces favorable conditions for coagulation", without even describing a mechanism for this.

In his 1972 paper Litvinov experimentally studied three industrial size combinations of dust removal equipment. In all three combinations the first unit is a precleaner for which he used cyclones or a combination cyclone and electrostatic precipitator. Next came a venturi followed by a one or two stage tray column. The dust used had a mean diameter of ≈0.8 μm. Here again no quantitative prediction of collection efficiency is given, only a description of Litvinov's experiments. This time the increase in collection efficiency is attributed to a change in the particle surface properties caused by water condensation.

Terebenin and Bykov (1972) describe an experiment where an aerosol of unrefined tin with an arithmetic mean diameter of 0.128 μm and saturated with steam was passed through a series of wetted wall rectangular ducts. They analyzed their scrubber for flux forces and increased sedimentation due to particle growth. Their conclusion is that the aerosol particles grew through condensation and then settled, largely due to the action of flux forces. Here again no attempt was made at generalizing the equation into a design method.

A study of steam injection into a laboratory scale wet scrubber was carried out by Lancaster and Strauss (1971).

They used redispersed dry agglomerates of ZnO whose size is defined only as having a mean diameter of 1 μm at low concentrations and a larger diameter at higher concentrations. The aerosol was injected into a 2" x 4" duct 6' long to which first steam and then water were injected. The water drops were then separated by a cyclone. They measured an increase in particle collection efficiency which was in direct proportion to the amount of steam injected rather than the amount condensed and they conclude that the increase in collection efficiency is due to particle growth. The use of hot water (same temperature as the temperature of the saturated air) rather than cold water in the sprays gave a slightly higher efficiency. This indicates that diffusio - and thermophoresis were ineffective in the spray section.

The peculiar dependence of collection efficiency on the amount of steam introduced rather than that condensed is attributed by the authors to the mechanism of steam condensation by self-nucleation on dust particles when the steam is quenched more by colder gas. The possibility of additional collection in the cyclone separator due to FF/C effects is not discussed, nor is sufficient information given so that it can be checked. One must conclude that the results of this experiment are valid only for direct steam injection with the specific geometry and operating conditions studied. No general design methods are presented in this paper.

Studies In Other Fields

The studies grouped under this category are more basic and more systematic than those in the first group. Very thorough analytical studies were carried out by Horst (1968), Hales et al. (1970), Hales et al. (1971), Hales and Schwendiman (1971). These studies were concerned with a reactor accident and explored the possibilities for aerosol removal in an enclosed environment at a condensing steam boundary layer. Thus, their analyses were confined to liquid sheets with only natural convection as the air moving mechanism, a situation which is very unlikely in a scrubber. These studies are further limited by the lack of experimental confirmation.

Goldsmith and May (1966) reported another very important study. They analyzed the removal of a radioactively tagged nickel-chromium aerosol 0.02 to 0.2 μm in diameter. The aerosol moved through a vapor gradient box and its deposition velocity was measured. They proved experimentally the validity of the Waldman equation for diffusiophoresis. In another experiment they showed that when the vapor pressure gradient was not closely controlled and supersaturation was permitted, collection was due to particle growth as well as flux forces.

Attempts At Analyzing The Flux Force/Condensation Scrubber

Only a few articles were found in the literature where the feasibility of a flux force or a FF/C scrubber was analyzed. These articles were also the ones that came closest to presenting design methods and design equations.

Sparks and Pilat (1970) presented an analysis of a spray column with condensation taking place on the drops. They showed that for example, when $K_p = 0.6$, where "K_p" is the Stokes number, the collection efficiency in a spray column, where the vapor pressure gradient is 10^5 mbar/cm, was 100% as compared to an efficiency of 0% with no vapor gradient present. While their equations can serve as a starting point for the design of a spray column they definitely need refinement and experimental verification.

Davis and Truitt (1972) present a rough economic analysis of a FF/C scrubber. However, a review of their work revealed sufficient errors in their theoretical analysis and experimental techniques that not much can be obtained from their work to facilitate evaluation and design.

Patent Literature

The patent literature is more obscure than any of the other groups. It does not describe the experimental work on which the patent is based and in some cases presents an idea that was never tried on a large scale. Patents usually contain much irrelevant information and their descriptive part usually centers on the equipment rather than on the design method. Some examples of the patents available which describe FF/C scrubbers are listed here. Japanese patent No. Sho 41-41184, Kazuo Matsuzaki - inventor, describes a FF/C venturi scrubber where the steam is injected tangentially upstream of the throat. No relationships are given which permit the design of such a scrubber.

An article by Takashi Mashita (1971) describes a system based on the Solivore scrubber. This system is based on several venturi's in parallel with water sprays saturating the air upstream of the venturi. Examples of actual installations are given which permit a rough estimation by extrapolation of the scrubber performance from the operating conditions. Other variants of the Solivore scrubber concept involve a single stage of saturation plus venturi and four stages in series, as described by Strauss (1966).

Nucleation and growth by condensation are claimed to be effective in the crossflow scrubber patented by Teller where saturated gas enters a packed section and is cooled with water. This device has been successfully applied to phosphate fertilizer plant particulate collection.

Background Summation

The studies discussed above are examples of the available background information on FF/C scrubbing. Table I, Selected References on FF/C Applications, summarizes the references and their high points is meant to be illustrative of significant studies rather than a complete listing of the literature. What can be distilled from a survey of the background information is a concept of where things stood at the onset of this feasibility study.

To see this status of knowledge with clarity it is helpful to consider first the question of what has to be known in order to design FF/C scrubbers so that their performance and costs can be predicted. In the next section, therefore, we will turn briefly to discussing what we need for design.

TABLE I - Selected References on FF/C Applications

AUTHORS	YEAR	HIGH POINTS OF STUDY	REFERENCE
Semrau K., Marynowski C., Lande K., Lapple C.	1958	Attributed increase in collection efficiency to scrubbing liquid temperature.	Ind. Eng. Chem. 50, 1615 (1958
Lapple C., Kamack H.J.	1955	Addition of steam reduced dust loss at a given air pressure drop.	Chem. Eng. Prog. 51, 110, (1955)
Schauer P.J.	1951	Addition of steam into a venturi scrubber increase removal of DOP smoke.	Ind. Eng. Chem. 43, 1532, (1951)
Rozen A.M., Kostin V.M.	1967	Studied experimentally the collection of fine oil mist in a plate column. They found that: 1. Collection efficiency increased with the quantity of steam condensed and proposed the empirical correlation $Pt = 12.5\ q^{-0.56}$ "Pt" is penetration and "q" = g steam condensed to g inlet particles. 2. Collection in each pair of plates is higher than in the preceding pair. (They attributed the increase in collection efficiency to particle growth.)	Intern. Chem. Eng., 7, 464 (1967)

AUTHORS	YEAR	HIGH POINTS OF STUDY	REFERENCE
Litvinov A.T.	1964A 1964B 1965 1967 1972	His studies concentrated on venturi scrubbers followed by cyclone or sieve tray for entrainment separation. In his 1967 and 1972 papers he reaches the following conclusions: 1. Phoretic forces are not important for particles larger than 0.1 μm in diameter. 2. Condensation of water vapor in a venturi and a sieve tray column increases particle removal efficiency. 3. He gives a design equation for the venturi based on an experimental optimum liquid film thickness, which permits calculation of the "optimum" quantity of condensed steam. 4. He gives the equation $N_{Nu}=0.78\ N_{Re}^{0.65}$ for the heat transfer coefficient from the gas to the liquid drops. 5. Particle growth does not affect collection efficiency. 6. Tray columns with condensation are more efficient than venturi with condensation in energy consumption.	Khim. prom. 8, (1964) Vestn. tekhn, i ekonom. inform. 5, (1964) Stal', 7, (1965) Zhurn, Priklad, Khim, 40, 353 (1967)

AUTHORS	YEAR	HIGH POINTS OF STUDY	REFERENCE
Terebenin A.N., Bykov, A.P.	1972	Analyzed the collection of particles 0.128 µm in diameter in cluster of wetted wall rectangular ducts. They concluded that in the presence of steam particle removal is attributed to growth and flux forces. They give reference to particle growth equation, the results of which do not agree with their experimental findings of particle diameter. No attempt to calculate penetration was made.	Zh. prikl. khim. 45, 1012, (1972)
Lancaster B.W., Strauss W.	1971	Studied the collection of ZnO agglomerates with a mean diameter of 1 µm in a 5 cm x 10 cm rectangular duct 1.85 m long. In different experiments steam was injected upstream or downstream of the aerosol injection port, and it was assumed that when steam was injected upstream of the aerosol it condensed on the aerosol particles. They concluded: 1. Particle build-up was the major mechanism responsible for improved scrubber performance. 2. Flux forces were not important. 3. For their system the dust penetration could be correlated with the rate of steam injection by: $Q = 0.2 \frac{1-\eta}{1-\eta_o} - 1$ where η and η_o are	Ind. Eng. Chem. Fund., 10, 362 (1971)

AUTHORS	YEAR	HIGH POINTS OF STUDY	REFERENCE
		the scrubber collection efficiency with and without steam addition and "Q" is the steam injection rate lb steam/lb air. 4. Steam was used inefficiently in this particular scrubber.	
Lohs W.	1969	Fine particle removal efficiency was studied in a spray column. Na_2SO_4 and polystyrene aerosol with median particle diameter varying from 0.43 to 0.8 μm and from 0.4 to 1.3 μm respectively. Collection efficiency was improved by steam addition for both aerosols. The increase in collection efficiency was higher for the soluble Na_2SO_4 aerosol. (0.3 - 0.5 μm particles can be removed at 60% efficiency) The separation of hydrophobic fine dust is also increased particularly if the particle surface is rendered hydrophilic by means of a wetting agent. Increased efficiency is attributed to particle growth only though Stefan flow is mentioned. No equations, correlations or design method are attempted.	Staub 29, 43, (1969)

AUTHORS	YEAR	HIGH POINTS OF STUDY	REFERENCE
Horst T.W.	1968	This series of studies carried out at Battelle Northwest was concerned with the transport and deposition of a radioactive aerosol expected to be generated by fuel overheating following an accident. Their solutions to the case of aerosol deposition through laminar naturally-convected boundry layer are more rigorous than for the parallel turbulent case. Their conclusions were: 1. In a laminar boundry layer the dominant mechanism is diffusiophoresis. In the turbulent case turbulent deposition may rival diffusiophoresis. 2. Relationships can be derived between steam consumption and particle deposition. 3. The rate of deposition of particles 0.5 - 2 μm in diameter in a laminar boundry layer is independent on particle diameter and depends only on the operating conditions within the air steam boundry layer. 4. When particle deposition is assumed at the mass average velocity of the fluid, values 20-60% lower than in the case of flux forces are calculated for a laminar boundry layer.	Battelle Northwest reports No. BNWL 848 (1968), BNWL 1125 (1970) BNWL SA-3592 (1971) BNBL-SA-3734 (1971)
Hales J.M., Horst T.W., Schwendiman	1970		
Hales J.M., Schwendiman L.C. Horst T.W.	1971		

AUTHORS	YEAR	HIGH POINTS OF STUDY	REFERENCE
Goldsmith P., Delafield H.J., Cox L.C.	1963	Experiments with radioactively tagged nickel-chromium aerosol (particles 0.02 to 0.2 μm in diameter) gave deposition velocities close to those predicted from the Waldman and Bakanov et al. equations. Comparison of thermophoretic velocities with theoretical predictions shows that for $r_p > \lambda$(r_p the particle radius, λ - the mean free path under the given conditions) they vary over a wider range. Derjaguin equation predicted a velocity 16% lower and Brock equation 40% higher than measured. Diffusiophoretic and thermophoretic forces are additive. Experiments of particle deposition efficiency were run in a Liebig condenser. The results show that collection efficiency could be plotted vs. the rate of steam condensation g/min.	Quart. J. of the Reg. Meteor. Soc. 89, 43, (1963)
Goldsmith P., May F.G.	1966		Chapt. VII in Aerosol Science, C.N. Davies ed (1966)
Sparks, L.E. Pilat M.J.	1970	Single droplet target efficiencies for particle collection by the combined mechanism of inertial impaction and diffusiophoresis were calculated. These values were used to calculate overall collection efficiency in a spray tower. It was found that condensation can greatly improve particle collection.	Atmos. Env. 4, 1, (1970)

AUTHORS	YEAR	HIGH POINTS OF STUDY	REFERENCE
Davis R.J. Truitt J.	1972	They concluded that diffusio and thermophoresis would be too expensive for use in scrubbers. Particle growth due to condensation followed by turbulent agglomeration is the best way to increase scrubber efficiency.	Instrum. and Control Systems pp. 68-70, (Nov 1972)
Matsuzaki K.	1970	The invention describes a venturi scrubber where steam is added tangentially upstream of the throat.	Japanese patent No. Sho 41-41184
Mashita T.	1971	Describes the Solivore scrubber which is composed of venturis with water sprays upstream and downstream of the throat. Several operating conditions are described.	Indus. Public Nuisance 7, 573, (1971)

ENGINEERING DESIGN

For an engineering design of an FF/C scrubber one needs design equations which tie the operating conditions to scrubber performance. Each scrubber type may require different equations. (See for example Chapter 5.3 of the Scrubber Handbook.) Thus, equations which describe a venturi scrubber would not be adequate for a tray column, etc.

To predict particle penetration, which is the basic measure of scrubber performance, one has to know the particle deposition velocity and the deposition surface area per unit of gas flow rate. The relevant deposition velocities are those due to the flux forces, inertial, gravitational and Brownian diffusional effects. Since the flux force deposition velocities are functions of the temperature and vapor pressure gradients, knowledge of the magnitude of these gradients at various distances (or residence times) along the gas path through the scrubber is needed.

Simultaneously, the inertial and gravitational deposition velocities are functions of the particle size and density which in turn change due to any vapor condensation on the particle. The critical vapor supersaturation required for nucleation depends upon the particle properties and the operating conditions. Therefore, to predict particle growth one must first know the vapor composition as a function of distance (or time) or travel inside the scrubber. Vapor composition depends on heat and mass transfer between gas/particles and gas/liquid. Thus, the computation of mole fraction water vapor in the gas requires knowledge of particle size and concentration, gas/liquid transfer area, heat and mass transfer coefficients, gas flow rate, and the critical saturation ratio required to nucleate condensation on the particles. All of these parameters change as the gas proceeds through the scrubber.

Figure 1 is a pictorial and verbal representation of the changes which take place as the gas moves through the liquid (foam) on a sieve plate, as an example. Comparable diagrams could be drawn for other types of scrubbers without much change in the major features which are shown. Also shown are the computations which are needed in order to compute the changes of magnitude for the variables shown.

Plots of Variables	Description	Computations Needed*
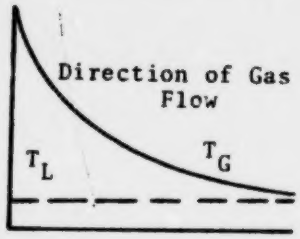	Gas temperature drops rapidly Liquid temperature is fairly uniform.	Ht. Tr. G/L, G/p Mass Tr. G/L, G/p Enthalpy Bal. Mass Bal.
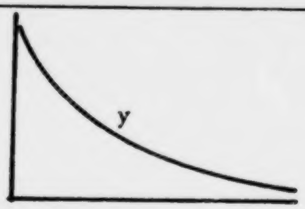	Mol fraction water vapor in gas reaches equilibrium rapidly.	Same as above.
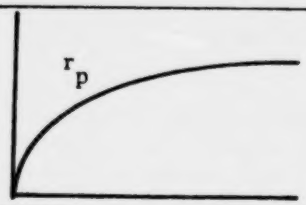	Particle radius grows rapidly while saturation ratio is high.	Mass Tr. G/p - (Need T_G, T_L, M_p, r_p, y)
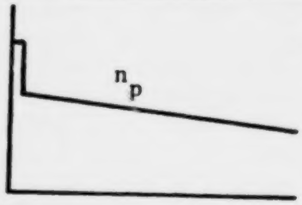	Particle concentration drops abruptly during bubble formation, then fairly uniformly.	Deposition Rate
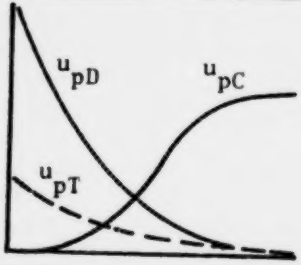	Diffusiophoretic vel. rapid when "y" high. Thermophoretic vel. drops quickly. Brownian diffusion is low for r_p > 0.05 μm. Inertial (centrifugal) dep. increases with "r_p".	Temp. gradient Composition grad. Slip correction Inertial parameter Centrif. force.

*Mass Tr. G/L = Mass transfer, gas to liquid, G/p = gas to particles, other symbols are as defined in "Nomenclature".

Figure 1 - Schematic representation for FF/C scrubbing on a sieve plate.

Because of the rapid changes in conditions and the competition between the particles and the liquid surface for the condensing water vapor, any realistic design method must consider the point-to-point conditions.

Availability Of Design Information

In order to carry out the design computations discussed above, several items of information are required. On the following page we discuss the various design computations and the state of knowledge regarding them, as of the time this research was started.

1. The particle growth equation

All the equations which are presented in the literature are based on a wide and varied set of assumptions which have to be checked experimentally in order to determine their applicability to the specific case at hand. First one must know what saturation ratio is required to cause nucleation of condensation on a particle of some specific substance (which probably has not been studied in this respect). Additional complications occur for particles 0.5 to 2 μm in diameter, which are in the slip flow regime under normal pressure and temperature, and for high vapor concentrations, such as are probable in an FF/C scrubber. Further, there are probably regions of higher saturation ratio than exists in the bulk of the gas phase, and condensation could be initiated there. It was, therefore, imperative to check the validity and applicability of the particle growth equation chosen.

2. The overall energy balance for the liquid interface.

This equation used to determine the interface temperature requires the knowledge of the gas/liquid heat and mass transfer coefficients, the liquid phase heat transfer coefficient, the nature of the interfacial area, and the flow patterns of the two major phases. The coefficients can be estimated from the two-film theory, the penetration theory, or empirical correlations. Experimental coefficients can be found in the literature but they play a major role in the prediction of FF/C scrubber performance (particle penetration) and even small errors in the coefficients can cause a large error in the predicted performance.

In the case of nonconventional designs, experimental coefficients were unavailable. The geometry of the interface must be idealized if predictive computations are to be made. We are aware, for instance, from the voluminous research on mass transfer in plate type equipment for distillation and gas absorption that simple models depicting the gas phase as spherical bubbles are not quite right but may yield some useful answers. Local gas velocity and the overall gas flow pattern will influence both the local transfer coefficients and the bulk conditions for the phases in contact in any region. Liquid phase hydrodynamics has similar effects and is likewise unpredictable.

3. Rate of vapor condensation.

Vapor may condense on the particles and on the collector liquid surface. These two phenomena are governed by the same equations and coefficients discussed earlier and the uncertainties which applied there apply also to this case. Because of the competition and the effect on the driving force for mass transfer the two rates must be evaluated simultaneously.

4. Rate of change of the gas temperature.

The gas temperature changes due to the latent heat of condensation on the liquid and on the particles, the heat transferred either to or from the liquid, and heat losses. All three effects are governed by the equations relating to particle growth, energy balance for the liquid interface and heat losses. The uncertainties and limitations of these equations have been discussed earlier.

5. Rate of particle removal.

Many uncertainties are piled one on top of the other in the equations used to calculate the particle concentration. We started by assuming that the particle fluxes due to the flux and centrifugal forces are additive. In addition we assumed that when particle collection is due to two consecutive mechanisms, the overall penetration is the product of the individual penetrations. Both these assumptions are accepted assumptions and are sound theoretically, however, they had not been proven experimentally.

The accuracy of the deposition velocity equations was questionable in that there was little experimental evidence in the range of particle sizes considered in this work. On top of this, there was the uncertainty as to the gas heat and mass transfer coefficients which in turn determine the gradients necessary for the calculation of the flux deposition velocities. Interwoven with this was the effect of unknown interfacial area for transfer and deposition. With regard to the centrifugal deposition there were questions concerning the gas flow radius of curvature and local velocity, especially when condensing vapor is added.

For plate type scrubbers, an additional removal mechanism is particle collection during bubble formation, which becomes especially important after particle growth takes place. Penetration during bubble formation is a function of foam density as well as particle properties, plate geometry, and gas velocity under normal operating conditions. However, foam characteristics can be different when condensing vapor is present and there were no experimental data on collection during bubble formation when vapor is condensing.

One faces the same kind of questions with other collection geometries, such as drops, packed bed and jets. No equations were available which would permit the calculation of drop target efficiency in the presence of flux forces and the same also applied to jets.

THEORETICAL BACKGROUND

General background on flux force deposition and particle growth by condensation of water vapor will be discussed in this section of the report before proceeding to the use of this knowledge in the development of FF/C scrubber models. As a starting point it is important to note that fine particles are in about the same size range as the mean free path of the gas molecules. Consequently, the interactions between the particles and the gas are not the same as they would be for plane surfaces and the gas.

A measure of the departure of the transport processes in the gas-particle system from the laws of continuum mechanics is provided by the Knudsen number, N_{Kn}.

$$N_{Kn} = \frac{\lambda}{r_p} \tag{2}$$

where "λ" is the mean free path of the gas molecules (about 0.07 µm for air at one atmosphere pressure and 40°C) and "r_p" is the particle radius. Only in the limit, when $N_{Kn} \to 0$ can the gas surrounding a particle be regarded as a continuum. The other extreme, when $N_{Kn} \to \infty$, is usually referred to as the free molecule regime. The "slip flow" regime, which applies roughly when $0.25 < N_{Kn} < 10.0$, is of importance in this program because for particles of 0.1 µm to 2.0 µm diameter, the Knudsen number runs from about 1.0 to 15. Maxwell (1890) suggested a procedure for treating the case of slip flow in which the transport processes in the bulk of the gas are described by the continuum equations, but in a very thin boundary layer of gas next to a surface the non-continuum effects are accounted for. Thus, the boundary conditions for slip flow allow for slip of the gas relative to the surface and analagous "jumps" in gas temperature and concentration between the surface and the gas.

DEPOSITION VELOCITIES

Several equations have been derived which relate the flux force deposition velocity of the aerosol particle in the slip flow regime with the appropriate gradient. For the influence of a temperature gradient on particle motion Epstein (1929) derived:

$$u_{pT} = - \frac{3\mu_G}{4\rho_G T} \left(\frac{2k_G}{2k_G + k_p} \right) \nabla T \qquad (3)$$

where "μ_G", "ρ_G", and "k_G" are respectively the gas viscosity, density and thermal conductivity, "T" is the temperature, "∇T" is the temperature gradient and "k_p" is the particle thermal conductivity.

Brock (1962) has corrected Epstein's equation by accounting not only for the thermal slip but also the temperature jump and the friction slip. His equation for the thermophoretic velocity is:

$$u_{pT} = - \frac{3\mu_G C' \left(k_G + C_t \frac{\lambda}{r_p} k_p \right)}{2\rho_G T \left(1 + 3C_m \frac{\lambda}{r_p} \right) \left(2k_G + k_p + C_t \frac{\lambda}{r_p} k_p \right)} \nabla T \qquad (4)$$

where "C'" is the Cunningham slip correction factor and "C_t" and "C_m" are the temperature jump coefficient and the isothermal slip coefficient respectively. The experimental values for "C_t" and "C_m" are $C_t = 2.3$ and $C_m = 1.25$.

Bakanov and Derjaguin (1962) claimed that the method of Epstein and Brock is invalid. They calculated that Maxwell's expression for thermal creep is too large by a factor of 35 and hence thermal creep is too small to account for thermophoresis. Instead they considered a term in the equation for the heat flux in the bulk of the gas which follows from the third order Chapman-Enskog theory. Applying Onsager's principle of symmetry of kinetic coefficients, they calculated an expression for the thermophoretic velocity. Derjaguin and Yalamov in (1965) improved this by accounting for velocity slip and temperature jump and got

$$u_{pT} = \frac{\mu_G \left(8k_G + k_p + 2C_t \frac{\lambda}{r_p} k_p \right)}{2\rho_G T \left(2k_G + k_p + 2C_t \frac{\lambda}{r_p} k_p \right)} \nabla T \qquad (5)$$

Diffusiophoresis

Diffusiophoresis in the slip flow regime was analyzed by Schmitt and Waldmann (1960) as a hydrodynamic problem, accounting for a finite gas velocity at the particle surface due to diffusion slip. For the case of vapor diffusing through a resting gas they got for the diffusiophoretic velocity:

$$u_{pD} = - \left(1 + \sigma_{12}\, y_G\right) \frac{D}{y_G} \nabla y_v \qquad (6)$$

where "y_G" and "y_v" are the mole fractions of the noncondensible gas and the water vapor, respectively, and "D" is the diffusivity of water vapor in the gas.

"σ_{12}" is a numerical constant called the diffusion slip factor. Kramer and Kistemaker (1943) calculated it as:

$$\sigma_{12} = \frac{M_v - M_G}{M + \sqrt{M_v\, M_G}} \qquad (7)$$

Combining equations 6 and 7 yields:

$$u_{pD} = - \left[\frac{\sqrt{M_v}}{y_v \sqrt{M_v} + y_G \sqrt{M_G}} \right] \frac{D}{y_G} \nabla y_v \qquad (8)$$

Derjaguin et al. (1966) derived an equation for diffusiophoresis of large particles ($r_p > \lambda$). Their derivation is similar to the one they used for thermophoresis. They give for the diffusiophoretic velocity near a condensing or evaporating drop:

$$u_{pD} = \frac{\rho_G}{\rho_m} D \nabla y_v \qquad (9)$$

where "ρ_G" is the density of the inert gas and "ρ_m" is the density of the mixture.

Experimental Results

Experiments by Schmitt (1959) with oil drops and by Schadt and Cadle (1961) with NaCl particles and with tricresyl phosphate drops (high conductivity) $0.05 < N_{Kn} < 1$ agree within ≈20% with the predictions of Brock's theory. Derjaguin, et al. (1966) on the other hand, pointed to convective currents as an uncontrolled source of error in the Millikan condenser apparatus. They devised new experiments and obtained data for $0.15 < N_{Kn} < 0.5$ which confirm their theory.

Measurements of thermophoresis by Goldsmith and May (1966) with Nichrome aerosol ($N_{Kn} \simeq 1$) appear to be bracketed by the opposing theories. Fulford et al. (1971) analyzed their experimental results together with those obtained by Derjaguin et al. (1966), Keng and Orr (1966), Brock (1967), Schmitt (1959), Schadt and Cadle (1961) and Calvert and Byers (1967). Their conclusion is that for particles in the size range of $1.\ \mu m \gtrsim r_p \gtrsim 0.1\ \mu m$ the Derjaguin equation agrees quite well with the experimental results. For larger particles they suggest an empirical correlation based on their experimental data.

Schmitt and Waldmann (1960) pointed out that equations (6) and (7) are accurate within ∿9% for the prediction of diffusiophoretic deposition velocity. Goldsmith and May experimental results with Nichrome aerosol ($N_{Kn} \simeq 1$) compares quite well with the theoretical results predicted by equations (6) and (7). Derjaguin et al. (1966) however, showed that Prokhorov and Leonov (1966) data are in better agreement with equation (9).

Condensation and Particle Growth

The water vapor contained in a saturated or supersaturated aerosol stream may condense on the particles, on the cold walls of the conduit, or on water surfaces, when passing through a scrubber. In our case the aerosol particles are ≈1 μm diameter, may be soluble, insoluble, wettable or nonwettable in water, and flow at the same velocity as the gas surrounding them. Under these conditions the following assumptions apply:

1. The vapor pressure increase due to particle curvature can be neglected for particles of interest.

2. The increase in heat and mass transfer caused by the relative velocity between the gas and the particles can be neglected.

3. There is no vapor pressure depression due to the colligative properties for insoluble particles.

4. Homogeneous nucleation is neglected because of the aerosol particles present.

Having limited our area of interest, we will look at the phenomena of nucleation and growth of water drops in a saturated and supersaturated atmosphere.

Nucleation - The conditions necessary for nucleation to occur on a surface may be predicted from equilibrium thermodynamic considerations for a system in stable equilibrium at a constant temperature when the Helmholz free energy is minimized. This fact is used to find the critical saturation ratio, S_c, for a surface exposed to the vapor. (See for example Abraham (1968), Fletcher (1966) and others.)

The saturation ratio is defined as the ratio of the vapor pressure at the point in question "p_g" to that of a plane water surface "p_i".

$$S = \frac{p_g}{p_i} \qquad (10)$$

It follows from the Kelvin equation that for a given drop diameter, water droplets grow by condensation if the saturation ratio is larger than a critical one. For drops 2 μm in diameter the critical saturation ratio is 1.001 and for drops 0.2 μm in diameter it is 1.01. The rate at which drops in this size range form spontaneously from the vapor increases very steeply with supersaturation. For water at 20°C as an example, the rate of nucleation will increase from $1.2\times10^{-4}/\mathrm{cm}^3$ -sec for S = 3.2 to $1.2\times10^{-2}/\mathrm{cm}^3$ -sec for S = 3.6 (Amelin, 1967). This is important since around the critical saturation ratio the rate of nucleation can be increased substantially by a small increase in the saturation ratio.

The critical saturation ratio is also a function of temperature. Figure 2 taken from Amelin (1967) shows the change in the critical saturation ratio for water vapor as a function of temperature. The critical saturation ratio for homogeneous water vapor nucleation is always above 2.0, within our temperature range of interest.

Nucleation by Insoluble Particles - Drops of the critical radius will form on the surface of insoluble particles at a higher rate than for self nucleation. Volmer (1939) developed a modification of the original Volmer-Weber nucleation theory to include the case of condensation on a plane surface. He showed that the critical saturation ratio for insoluble surfaces is a function of the contact angle between the condensed vapor and the surface. Figure 3 shows the effect of contact angle on critical saturation ratio for water at 20°C. The contact angle is that which is measured between the solid surface and the liquid surface at the line of contact, and which includes the liquid phase.

This analysis was extended to condensation on insoluble particles by Fletcher (1958), and the results of his theoretical calculations are plotted in Figure 4 as the critical saturation ratio vs. drop radius with cos α, the cosine of the contact angle, as a parameter for water vapor at 20°C. This plot shows that for fine particles a saturation ratio of a little over 1.0 will suffice for highly wettable particles ($\alpha = 0°$, $\cos \alpha = 1.0$). In the case of non-wettable particles (α approaching 180°) the critical saturation ratio required for nucleation to occur is equal to that required for homogeneous condensation. Thus, most particles will cause nucleation to occur at lower saturation ratios than for homogeneous nucleation.

Nucleation By Soluble Particles - Nucleation occurs more readily on soluble particles than insoluble particles. Raoult's law states that the equilibrium vapor pressure over a solution is less than that over pure water by a factor equal to the mole fraction of water in the solution. Using the Van't Hoff factor, i, to take into account the dissociation of inorganic salts, Howell (1969) derived an expression for the equilibrium saturation ratio over a solution droplet containing "m" moles of a solute. Figure 5 is a plot of $(p_i/p_\infty - 1) \times 10^2$ vs. droplet radius with "im" as a parameter, "p_i" is the vapor pressure above a droplet of solution containing "m" moles of solute, and "p_∞" is the vapor pressure above a plane surface of pure

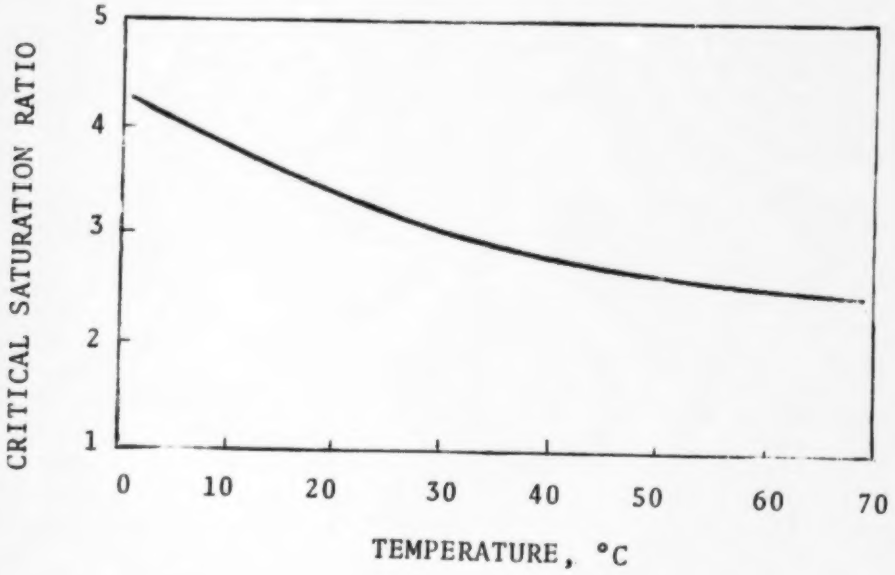

Figure 2 - Critical saturation ratio for homogeneous nucleation of water (After Amelin (1967))

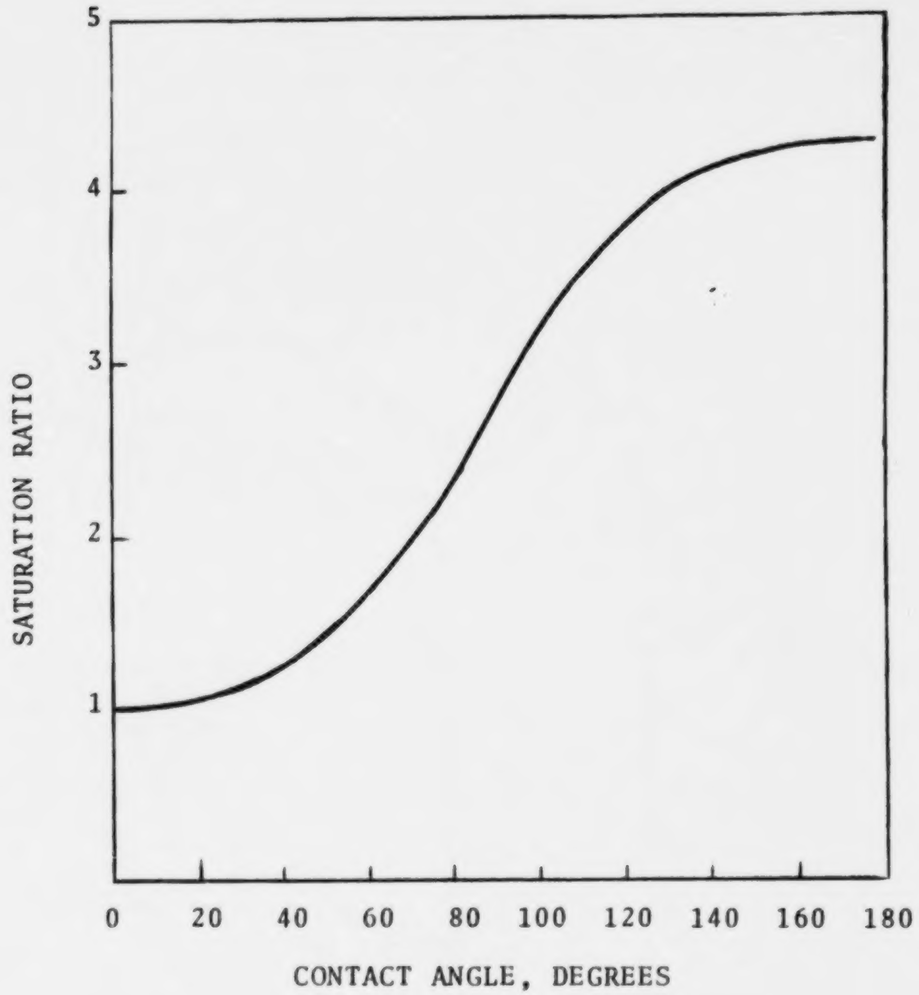

Figure 3 - Critical saturation ratio for water upon a plane substrate of given contact angle - water at 20°C (After Fletcher 1966).

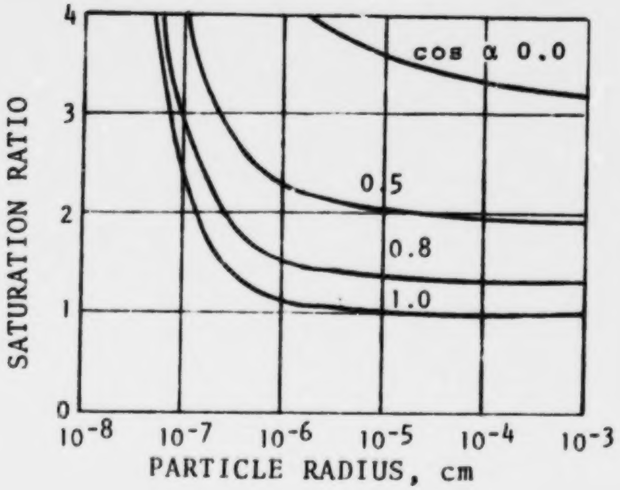

Figure 4 - Critical saturation ratio for nucleation of water droplets upon a particle of given radius with cos α at 20°C as parameter. (After Fletcher 1966).

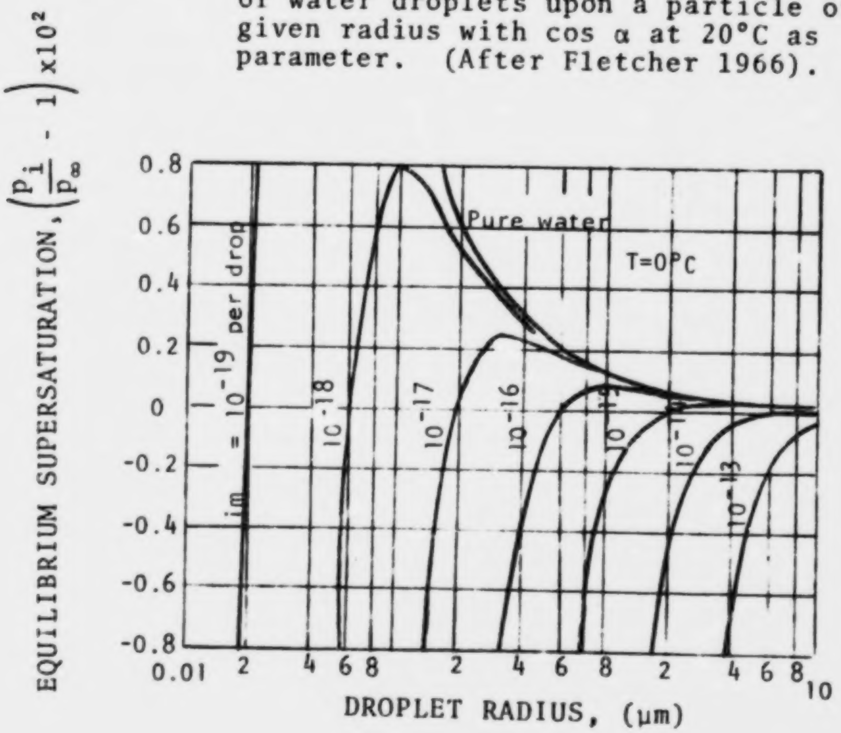

Figure 5 - Equilibrium supersaturation as a function of droplet radius with (im) as a parameter. (After Howell 1949).

water. If, for a given value of "im", the ambient saturation is raised to a value below the peak of the equilibrium saturation curve on Figure 5, an equilibrium drop size will be formed. If, however, the ambient saturation reaches the peak of the curve or higher, spontaneous nucleation, condensation and growth will occur.

The curves presented in Figure 5 apply only when the vapor concentration is higher than the concentration which is in equilibrium with saturated solution at this temperature. For example, a saturated solution of NaCl will reduce the equilibrium vapor pressure of the water by ≈22%; thus no condensation on the NaCl particles is expected unless the relative humidity is higher than 78%, which was found to be the case experimentally (Junge, 1952). In the case of NaCl, Figure 5 will apply only when the relative humidity is higher than 78%.

Mixed Nuclei - In any real situation it is unlikely that the natural condensation nuclei will be described completely by one of the types we have considered. It is more likely that a mixture of soluble, insoluble, wettable and nonwettable particles will be present. In such a mixture we should consider two cases:

1. How the mixture would behave as condensation nuclei.

2. How a particle formed by agglomeration of two different type particles would behave as a condensation nucleus.

The first case is fairly simple because those particles which require lower saturation ratios to nucleate will nucleate first and grow, thus reducing the degree of supersaturation in the aerosol. In order to find the exact proportion of nucleation on the various particles at a given supersaturation, one should examine the rate of nucleation and the rate of decrease of supersaturation. In reality the situation may be complicated by the inhomogeneity of the saturation ratio within the aerosol stream, as is discussed later. However, when the saturation ratio is below the critical value for each of the different cases, no nucleation and growth will take place.

The second case, that of a mixed particle, is more difficult to analyze. Even when all the components of a coagulated nucleus are similar particles, it may possess properties differing from those of a simple particle of the same size. This is due to the fact that its surface will contain cracks and cavities between the particles, and these are favoured condensation sites.

If the nucleus consists of a mixture of soluble and insoluble particles, the nucleation behavior is dominated by the soluble component. Above the phase transition of these components the particle is enveloped in a film of solution, and behaves as a solution droplet in the way we have already considered. The presence of the insoluble components enhances the effectiveness of the soluble salts since less water is required to make a droplet of a given size and the resulting solution is more concentrated. The behavior of such mixed nuclei has been examined in some detail by Junge (1952).

Particle Growth After a drop of critical size has been nucleated, it grows at a rate determined by the ambient environment and conditions at its surface. However, as vapor condenses on the drop, the drop temperature rises and hence the conditions at its surface change. Several equations can be found in the literature describing the rate of growth, Fletcher (1966), Nuzhnyi et al. (1965) and Fuchs (1959). In general they all make the same assumptions and use the same three basis relations: rate of mass transfer, rate of heat transfer and phase equilibrium. Fletcher's equation, which accomodates soluble and insoluble nuclei and is integrated to a comparatively simple form was used in our early modeling. In our later and more refined models for particle growth and collection, however, we use the basic heat and mass transfer equations in order to avoid some of Fletcher's approximations.

Rate of growth during a condition of constant saturation ratio is given by Fletcher as:

$$r_p \frac{dr_p}{dt} = G_F \left(S - 1 - \frac{a}{r_p} + \frac{b}{r_p^3} \right) f(N_{Re}, N_{Sc}) \qquad (11)$$

"r_p" is the particle radius (cm) at time "t", "S" is the saturation ratio defined in equation 10, a/r_p describes the effect of surface curvature in increasing the vapor pressure of small drops and "b/r_p^3" describes the effect of solute content on vapor pressure. "a" and "b" can be approximated by

$$a \approx \frac{3.3\text{x}10^{-5}}{T} \quad \left(\frac{\text{cm}}{°\text{K}}\right) \tag{12}$$

$$b \approx 4.3 \; i \; m \quad \left(\frac{\text{cm - gmol}}{\text{drop}}\right) \tag{13}$$

Where "im" is the number of moles of solute in a drop and "G_F" is defined as:

$$G_F = \frac{D_G \; \rho_v}{\rho_L} \left[1 + \frac{D_G \; L_M^2 \; \rho_v \; M_v \; f(N_{Re}, N_{Sc})}{R \; T^2 \; k_G \; f(N_{Re}, N_{Pr})}\right]^{-1} \tag{14}$$

"D_G" is the vapor diffusivity in air, "ρ_v" and "ρ_L" are respectively the density of the vapor and the liquid, "L_M" is the latent heat of evaporation, "M_v" the molecular weight of the vapor, "R" the gas constant = 1.987 (cal/gmole - °K) and "k_G" is the gas thermal conductivity. $f(N_{Re}, N_{Sc})$ and $f(N_{Re}, N_{Pr})$ represent the increase in the heat and mass transfer coefficients due to the relative velocity between the gas and the growing nuclei, which is negligible for fine particles. The correction due to the surface curvature of the particle, "a/r_p", can also be neglected and "b/r_p" applies only in the case of soluble particles. Thus Fletcher's equation reduces to:

$$r_p \frac{dr_p}{dt} = G_F \left(S - 1 + \frac{b}{r_p^3}\right) \tag{15}$$

where:

$$G_F = \frac{D_G \; \rho_v}{\rho_L} \left[1 + \frac{D_G \; L_M^2 \; \rho_v \; M_v}{R \; T^2 \; k_G}\right]^{-1} \tag{16}$$

Particles 1 µm in diameter are in the slip flow regime, and from Hidy and Brock (1970) we obtain:

$$G_F \sim \frac{D_G \; \rho_v}{(1 + 1.2 N_{Kn}) \rho_L} \left[1 + \frac{D_G \; L_M^2 \; \rho_v \; M_v}{R \; T^2 \; k_G}\right]^{-1} \tag{17}$$

For high vapor concentrations a second correction is required due to the Stefan flow. From Fuchs (1959) this correction is approximated by

$$G_F \simeq \frac{D_G \left(1 + \frac{p_i + p_G}{2P}\right) \rho_v}{(1+1.2\ N_{Kn})\ \rho_L} \left[1 + \frac{D_G \left(1 + \frac{p_i + p_G}{2P}\right) L_M^2\ \rho_v\ M_v}{R\ T^2\ k_s}\right]^{-1} \quad (18)$$

where "p_i" is the vapor pressure at the drop surface, "p_G" is the partial pressure in the gas stream and "k_s" is the thermal conductivity of the gas corrected for the Stefan flow.

Saturation Ratio in Boundary Layer - When considering the conditions under which particles will nucleate condensation, it is important to note that the saturation ratio can be higher in the boundary layer than it is in the bulk of the gas. This can cause the onset of particle growth sooner than would be expected based on bulk conditions. Once the particle surface has been wetted it can serve as a site for further condensation so long as the saturation ratio exceeds 1.0. The particles grown by condensation will be more susceptible to collection by mechanisms dependent on their mass.

As an example, let us take the case of particle collection from the interiors of bubbles, and for simplicity we will treat the boundary layer in terms of penetration theory. We will discuss the behavior of an element of gas which is undergoing simultaneous heat and mass transfer as it moves around the bubble due to gas circulation inside the bubble. Both composition and temperature distributions in the gas contacting the water surface are assumed to be the same as unsteady-state diffusion into (or out of) a semi-infinite plane sheet. Crank's (Crank, 1956) solution for this case is shown in Figure 6, a plot of dimensionless concentration or dimensionless temperature versus dimensionless distance. The dimensionless concentration is the difference in water partial pressure between any point and the gas-liquid interface divided by the difference in partial pressure between the bulk gas and the interface. Dimensionless temperature is defined in an analogous way

$$\text{Dimensionless concentration} \equiv \frac{p - p_i}{p_G - p_i} \quad (19)$$

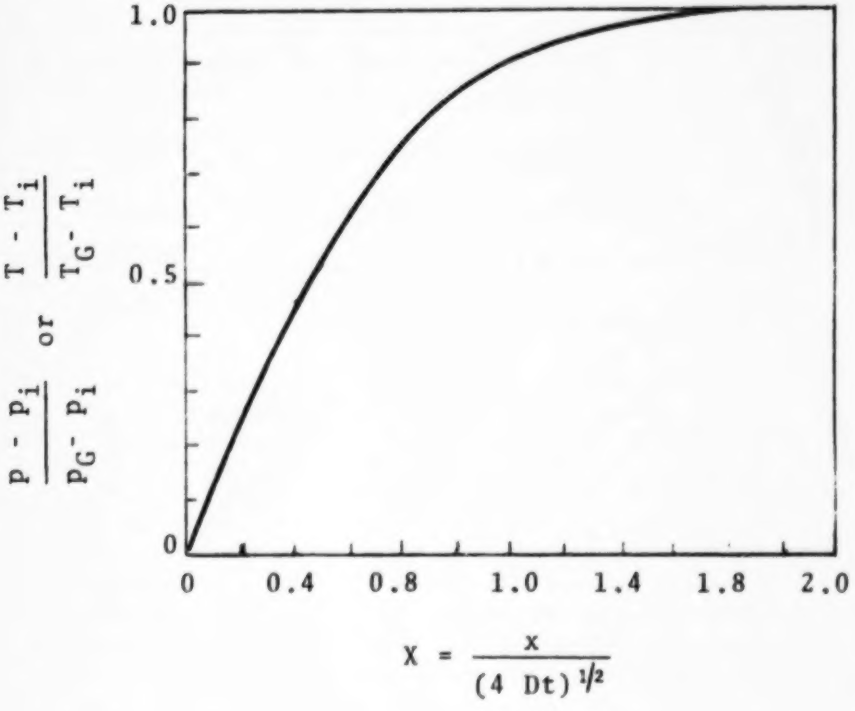

Figure 6 - Dimensionless concentration or temperature versus dimensionless distance

and

$$\text{Dimensionless temperature} \equiv \frac{T - T_i}{T_G - T_i} \qquad (20)$$

$$\text{Dimensionless distance} \equiv \frac{x}{(4\ Dt)^{1/2}} = X \qquad (21)$$

Where:

p = partial pressure of transferring component at a position "x", atm.

T = temperature of gas at position "x", °K or °C

x = distance from interface, cm

D = diffusivity of mass or heat, cm^2/sec

t = penetration time, sec

To get some idea of the magnitudes involved, consider the common case of a 0.4 cm diameter bubble rising at 20 cm/sec and let us use representative values of the properties involved. The penetration time for a circulating bubble is estimated from the time it takes for a 1 dia. rise; or 0.02 sec. The diffusivity of water vapor in air is about 0.25 cm^2/sec, so the value of "x" at a dimensionless distance, X, of 1.0 would be 0.14 cm. The diffusivity of heat, $(k/\rho C_p)$, is approximately 0.2 cm^2/sec and the value of "x" for "t" = 0.02 sec and a dimensionless distance of 1.0 would be 0.136 cm.

From the above example, it can be seen that the dimensionless composition and temperature distributions can be considered identical on the same real distance scale. To illustrate, we see that at X = 1.0 the real distance to the interface is about the same (i.e., 0.14 cm) for heat and mass transfer and that the values of dimensionless temperature and composition are the same. One can also note that most of the volume of a circulating bubble 0.2 cm radius would become involved in the boundary layer, which grows to about 0.14 cm at the bottom of a rising bubble.

Some examples of gas and liquid conditions were chosen for illustrative purposes and the saturation ratios which would occur because of the heat and mass transfer were computed for various positions in the boundary layer as given by Figure 6. The results are shown in Figure 7, a plot of saturation ratio vs. dimensionless distance from the gas/liquid interface. It can be seen that the curves for a water interface temperature of 20°C and bulk gas phase conditions of 45°C, S = 1.0 and 60°C, S = 1.0 have maxima where the saturation ratio goes considerably above 1.0 at a position within the boundary layer.

For the case of a 20°C liquid interface temperature, gas phase temperature of 30°C, and S = 1.4, there is no maximum in the curve. It can be seen from these examples that it is possible for the saturation ratio in the boundary layer to be higher than that in the bulk of the gas phase, depending on the temperatures of the gas and liquid. Consequently, a substance which requires a critical saturation ratio of 1.5 in order for water to condense on it could nucleate growth under the 60°C gas temperature condition, even though the saturation ratio for the bulk gas phase is only 1.0. Once condensation starts on a particle it can continue to grow so long as the saturation ratio is 1.0 or larger.

Curve No.	T_G,°C	T_L,°C	S
1	60	20	1.0
2	45	20	1.0
3	30	20	1.4
4	45	20	1.1

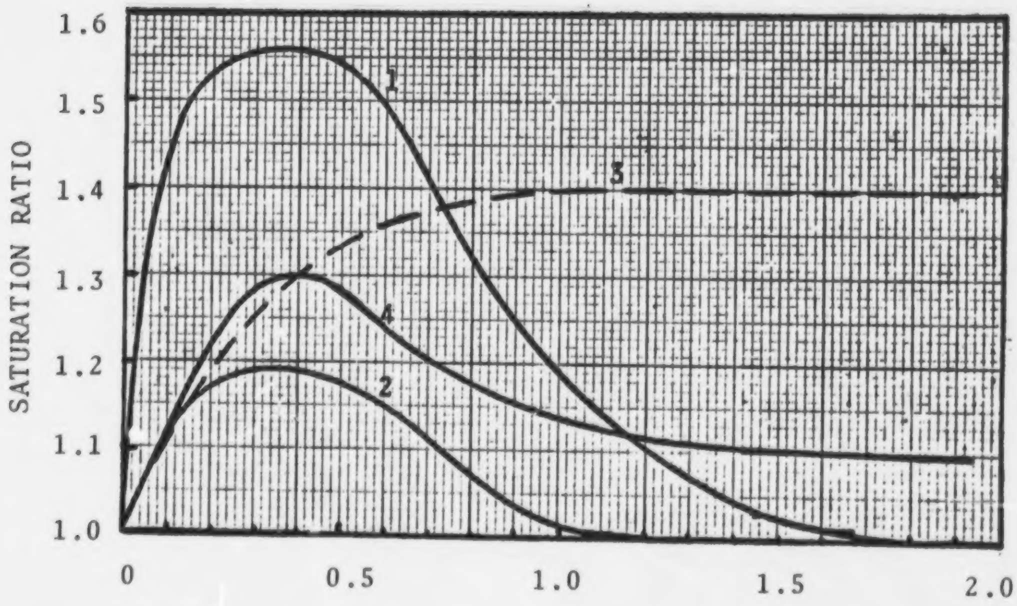

$$X = \frac{x}{(4\ Dt)^{1/2}}$$

Figure 7 - Saturation ratio versus dimensionless distance

MATHEMATICAL MODEL, SPRAYS

Mathematical models were developed for three principal types of scrubbers; spray, plate, and liquid sheets. The models were to be used first for the exploration of possible operating conditions and design variations in order to assess the capability of each scrubber type when operated in the FF/C mode and to locate an approximately optimum operating range. Next, the models would be used for the correlation of experimental data and then the evaluation and possible modification of the model in the light of the data.

The models which were developed early in this research were for plates, as represented by the unit mechanism of collection from bubbles. They did not allow for particle growth, simultaneous transfer to particles from liquid, and other factors. In the course of the program the plate models were refined; especially since our experimental work was on plates. As it happened, the mathematical model for sprays was developed fairly early in the program and was not revised at the time of writing. Because it is the oldest model, that for sprays will be presented first, so that the progressive development of more realistic and complex models during the research will be reported in order of our increasing understanding of FF/C system modeling.

Spray type scrubbers are represented in fundamental terms by the unit mechanism of particle collection by drops or spheres. Collection of particles by spheres due to inertia alone is discussed in the literature and target efficiencies have been calculated by many: Langmuir and Blodget (1946), Ranz and Wong (1952), Herne (1960) and others. When additional forces are involved, the equations of motion are different and new solutions are required. We adopted Sparks and Pilat (1970) approach and solved the equations of motion of the particle in the "X" and "Y" direction after including the additional flux force.

A force balance on the particle in the "x" direction gives for the case where Stokes law applies:

$$\frac{du_x}{dt} = \frac{1}{\tau}(v_x - u_x) + \frac{F_x}{m_p} \qquad (22)$$

and

$$F_x = 6\pi \mu_G r_p u_F \tag{23}$$

τ = particle relaxation time $\equiv \frac{2 r_p^2 \rho_p}{9 \mu_G}$ (sec)

v_x = gas velocity in "x" direction, cm/sec

u_x = particle velocity in "x" direction, cm/sec

m_p = particle mass, g

F_x = flux force acting on particle in "x" direction, dynes

u_F = particle velocity due to flux force, cm/sec

The equations of motion can be put in dimensionless form by the use of the following new dimensionless parameters and variables:

$$\tilde{X} \equiv \frac{X}{r_d}; \quad \tilde{Y} \equiv \frac{Y}{r_d}; \quad \tilde{v}_X \equiv \frac{v_X}{v_o}; \quad \tilde{v}_Y \equiv \frac{v_Y}{v_o}; \quad \tilde{t} \equiv \frac{t\, v_o}{r_d}$$

$$K_p \equiv \frac{2 \rho_p r_p^2 v_o}{9 \mu_G r_d} = \text{inertial impaction parameter} \tag{24}$$

and

$$G_F \equiv \frac{u_F}{K_p v_o} \tag{25}$$

Where:

X = distance from center of drop in "x" direction, cm

Y = distance from center of drop in "y" direction, cm

v_o = velocity of undisturbed gas stream relative to sphere, cm/sec

Substituting values of "v_x" for potential flow, from Fuchs (1964), we obtain the differential equations in their final form:

$$\frac{d^2\,\tilde{X}}{d\tilde{t}^2} + \frac{1}{K_p}\,\frac{d\tilde{X}}{d\tilde{t}} + \frac{2\,\tilde{X}^2 - \tilde{Y}^2}{2\,K_p(\tilde{X}^2 + \tilde{Y}^2)^{2.5}} - \frac{G_F\,X}{(\tilde{X}^2 + \tilde{Y}^2)^{1/2}} = \frac{1}{K_p} \qquad (26)$$

$$\frac{d^2\,\tilde{Y}}{d\tilde{t}^2} + \frac{1}{K_p}\,\frac{d\tilde{Y}}{d\tilde{t}} + \frac{3\,\tilde{X}\,\tilde{Y}}{2\,K_p(\tilde{X}^2 + \tilde{Y}^2)^{2.5}} - \frac{G_F\,\tilde{Y}}{(\tilde{X}^2 + \tilde{Y}^2)^{1/2}} = 0 \qquad (27)$$

Equations (26) and (27) can be solved if boundary conditions are specified and if an expression for "G_F" is available.

FLUX DEPOSITION

Equations (26) and (27) show that the two parameters, K_p and G_F, are required to define particle motion under the influence of inertial and flux forces. It will be shown later that the product of these parameters is a new parameter which defines the effect of adding flux forces to a system involving only inertial force. Equation (25) can be rearranged to yield the product:

$$K_p\ G_F = \frac{u_F}{v_o} = \frac{\text{Particle transport by flux forces}}{\text{Particle transport by fluid flow}} = N_{FD} \qquad (25)$$

The dimensionless parameter "v_o/u_F" is related to the Peclet number since it is an indication of the relationship between convective and flux force transfer of particles diffusing to a boundary surface. The Peclet number, usually given $N_{Pe} = v_o d/D$, is the characteristic ratio for convective diffusion. It represents the ratio of the rate of transport by fluid motion to the rate of transport by molecular processes. We will refer to the ratio "u_F/v_o" as the Flux Deposition number, N_{FD}.

Significance of Flux Deposition Number

To show the relationship of N_{FD} to N_{Pe}, we can start with consideration of a diffusional process where the flux is given by:

$$N_A = -D\,\frac{dc}{dx} = u_{DM}\ c_A\ \ (\text{gmol/cm}^2\text{-sec}) \qquad (28)$$

where:

u_{DM} = deposition velocity for mass transfer, cm/sec

c_A = concentration of transferring component ("A"), gmol/cm^3

If the concentration gradient is linear, there is no equilibrium pressure above the interface (i.e., no "back-pressure") and the boundary layer thickness, "δ", is proportional to drop diameter, "d":

$$\frac{dc}{dx} \simeq \frac{c - o}{\delta} \; \alpha \; \frac{c}{d} \tag{29}$$

Therefore:

$$\frac{D}{d} \; \alpha \; u_{DM}, \text{ and, } N_{Pe} \; \alpha \; \frac{v_o}{u_{DM}}$$

or:

$$N_{Pe} \simeq \frac{V_o}{u_{DM}}, \text{ if } \delta \simeq d \tag{30}$$

The form of the modificed Peclet number in equation (30) will apply to any deposition process for which the flux can be described by equation (28). Thus we should expect to find comparable mathematical models and empirical correlations for deposition with diffusion and that with flux forces.

It is instructive to look for an estimate of the quantitative significance of N_{FD}. Deposition rate on a sphere by any flux or diffusional mechanism will follow the same form as the following equation

$$(4\pi r_d^2)N_F = u_F n_p (4\pi r_d^2), \text{ no./sec} \tag{31}$$

The rate at which particles approach the sphere is given by:

$$v_o n_p (\pi r_d^2) = \text{convection rate to sphere} \tag{32}$$

The fraction of the particles convected to the sphere which deposit on the sphere (i.e., the collection efficiency) is:

$$\eta = \frac{4\pi\ r_d{}^2\ u_F\ n_p}{\pi r^2\ v_o\ c} = \frac{4\ u_F}{v_o} = 4\ N_{FD} \tag{33}$$

Thus, for a single drop if N_{FD} is greater than 0.1, collection efficiency is good. If N_{FD} number is less than 0.01, collection efficiency will be only a few percent or less. In situations where there is collection on a series of drops, the efficiency of each drop need not be so high in order to obtain a suitable overall efficiency for the sequence of drop contacts. For example, the particle penetration of a counter-current spray tower with a water/gas ratio of 1.0ℓ/m³, drops 0.04 cm diameter, a height of 3 meters, and a gas velocity of 120 cm/sec and spray losses on the walls equal to 80% of the inlet water is approximately:

$$Pt \simeq \exp(-10.0\eta) \tag{34}$$

If a penetration of 0.1 (i.e. 90% collection efficiency) is desired, the collection efficiency for a single drop would have to be 0.23 (23%). If the single sphere efficiency were 0.023, the overall penetration would be about 0.8. Thus the approximate N_{FD} range of 0.1 to 0.01 to distinguish good from poor performance for a single sphere is also about the right magnitude for a spray scrubber.

SOLUTION OF THE EQUATIONS OF MOTION

Let us now take up the solution of equations (26) and (27) for particle collection under the influence of flux forces. The velocity and trajectory of the particle is determined by the resultant force and the air flow field around the particle. In order to formulate this situation mathematically, the following assumptions are made:

1. All the assumptions made by Langmuir and Blodgett (1946) for collection due to inertia alone apply also in this case.

2. The time scale for the interaction between a single particle and a single drop is small compared to the time scale of changes in the drop and gas temperature and humidity. Thus the temperature difference between the gas and the drop is assumed constant. This assumption was checked numerically and found correct within 1%.

3. All the resistance to heat transfer is assumed to be in the thermal boundary layer. The boundary layer thickness is estimated from the heat transfer coefficient obtained from the Whitaker (1972) equation:

$$N_{Nu} = 2 + 0.4\ N_{RE}^{0.5}\ N_{Pr}^{0.4} \left(\frac{\mu_G}{\mu_{Gi}}\right)^{0.25} \tag{35}$$

A heat balance around the drop gives:

$$Q = h\ \Delta T = \frac{k_G}{\delta}\ \Delta T \tag{96}$$

Substituting for "h" in $N_{Nu} = \frac{h'\ d_d}{k_G} = \frac{d_d}{\delta}$

Other equations for the boundary layer thickness yield other values for "δ". These values range from $\approx 0.5\ r_d$ to $\approx 2\ r_d$.

4. The thermal boundary layer was assumed to be of a constant thickness in the front half of the sphere. The thickness varies with the Reynolds number of the sphere as can be seen from the previous assumption. This is an approximation, since the velocity boundary layer thickness approximately doubles from the stagnation point to an angle of 90°, Schlichting (1960).

5. The temperature gradient in the thermal boundary layer is assumed constant. This was calculated to be approximately the case for a flat plate and $N_{Pr} \approx 0.6$, Schlichting (1960).

6. The thermophoretic force acts on the particle only inside the thermal boundary layer.

7. Collection in the back of the drop was neglected. This assumption is correct for low drop Reynolds numbers.

8. G_F is constant inside the boundary layer.

Integration

Equations (26) and (27) were integrated for boundary conditions which are consistent with the assumptions given above. The boundary conditions are:

$$\left.\begin{aligned} \tilde{X} &= -\infty \\ \tilde{Y} &= \tilde{Y}_o \\ \frac{d\tilde{X}}{d\tilde{t}} &= 1 \\ \frac{d\tilde{Y}}{d\tilde{t}} &= 0 \end{aligned}\right\}\quad \text{at } \tilde{t} = 0 \tag{37}$$

$$G_F = 0 \text{ for } (\tilde{X}^2 + \tilde{Y}^2) > (1 + \tilde{\delta})^2$$

$$G_F = G_F \text{ for } (\tilde{X}^2 + \tilde{Y}^2) \leq (1 + \tilde{\delta})^2$$

These equations were solved numerically on a digital computer using a Runge-Kutta method. The solution was started at $\tilde{X} = -5.0$. Figure 8 is a plot of target efficiency vs. "K_p" with N_{Pe}' as a parameter for $N_{Red} = 9.6$.

To illustrate the significance of Figure 8, we might consider a case with initial gas temperature of 100°C and initial liquid temperature of 20°C, for which we compute $u_{pT} \approx 0.03$ cm/sec. It follows from Figure 8 that under these conditions the effect of thermophoresis is very small. If the drop diameter were, say 200 μm, its settling velocity would be about 74 cm/sec, and N_{FD} would be about 2.5×10^{-4}, which is indicative of very poor collection efficiency due to flux force.

DIFFUSIOPHORESIS AND INERTIA

The solutions of equations (26) and (27) and the resulting Figure 8 are valid for the case of diffusiophoresis and inertia and the sum of thermophoresis and inertia. Figure 8 is also a representation of collection efficiency when any number of forces are acting simultaneously; given that deposition velocity, u_F, is defined as:

$$u_F = u_{pD} + u_{pT} + \text{any other deposition velocity} \qquad (38)$$

and:

$$G_F \equiv \frac{u_F}{K_p \, v_o} \qquad (39)$$

Three dimensionless numbers, K_p, N_{FD}, and N_{Re} determine the collection efficiency of particles by drops when the particles are subjected to the simultaneous action of inertia and flux forces. We have reduced the role of the Reynolds number by assuming potential flow around the drop.

From Figures 8 and 9, which is a cross plot of Figure 8, several conclusions can be drawn:

1. Collection efficiency increases with the increase in "K_p" and "N_{FD}".

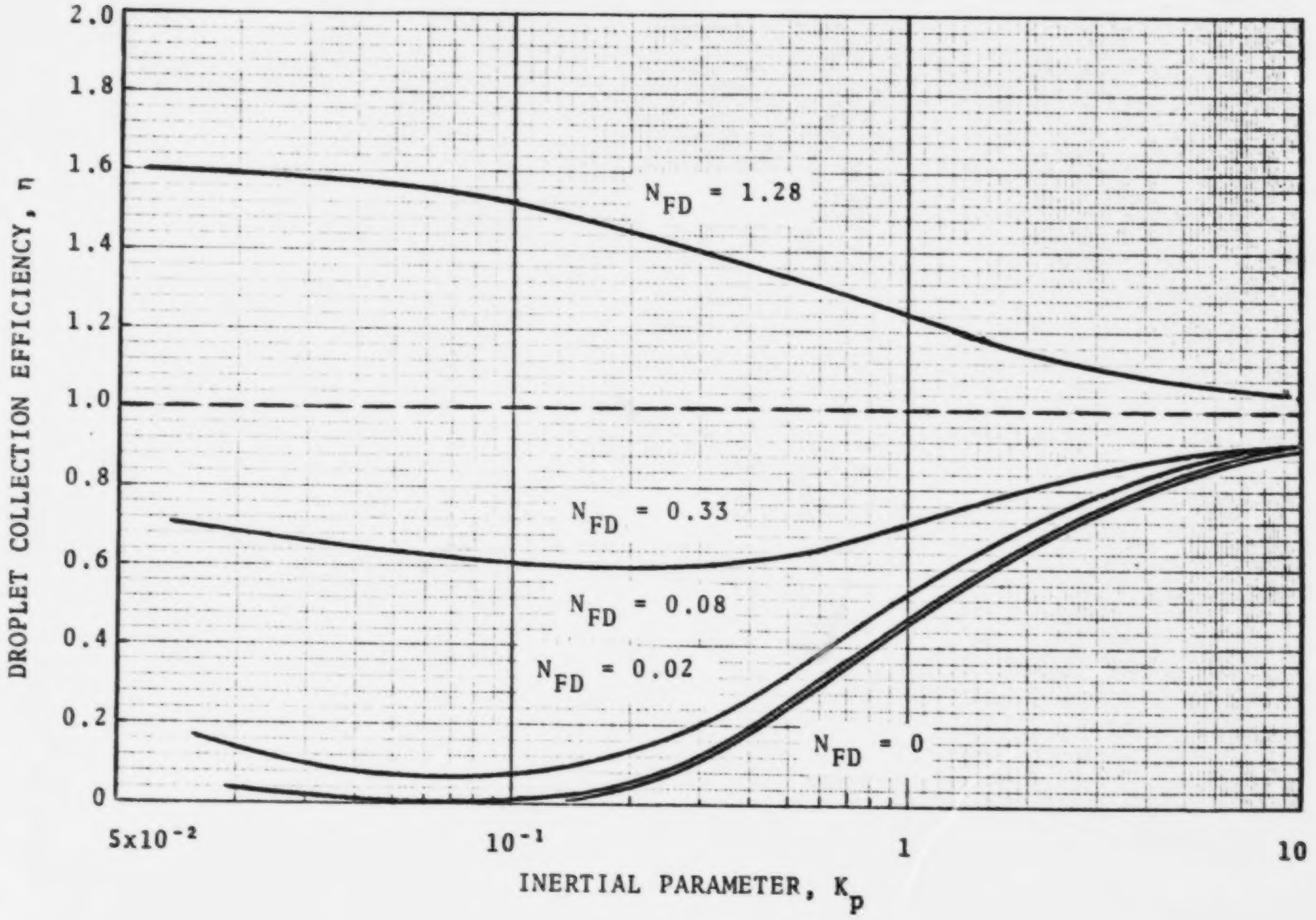

Figure 8 - Efficiency of single drop versus inertia parameter at N_{Red} = 9.6 with N_{FD} as parameter

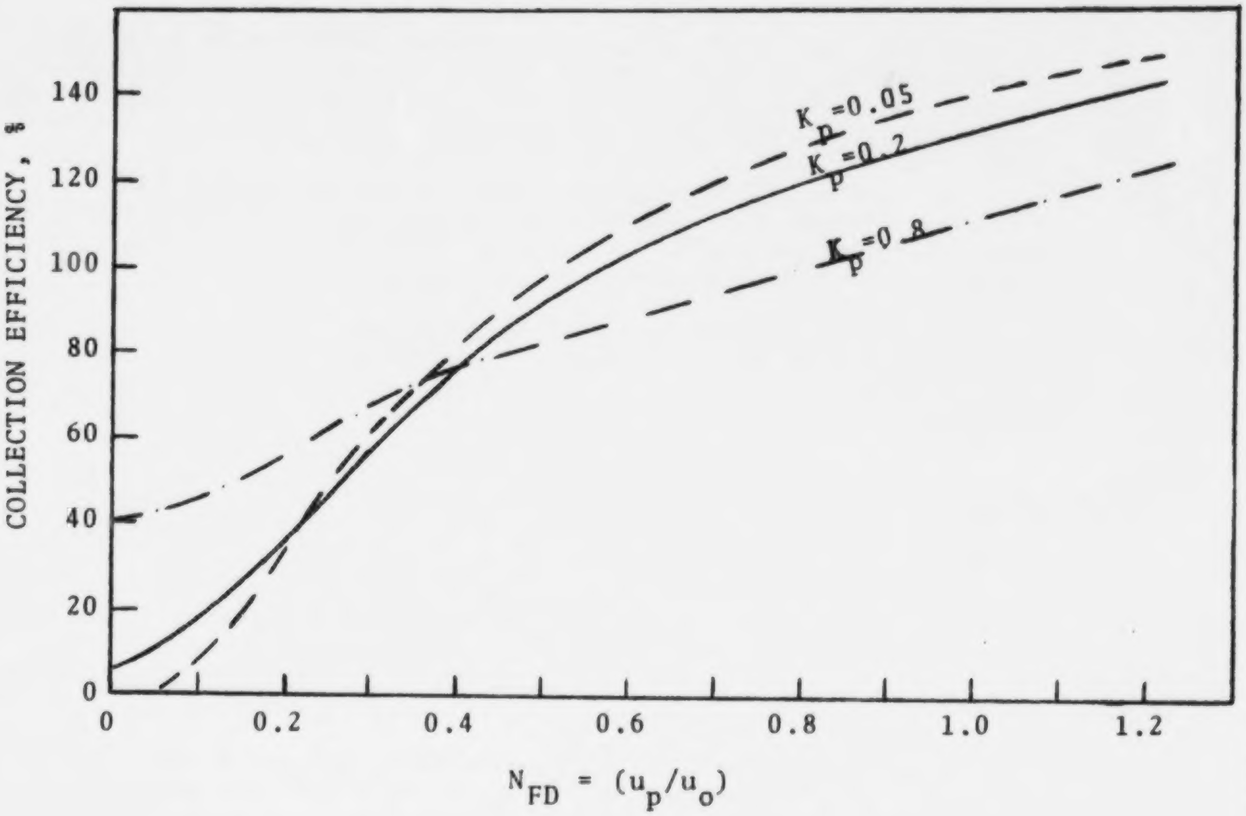

Figure 9 - Efficiency of a single drop, η, versus N_{FD} with K_p as a parameter ($N_{Red} = 9.6$).

2. The higher "K_p" is (and the larger the particles), the smaller is the effect of the flux force on collection efficiency.

3. At low "K_p" values collection efficiency increases with decrease in "K_p". This may be attributed to the lower stream velocities and the longer time in which the particle is subjected to the flux forces.

4. Collection efficiency can increase above 100% for high values of "u_p/u". This stems from the fact that particles can be moved to the drop from positions outside the projected frontal area in the gas stream.

We can make some general observations about the probable importance of flux force deposition mechanisms by estimating ranges of N_{FD} and then interpreting these values in the light of Figures 8 and 9. For example:

1. For poorly conducting particles in the fine size range and a temperature range of $0°C < \Delta T < 80°C$, flux deposition number is $0.04 > N_{FD} > 0.0007$. This means that in this range thermophoresis is not important.

2. Diffusiophoresis can be very important for fine particles because with a water vapor partial pressure range of $0.13 \lesssim p_v \lesssim 0.65$ atmospheres, the flux deposition number range is $2.5 > N_{FD} > 0.01$.

Collection efficiency as shown in Figures 8 and 9 is for $N_{Re} = 9.6$ which is the N_{Re} of a free-falling 200 μm diameter water drop. The boundary thickness, as already mentioned, is a function of the Reynolds number and for the case presented in Figure 8 and 9 it was taken as $0.56(r_d)$. Since these calculations are for potential flow, a change in the Reynolds number will change only the thickness of the boundary layer. To see the effect of changing the boundary layer thickness on the collection efficiency, Table II shows the change in

$$\eta \text{ vs. } \tilde{\delta} = \frac{\delta}{r_d}, \text{ at } K_p = 1.1 \text{ and } G_F = 0.1.$$

TABLE II

Collection Efficiency of Particles by Drops for $K_p = 1.1$ and $G_F = 0.1$ at Various Boundary Layer Thickness

$\tilde{\delta}$	0	0.56	1	2.2
η	0.5	0.58	0.62	0.69

We see that the thickness of the boundary layer has a small but noticeable effect on collection efficiency.

PARTICLE GROWTH

When humid hot air is passed through a spray column, cooling and dehumidification take place. Transfer of heat and vapor from the gas to the drops occurs and particles are collected by the drops due to the combined effect of inertia, diffusiophoresis, and thermophoresis. At the same time, if the saturation ratio is high enough, particle growth starts. As shown in the previous section, diffusiophoresis is significant for the temperature range of interest, but thermophoresis can be neglected.

A mathematical model for particle collection by diffusiophoresis and inertial impaction in a spray column was developed and solved as follows:

1. Computations were made for small increments of the spray column; ranging from 0.1 to 2.0 cm high. After the increment height was chosen the conditions calculated and compared to the conditions calculated from one half of this height. If the difference was not significant the original increment height was used for further calculations.

2. Gas humidity and temperature, liquid temperature, and interfacial humidity and temperature were calculated for each section in the method presented in Brown (1950). These conditions were assumed constant throughout the section. "h_L" and "h_G", the heat transfer coefficients inside the drop and on the gas side, were estimated from penetration theory and equation (35).

3. Particle growth was computed by means of Fletcher's equation, modified by the use of a factor "α", so that:

$$r_p\left(\frac{dr_p}{dt}\right) = \frac{\left(\frac{D_G \rho_G}{\rho_L}\right) (S - 1) \alpha}{\left(1 + \frac{\alpha D_G L^2 \rho_G M_v}{R T^2 k_G}\right)} \tag{40}$$

"α" is an arbitrary factor less than or equal to one, which is introduced to permit exploration of effects due to variance in surface conditions and other factors which can influence the competition between particles and liquid surface for condensing water. By varying "α" one can calculate what will occur if, for example, only 50% growth is realized.

4. Vapor concentration gradient was calculated from:

$$\frac{dy}{dx} = \frac{y - y_i}{\delta}$$

where "y_G" and "y_i" are the mole fractions of water vapor at the bulk and at the drop interface.

5. Particle radius after growth, "K_p" and, "N_{FD}" were calculated for each increment.

6. Target efficiency was estimated from Figure 8 for each increment.

7. For comparison of various operating conditions, the collection efficiency of a 1 meter column was calculated.

8. Penetration for each increment was calculated from the equation for a countercurrent spray column:

$$Pt_i = \exp - \left[\frac{3 Q_L u_t \Delta Z}{4 Q_G r_d (u_t - u_G)}\right] \eta_i \tag{41}$$

Where:

Pt_i = particle penetration for the increment, fractional

Q_L = liquid flow rate, m^3/sec

Q_G = gas flow rate, m³/sec

u_t = terminal settling velocity of drop, cm/sec

u_G = linear velocity of gas, cm/sec

ΔZ = height of increment, cm

η_i = collection efficiency of drop under increment conditions, fractional

The overall penetration of the increments where cooling and dehumidification take place was calculated from

$$Pt_c = \prod_{i=1}^{n} Pt_i = \exp - \left[\frac{3\, Q_L\, u_t\, \Delta Z}{4\, Q_G\, r_d\, (u_t - u_G)} \sum_{i=1}^{n} \eta_i \right] \qquad (42)$$

Penetration for the rest of the column, where heat and mass transfer are small and affect collection efficiency only slightly, was calculated from

$$Pt_n = \exp - \left[\frac{3\, Q_L\, u_t\, (Z - n\,\Delta Z)}{4\, Q_G\, r_d\, (u_t - u_G)}\, \eta \right] \qquad (43)$$

where $\eta = \eta_n$.

The overall collection efficiency is:

$$E = 1 - Pt_T = 1 - (Pt_c\, Pt_n) \qquad (44)$$

Figure 10 shows $E_c = (1 - Pt_c)$ and $E_T = (1 - Pt_T)$ for a 1 meter countercurrent spray column as a function of "α" for 0.5 μm diameter particles of density 1 g/cm³ and inlet concentration of 10^6/cm³. The gas entered at 35°C and left at 33.2°C, while the liquid entered at 20°C and left at 25.3°C. Gas inlet humidity, "Y_o" was 0.155 g/g, corresponding to a saturation ratio of about 3.5 at 35°C; and the outlet was 0.077 g/g, corresponding to a saturation ratio of about 2.1. Liquid to gas flow ratio was 5ℓ/m³, drop size 0.05 cm diameter, and linear gas velocity 60 cm/sec.

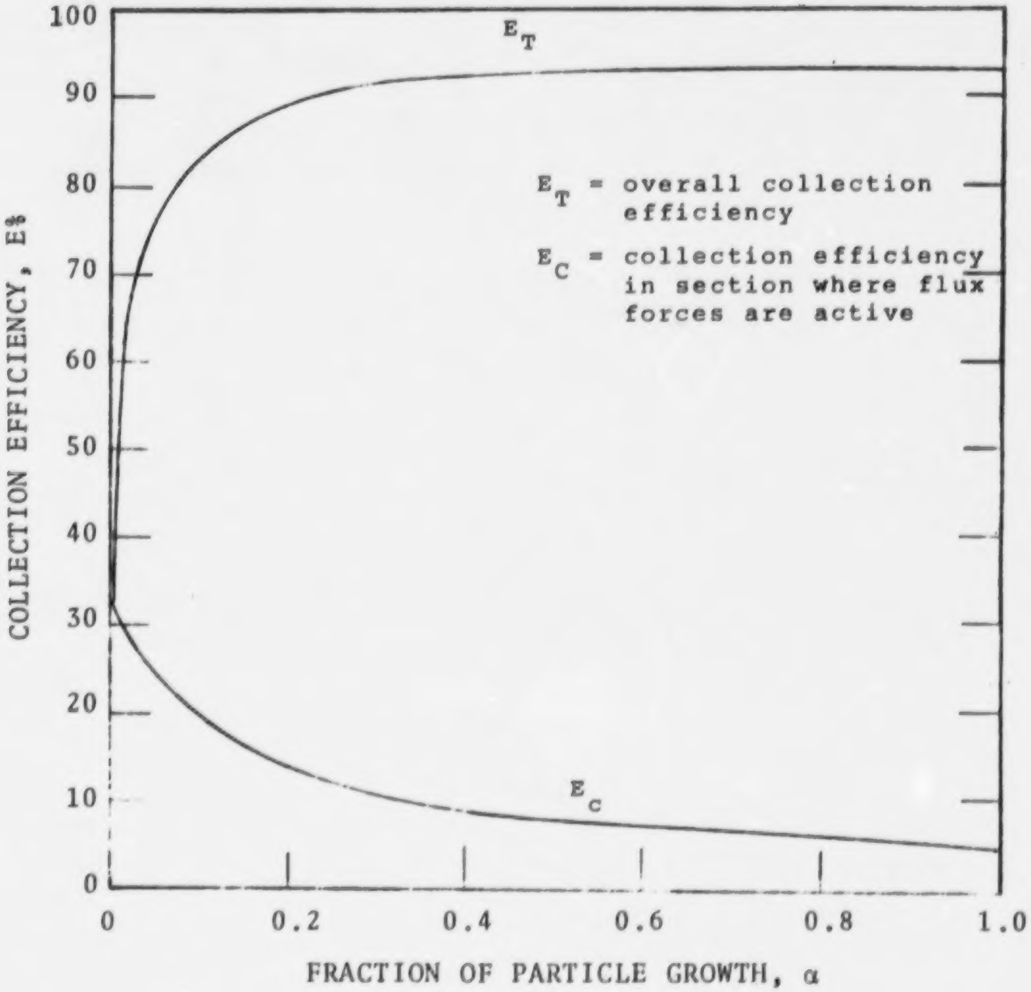

Figure 10 - Collection efficiency for 0.5 μm diameter particles in a 1 meter spray column

It can be seen that with no particle growth, a collection efficiency of 33% was calculated, while for full particle growth collection efficiency rose to 92%. It should be borne in mind that there are several points of uncertainty in the computation so that one should view these results as being only approximate. For one thing, the liquid to gas ratio is rather high so the wall losses and agglomeration of drops would cause the active spray holdup and its efficiency to be less than assumed. If, as might realistically be assumed, half of the spray were lost to the walls, the efficiency would drop from 92% to 74%.

Reducing the degree of supersaturation in the incoming gas by raising its temperature, reduces collection efficiency markedly even if the humidity is not changed. At the time these calculations were made it seemed reasonable to assume that as high a saturation ratio as 3.5 could be attained in the inlet gas. Experimental experience obtained later in this program leads us to have serious doubt that saturation ratios much higher than 1.0 can be attained in realistically dirty effluent gas streams. For these and other reasons relating to computational techniques, the present spray model should be considered as a first exploratory step.

MATHEMATICAL MODEL, PLATES

Plate type scrubbers are represented to a first approximation by the unit mechamism of transfer from bubbles. Thus, while the model which is described in the following section is defined in the specific terms of a sieve plate, it is suitable for expressing the particle collection behavior of scrubbers in which bubble formation and rise through liquid are the principle mode of gas/liquid contacting. In order to compute the simultaneous effects of transport and particle deposition phenomena in plate type scrubbers, a set of equations was developed as described below. The final set of equations describes the following phenomena:

1. Heat and mass transfer between bubbles and liquid.
2. Heat and mass transfer between bubbles and particles suspended in bubbles.
3. Particle growth due to condensation.
4. Particle deposition by:
    a. Diffusiophoresis
    b. Thermophoresis
    c. Centrifugation during bubble rise

The following general assumptions were made:

1. Gas bubbles are spherical, constant diameter (d_b = 0.4 cm, usually), and perfectly mixed internally (except for the interfaces).

2. Gas properties are as for air and water vapor.

3. Foam density is constant throughout the foam layer on the plate.

4. Liquid bulk temperature is constant throughout the foam, although the liquid-bubble interface temperature can vary.

5. Particles are mono-disperse, wettable, insoluble spheres.

6. Condensation on particles can occur whenever the saturation ratio is 1.0 or larger.

7. All the particles are subjected to condensation and growth.

PARTICLE GROWTH

The rate of change of particle radius is given by a mass balance,

$$\frac{dr_p}{dt} = \frac{k'_{pG}\ (p_G - p_{pi})}{\rho_M} \quad \left(\frac{cm}{sec}\right) \tag{45}$$

Where:

$$k'_{pG} = \frac{2\ D_G\ P}{RT_G\ d_p\ p_{BM}} \quad \left(\frac{gmol}{cm^2\text{-sec-atm}}\right) = \text{mass transfer coefficient particle to gas} \tag{46}$$

p_G = water vapor partial pressure in bulk of gas bubble, atm

P = total pressure, atm

p_{BM}= mean partial pressure of non-transferring gas, atm

d_p = particle dia, cm

T_G = gas bulk temperature, °K

ρ_M = molar density of water, gmol/cm³

For air and water:

$$D_G \simeq 0.256 \left(\frac{T_G}{300}\right)^{1.75}$$

so

$$k'_{pG} \simeq \frac{2.85\text{x}10^{-7}\,(T_G)^{0.75}}{d_p\left(\frac{2-p_{pi}-p_G}{2}\right)} \tag{47}$$

It can be shown that "p_{pi}" is close to "p_G" so that $p_{BM} \simeq (1-p_G)$ for the case of particle growth.

Particle growth over a finite period is given by the integration of equation (45) after substitution of equation (46).

$$r_2^2 - r_1^2 = \frac{2\ D_G\ P(p_G - p_{pi})\Delta t}{RT_G\ \rho_M\ p_{BM}} (\mathrm{cm}^2) \qquad (48)$$

where Δt = time of growth, sec.

In our present computational programs, equation (48) is not applied when $p_{pi} > p_G$, because this would imply particle evaporation. It would be possible to write a computer program which would allow the evaporation of only the water film on a particle, but this has not been necessary thus far.

The vapor-liquid equilibrium relationship for water can be approximated within a few percent by:

$$p_{eq} = \exp\left(13.64 - \frac{5.1\mathrm{x}10^3}{T}\right) \ (\mathrm{atm}) \qquad (49)$$

p_{eq} = water vapor partial pressure in equlibrium at T °K

Particle temperature can be computed from an energy balance:

$$h_{pG}(T_{pi} - T_G) + \left(\frac{\rho_p\ C_{pp}\ r_p}{3}\right)\frac{d\ T_{pi}}{dt} = k'_{pG}\ L_M\ (p_G - p_{pi}) \qquad (50)$$

Where:

$$h_{pG} = \frac{2k}{d_p} \simeq \frac{7.5\mathrm{x}10^{-5}}{r_p}\left(\frac{\mathrm{cal}}{\mathrm{cm}^2\text{-sec-°K}}\right) = \text{particle to gas heat transfer coefficient} \qquad (51)$$

C_{pp} = heat capacity of particle, cal/g-°K

k = thermal conductivity of gas, cal/cm²-sec-°K/cm

and

$L_M \simeq 10^4 \left(\frac{\mathrm{cal}}{\mathrm{gmol}}\right)$ = latent heat of vaporization for water

The second term on the left side of equation (50) represents the effect of particle heat capacity and it is neglected in the computation. It can be shown that the product of particle mass and heat capacity is a very small percentage (generally less than 1%) of the product of gas mass and heat capacity. Thus, for a given change in temperature, most of the energy goes into increasing gas enthalpy.

An explicit solution for particle surface temperature was provided by an alternate solution to equation (50). This solution involves the approximation that the vapor-liquid equilibrium relationship is linear over a small range of temperature or vapor pressure (see equation 54). If we define a temperature, T*, which is the saturation (equilibrium) temperature corresponding to the partial pressure of water in the bulk gas, p_G, we can show that:

$$\frac{p_G - p_{pi}}{T_{pi} - T_G} = \frac{h_{pG}}{k'_{pG} \, L_M} = C_2 \tag{52}$$

and

$$T_{pi} - T_G = \left[\frac{1}{1 + \frac{C_2}{m}} \right] (T^* - T_G) \tag{53}$$

Where:

$$m = \text{slope of eq. line} \approx \left[(0.042)\, p_G + 5\text{x}10^{-4} \right] \left(\frac{\text{atm}}{°\text{K}} \right) \tag{54}$$

and

$$T^* = \frac{5{,}100}{13.64 - \ln p_G} \tag{55}$$

Because $C_2 \approx 4\text{x}10^{-4}$ (atm/°K), the particle temperature, T_{pi}, will be within a few degrees of T*, rather than being at approximately the gas temperature, T_G. For example, at $p_G = 0.1$, $m = 4.7\text{x}10^{-3}$ and $C_2/m = 0.085$. Thus,

$$T_{pi} - T_G \approx 0.925\ (T^* - T_G)$$

HEAT AND MASS TRANSFER IN BUBBLES

The overall energy balance for a bubble interface is given by

$$k'_{bG}\, a_b\, L_M (p_G - p_{Li}) A_p\, dZ =$$

$$h_{bL}\, a_b (T_{Li} - T_L) A_p\, dZ + h_{bG}\, a_b (T_{Li} - T_G) A_p\, dZ \qquad (56)$$

where:

$$k'_{bG} = \frac{\hat{k}_G P}{p_{BM}} \simeq \frac{1.13P}{RT_G\, p_{BM}} \left(\frac{D_G}{\Theta_B}\right)^{1/2} \quad \frac{\text{gmol}}{\text{cm}^2\text{-sec-atm}}$$ = mass transfer coefficient, bubble to liquid (57)

a_b = surface area of bubbles/unit volume of foam, cm^2/cm^3

A_p = area of plate, cm^2

Θ_B = surface renewal time, sec

$$h_{bG} = 2\left(\frac{\rho\, C_p\, k}{\pi\, \Theta_B}\right)^{1/2} \left(\frac{\text{cal}}{\text{cm -sec-°K}}\right) \qquad (58)$$

T_L = temperature of liquid bulk, °K

For a bubble diameter = 0.4 cm and bubble rise velocity = 20 cm/sec, the time to rise 1 diameter = 0.02 sec. If "Θ_B" is evaluated as 0.02 sec for the penetration theory models represented by equations (57) and (58), the coefficients for air and water properties are as follows:

$$\hat{k}_G = 1.6\text{x}10^{-4} \text{ gmol/cm}^2\text{-sec-atm} \qquad (59)$$

$$h_{bG} \simeq 0.022\ (T_G)^{-1/2} \text{ cal/cm}^2\text{-sec-°K} \qquad (60)$$

It should be noted that boundary layer theory would predict coefficients about half these and that the computation of diffusiophoresis deposition from equation (59) yields a very high velocity. Thus, we are cautioned to view equations

(59) and (60) as rough approximations which may be used until experimental data are available.

The heat transfer coefficient from the interface to the bulk liquid is approximated through penetration theory as:

$$h_{bL} = 2 \left(\frac{\rho \; C_p \; k}{\pi \quad \theta_B} \right)^{1/2} = 0.31 \left(\frac{\text{cal}}{\text{cm}^2\text{-sec-°K}} \right) \tag{61}$$

Combining equations (55), (50), (60), and (61) yields:

$$\frac{1.6(p_G - p_{Li})}{(1 - p_G/2)} - 0.31 \; (T_{Li} - T_L) - \left(\frac{0.022}{T_G^{1/2}} \right) (T_{Li} - T_G) = 0 \tag{62}$$

In equation (62), p_{BM} is approximated as $(1 - p_G/2)$ because p_{Li} is usually very low.

Condensation of water from the gas bubble will cause both a decrease in gas flow rate and composition, as given by:

$$-d(G\;y) = - \frac{G \; dp_G}{(1-p_G)} = \frac{dM_t}{dt} \quad \frac{\text{gmol } H_2O \text{ vapor}}{\text{cm}^2 \text{ of plate area-sec}} \tag{63}$$

where G = molal gas flow rate per unit area of plate, gmol/cm^2-sec

y = mol fraction water vapor

The mass of water vapor transferred is given by:

$$dM_T = dM_p + dM_b = \frac{\text{gmol } H_2O \text{ vapor}}{\text{cm}^2 \text{ of plate area}} \tag{64}$$

The transfer rate to particles is,

$$A_p \frac{dM_p}{dt} = \frac{4\pi \quad (r_2{}^3 - r_1{}^3)}{3(18) \; \Delta t} (n_p \; A_p \; V_b \; dZ) \; \left(\frac{\text{gmol}}{\text{sec}} \right) \tag{65}$$

where:

n_p = number concentration of particles in gas, no./cm^3

t = time interval, sec

V_b = volume fraction bubbles in froth, cm^3/cm^3

and the mass transfer rate to the bubble interface is,

$$A_p \frac{dM_b}{dt} = k'_{bG}\, a_b\, (p_G - p_{Li})\, A_p\, dZ \left(\frac{\text{gmol}}{\text{sec}}\right) \tag{66}$$

where: dZ = height of bubble rise in time "dt"

In the difference calculation procedure used for the machine computations, equations (64), (65), and (66) are combined to give:

$$\frac{\Delta M_T}{\Delta t} = k'_{bG}\, a_b\, (p_G - p_{Li})\, \Delta Z + \frac{4\pi}{54}\, (r_2{}^3 - r_1{}^3)\, n_p\, V_b\, \Delta Z \left(\frac{\text{gmol}}{\text{cm}^2\text{-sec}}\right) \tag{65}$$

The change of gas temperature due to sensible heat transfer is defined by an energy balance as follows:

$$G\, C_{pM}\, \Delta T_G = h_{bG}\, a_b\, (T_{Li} - T_G)\, \Delta Z + \Delta M_p \times 10^4 \left(\frac{\text{cal}}{\text{cm}^2\text{-sec}}\right) \tag{66}$$

or

$$G\, C_{pM}\, T_b = \frac{\Delta Q_b + \Delta Q_p}{\Delta \Theta} \qquad \left(\frac{\text{cal}}{\text{cm}^2\text{-sec}}\right) \tag{67}$$

Where C_{pM} = molar heat capacity of gas, cal/mol-°K

and ΔQ = heat transferred in time $\Delta\Theta$, per cm^2 of plate area

The particle area per cm^3 foam is:

$$a_p = n_p\, (4\pi\, r_p{}^2)\, (1-F) = n_p\, V_b\, (4\,\pi r_p{}^2) \left(\frac{\text{cm}^2}{\text{cm}^3}\right) \tag{68}$$

The bubble surface area per cm^3 foam is assumed constant and given by:

$$a_b = v_b\left(\frac{G}{d_b}\right)\left(\frac{cm^2}{cm^3}\right) \tag{69}$$

The change in gas flow rate is approximated by:

$$G = \frac{M_T}{\Delta t}\left(\frac{gmol}{cm^2\text{-}sec}\right) \tag{70}$$

PARTICLE DEPOSITION

Particle deposition by Brownian diffusion is not very effective on particles in the >0.1 μm dia. size range, and was not included, although it could have been included with little difficulty. The collection which occurs during the period of bubble formation can be predicted separately by means of equation (71) and it was not included in this model.

$$Pt_F = \exp - (40\ F_\ell^{\,2}\ \ K_p) \tag{71}$$

where

F_ℓ = foam density, volume fraction liquid

Pt_F = particle penetration for collection during bubble formation, fraction

K_p = inertial impaction parameter

$K_p = \dfrac{d_{pa}^{\;2}\ v_h}{9\ \mu_G\ d_h}$

d_{pa} = aerodynamic diameter of particle

$= d_p(\rho_p\ C')^{1/2}$

It should be noted that collection by impaction during bubble formation is not very important for one tray and particle diameter smaller than 1 μm. But if the particles grow during their stay in the first tray, this mechanism will become very important in collecting the particles on the second tray and following trays.

For the present, we are looking at what happens after the initial collection by impaction. The total particle flux from the gas to the liquid is defined as the sum of fluxes due to diffusiophoresis, thermophoresis, and centrifugation.

$$N_s = N_D + N_T + N_C \left(\frac{\text{no. particles}}{\text{cm}^2\text{-sec}} \right) \tag{72}$$

and the flux is related to the deposition velocity and particle concentration by:

$$N_s = u_{ps}\, n_p \tag{73}$$

For a spherical bubble of radius "r_b", the rate of change of particle concentration is:

$$\frac{dn_p}{dt} = \left(\frac{3}{r_b} \right) N_s = \left(\frac{3n_p}{r_b} \right) u_{ps} \tag{74}$$

Where,

$$u_{ps} = u_{pD} + u_{pT} + u_{pC} = \text{sum of deposition velocities} \tag{75}$$

and the penetration for a period = Δt:

$$Pt = \exp - \left[\frac{3}{r_b} \; (u_{ps}) \; \Delta t \right] \tag{76}$$

Diffusiophoretic deposition velocity is:

$$u_{pD} = \frac{\sqrt{M_1}\; D_G}{y \; \left| \sqrt{M_1} + (1-y) \; \sqrt{M_2} \right| \; (1-y)} \frac{dy}{dr} \quad \left(\frac{\text{cm}}{\text{sec}} \right) \tag{77}$$

$$u_{pD} = C_1\ D_G \left(\frac{1}{1-y}\right) \frac{dy}{dr}$$

where M_1 = molecular weight of water, g/mol

M_2 = molecular weight of non-transferring gas, g/mol

and for air and water it can be shown that:

$C_1 \approx 0.85$ (dimensionless) over the range from $y = 0.1$ to 0.5

The composition gradient can be related to the mass transfer coefficient as:

$$\frac{dy}{dr} = \frac{dp}{dr} = \frac{RT_G\ k'_{bG}(p_G - p_{Li})}{D_G} \tag{78}$$

Therefore, substitution from equations (57), (59) and (78) into (77) yields:

$$u_{pD} \approx 0.85\ RT_G(1.6\times10^{-4})\ \frac{(p_G - p_{Li})}{(1 - p_G/2)} \tag{79}$$

$$u_{pD} \approx 0.0112\ \frac{(p_G - p_{Li})T_G}{(1 - p_G/2)}\ \text{(cm/sec)} \tag{80}$$

Thermophoretic deposition velocity is:

$$u_{pT} = -Z'\ \frac{\mu_G}{\rho_G\ T_G}\ \frac{dT}{dx} \tag{81}$$

and the gradient is estimated from:

$$\frac{dT_G}{dx} = \frac{h_{bG}}{k}\ (T_G - T_{Li})\ \left(\frac{°K}{cm}\right) \tag{82}$$

Using Brock's value for $Z' \approx 0.25\ C'$, we have for air and water vapor:

$$u_{pT} \simeq 1.35\text{x}10^{-4} \; (C' T_b^{1/2} \;\; \Delta T) \; (\text{cm/sec}) \tag{83}$$

Where:

$$\Delta T_G = (T_G - T_{Li}) \, (°K) \tag{84}$$

$$C' \simeq \left(1 + \frac{1.6\text{x}10^{-5}}{d_p}\right) = \text{Cunningham slip correction} \tag{85}$$

Centrifugal deposition velocity is:

$$u_{pC} = \frac{2 \; r_p^{\,2} \; \rho_p \; C' \; v_t^{\,2}}{9\mu \; r_b} = K \; v_t \tag{86}$$

and for $r_b = 0.2$ cm, $\rho_p = 1.0$ g/cm³, and $v_t = v_b = 20$ cm/sec,

$$u_{pC} = \frac{r_p^2 \; C'}{T_G} \; (7.4\text{x}10^{8}) \; (\text{cm/sec}) \tag{87}$$

Note that "u_{pC}" is dependent upon "$v_t^{\,2}$" and is quite sensitive to the assumed values of "v_b" and "r_b".

PREDICTIONS

A computer program was written to solve the mathematical model comprising the equations given above, and some predictions of performance were computed. As a representative case, we took bubble diameter to be 0.4 cm, foam density 0.5 (volume fraction gas), and bubble rise velocity to be 20 cm/sec. The first computations were for the following conditions:

particle radius = 0.5 μm

particle concentration = 1x10⁶ particles/cm³

gas molar flow rate = 0.003 gmol/cm²-sec

foam height = 8.0 cm

The predicted penetration for these conditions was much lower than experimental data such as Rosen and Kostin (see Figure 4.6.4-7 in Scrubber Handbook). Because of this and the uncertainties about the transfer coefficients, the heat and mass transfer coefficients for the gas phase, bubble to liquid transfer were decreased to 1/2 the values given by equations (59) and (60). The lower values are in line with the predictions given by boundary layer theory and the penetration resulting from their use are of a more realistic magnitude. The predictions which are discussed in the remainder of this section were made on the basis of 1/2 the values given by equations (59) and (60) until experimental data was available.

As will be seen later, under experimental work, the liquid phase heat transfer coefficient and the interfacial area for transfer seem to be quite different than those assumed. The approach we have taken is to devise the best model possible based on existing information, devise and perform experiments to test the predictions of the model, and then revise the model to fit experimental findings. Because of that, we will describe only the general features of the predictions based on 1/2 the simple penetration theory transfer coefficients in this section.

It is enlightening to explore the predicted effects of process variables as shown in Figures 11 through 15 and Table III. Table III summarizes the conditions and results for 20 computer runs. Bear in mind that while the general trends are in line with experimental results, the predictions give lower penetrations than experimentally observed, apparently because of the liquid phase heat transfer coefficient used. In all of these runs the total foam height was 6 cm; so the bubble residence time was 0.3 sec.

In all figures, the "Y" axis ranges from 0. to 1.0 and the "X" axis denotes time, with each increment of the digital computation, Δt = 0.02 sec. In order to fit all four curves into the range from 0. to 1.0, we plotted the following:

$$S' = \frac{S}{2} = \frac{P_G}{2[\exp\ (13.64) - 5{,}100/T_G)]} \tag{88}$$

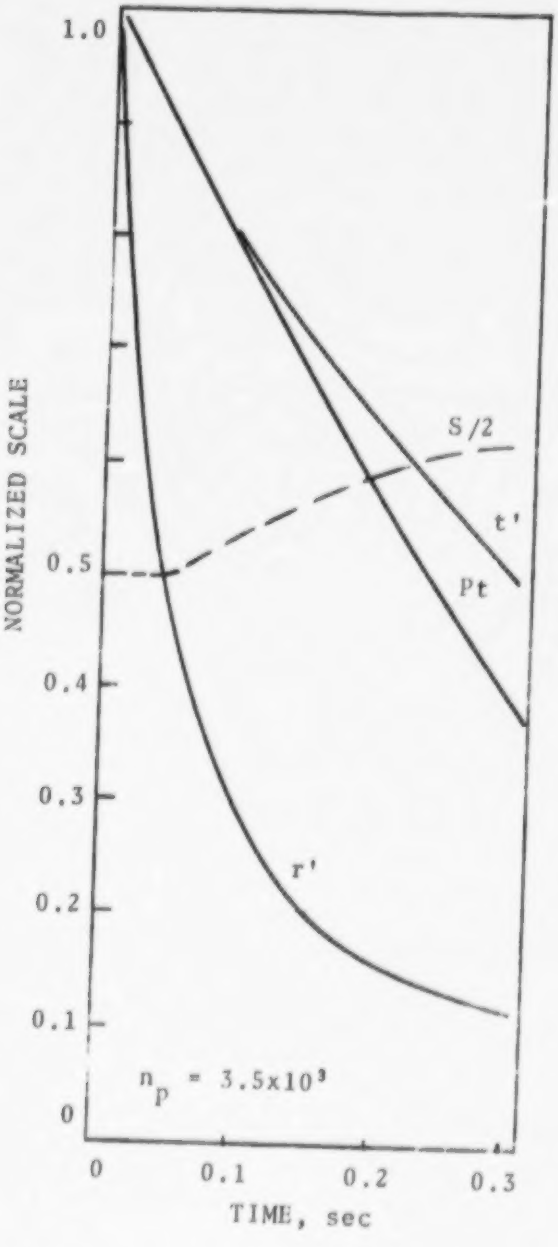

Figure 11
Computed prediction
Run #3 for sieve plate

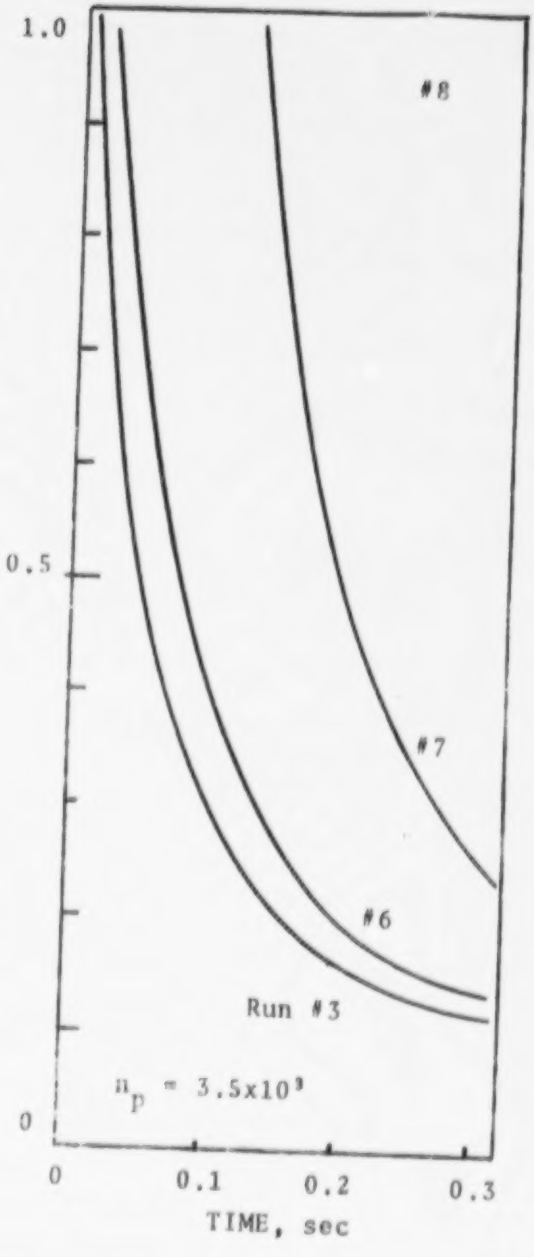

Figure 12
Prediction of effect of water vapor concentration on particle radius.

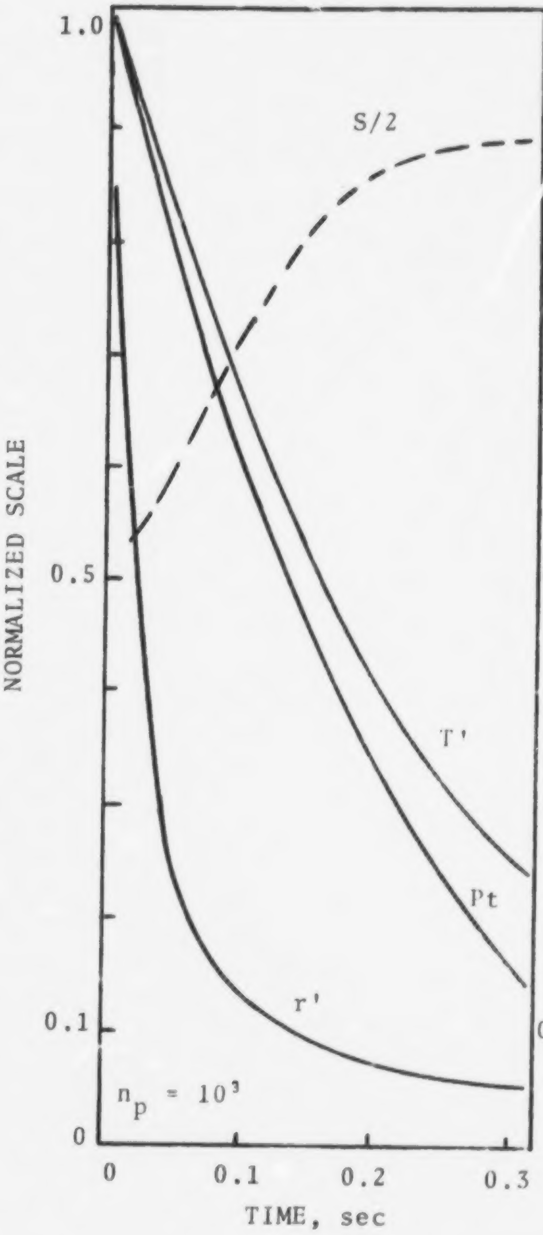

Figure 13
Computed predictions
Run # 16

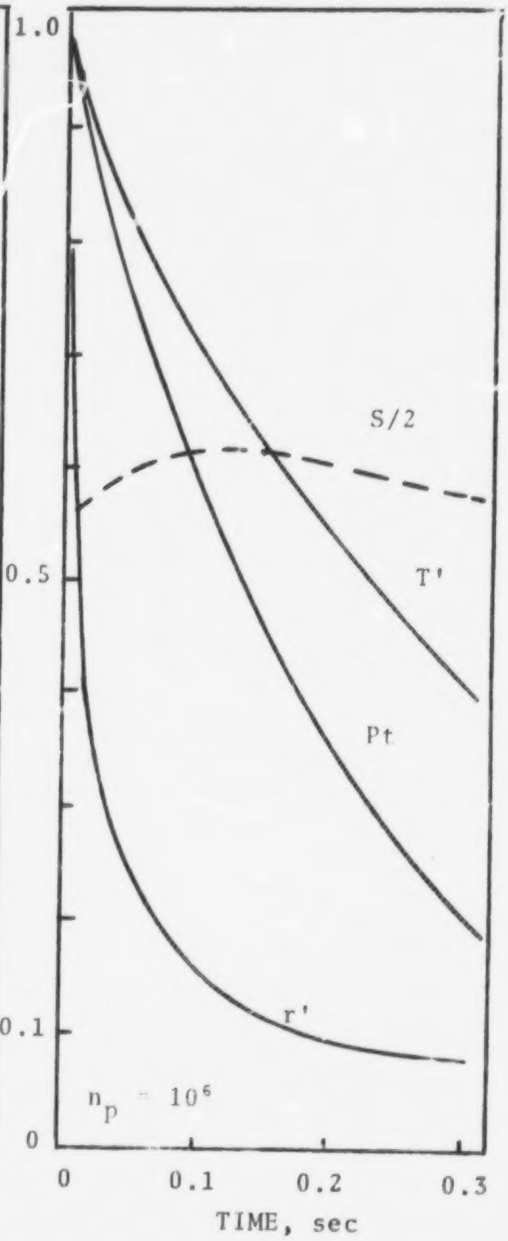

Figure 14
Computed predictions
Run # 18

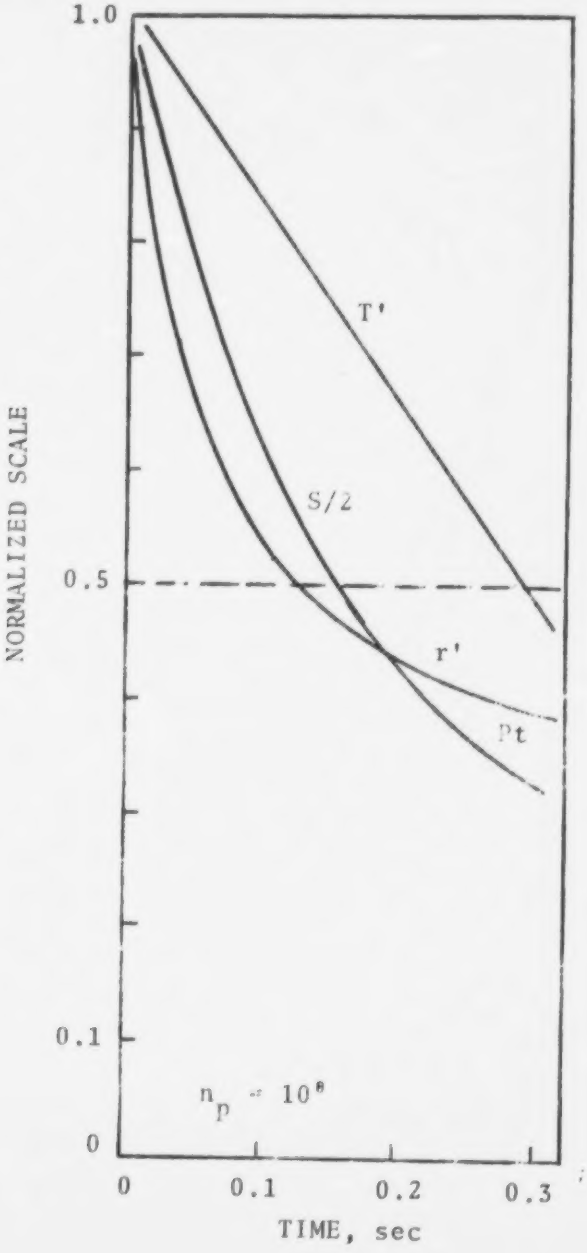

Figure 15

Computed predictions
Run #20

Table III

SUMMARY OF PLATE COMPUTATIONS WITH PENETRATION THEORY PREDICTED COEFFICIENTS

Run #	T_G °C	p_G Atm	T_L °C	Initial r_p, µm	n_p #/cm³	G gmol/cm²-sec	Final r_p, µm	Final Pt
1	30	0.093	19	0.33	3,500	0.003	4.7	0.1
2	45	0.093	19	0.33	3,500	0.003	3.0	0.38
3	45	0.093	19	0.33	3,500	0.006	2.8	0.37
4	30	0.093	19	0.33	3,500	0.006	6.6	0.09
5	45	0.093	21	0.33	3,500	0.006	2.55	0.39
6	45	0.09	21	0.33	3,500	0.006	2.35	0.43
7	45	0.08	21	0.33	3,500	0.006	1.3	0.55
8	45	0.07	21	0.33	3,500	0.006	0.36	0.62
9	45	0.03	21	0.33	3,500	0.006	0.33	0.83
10	45	0.025	21	0.33	3,500	0.006	0.33	0.85
11	45	0.093	21	0.33	3,500	0.009	2.55	0.39
12	45	0.093	19	0.33	10^5	0.006	2.55	0.38
13	30	0.093	19	0.33	10^5	0.006	4.7	0.09
14	30	0.093	19	0.33	10^6	0.006	3.3	0.23
15	45	0.08	21	0.33	10^5	0.006	1.32	0.55
16	60	0.19	20	0.25	10^3	0.003	4.2	0.13
17	60	0.19	20	0.25	10^7	0.003	1.4	0.28
18	60	0.19	20	0.25	10^6	0.003	3.1	0.19
19	60	0.19	20	0.25	10^5	0.003	4.0	0.15
20	60	0.19	20	0.25	10^8	0.003	0.68	0.31

$$T' = \frac{T_G - T_L}{T_{Go} - T_L} \quad \frac{\text{present } \Delta T}{\text{original } \Delta T} \tag{89}$$

$$Pt = n_p/n_{po} = \frac{\text{present particle conc.}}{\text{original particle conc.}} \tag{90}$$

$$r_p' = \frac{r_{po}}{r_p} = \frac{\text{original particle radius}}{\text{present particle radius}} \tag{91}$$

Figure 11 shows the predicted results for computer run #3, in which the air starts out saturated at 45°C and contacts water at a constant temperature of 19°C. The saturation ratio rises above 1.0 so there is particle growth, as shown by the curve for "r'" (which decreases as particle size increases). Particle penetration decreases almost linearly with time (or bubble rise distance), as does air temperature.

Figure 12 shows only the predicted particle time parameter for runs #3, 6, 7, and 8. It can be seen that as the initial air saturation decreases (all other factors being the same for runs #6, 7, and 8) the amount of condensation decreases. In run #8 there is a small amount of particle growth (about 5%) at the end of the 0.3 sec (corresponding to 6 cm of rise at 20 cm/sec for a 0.4 cm dia. bubble).

Figures 13, 14, and 15 show the predictions for runs 16, 18, and 20, respectively. The only output parameter changing in these runs is particle concentration, which is 10^3 particles/cm^3 for Figure 13, 10^6 for Figure 14, and 10^8 for Figure 15. One can see the effect of increasing particle concentration as it decreases the saturation ratio and particle growth, while increasing the outlet air temperature and particle penetration.

To get some perspective in accustomed engineering units, one might note that 10^6 particles/cm^3 corresponds to about 0.137 g/m^3 (0.06 grains/ft^3) if particle density is 2.0 g/cm^3 and particle diameter is 0.5 μm. This would represent a few percent of the particulate mass if the concentration from a source were 2.3 to 4.6 g/m^3 (1 or 2 grains/ft^3), so it would be on the order of a realistic fine particulate concentration. Obviously, it would be advantageous to remove as much of the larger particles as possible before raising the saturation ratio above 1.0. This last statement will be even more important for higher fine particle concentrations, such as have been reported for ferroalloy furnace emissions.

The plate scrubber model and the computation procedure described in this section proved to be of proper form to describe FF/C scrubbing to the extent that theoretical and empirical information is available. The various coefficients and quantities used may be adjusted to fit new experimental data as it becomes available. As discussed previously, the development of a useful and reliable design method is an iterative procedure which can continue to upgrade the method as well as to increase our perception of experimental reality.

MATHEMATICAL MODEL, IMPINGING JET

The approach to calculating the collection efficiency of particles from a jet impinging on a plate was similar to that taken for predicting collection efficiency by a drop. The particle trajectory was calculated from its initial conditions and the forces acting on it. In deriving the equations of motion we followed the method outlined by Mercer and Chow (1968) adding an additional term to the equation which described the flux force. To simplify the solution we assumed a constant flux force gradient in the space between the jet and the impaction plate.

A force balance leads to the following set of differential equations in dimensionless form, comparable to equations (26) and (27), where vapor gradient exists in the jet space:

$$\frac{d^2\tilde{X}}{d\tilde{t}^2} = \frac{1}{K_p}\left(\tilde{v}_X - \tilde{u}_X\right) + K_D\,\frac{dy}{d\tilde{X}} \qquad (92)$$

$$\frac{d^2\tilde{Y}}{d\tilde{t}^2} = \frac{1}{K_p}\left(\tilde{v}_Y - \tilde{u}_Y\right) - K_D\,\frac{dy}{d\tilde{Y}} \qquad (93)$$

Where

$$K_D = \frac{9\ \mu_G\ (0.85)\ D}{2\ \rho_p\ r_p^{\,2}\ u_o^{\,2}\ (1 - y)} \qquad (94)$$

The same equations will result when a thermal gradient is present, with "K_D" replaced by "K_T" and "dy" by "dT_G".

The flow field assumed by Mercer and Chow is

$$\left.\begin{aligned} \tilde{v}_X &= -\frac{\tilde{X}}{\beta} \\ \tilde{v}_Y &= \frac{\tilde{Y}}{\beta} \end{aligned}\right\} \text{ for } \left\{\begin{aligned} &-(1 + \Delta\tilde{Y}) < \tilde{Y} < (1 + \Delta\tilde{Y}) \\ &-\beta < \tilde{X} < 0 \end{aligned}\right. \qquad (95)$$

$$\tilde{v}_X = 0 \qquad \text{for} \quad \begin{cases} -(1 + \Delta\tilde{Y}) > \tilde{Y} > (1 + \Delta\tilde{Y}) \\ -\beta < \tilde{X} < 0 \end{cases}$$

The boundary conditions are:

$$\tilde{v}_X = \tilde{u}_X = 1 \text{ for } \tilde{X} = -\beta \tag{96}$$

$$\tilde{u}_Y = 0 \text{ for } \tilde{t} = 0$$

The flux force is defined by:

$$\frac{dy}{d\tilde{X}} = \text{const. and } \frac{dy}{d\tilde{Y}} = 0 \text{ for } -(1 + \Delta\tilde{Y}) < \tilde{Y} < (1 + \Delta\tilde{Y}) \tag{97}$$

$$\frac{dy}{d\tilde{X}} = \frac{dy}{d\tilde{Y}} = 0 \text{ for } -(1 + \Delta\tilde{Y}) > \tilde{Y} > (1 + \Delta\tilde{Y}) \tag{98}$$

Where

$\tilde{X} = \frac{2X}{W}$ = dimensionless distance

$\tilde{Y} = \frac{2Y}{W}$ = dimensionless distance

$\tilde{v}_x = \frac{v_x}{v_o}$ = dimensionless velocity

$\tilde{v}_y = \frac{v_y}{v_o}$ = dimensionless velocity

$\tilde{t} = \frac{2t\,u_o}{W}$ = dimensionless time

W = jet width, cm

s = distance from jet nozzle to plate, cm

$\beta = \frac{2s}{W}$ = dimensionless jet spacing

$Y = |Y_o|$, the ordinate of a given streamline
at $X = -\beta$

y = mol fraction water vapor

Note that the factor 0.85, which accounts for molecular weight gradient effect, is as discussed previously, and

$$K_T = \frac{9\ \mu_G^{\ 2}}{2\ \rho_p\ r_p^{\ 2}\ u_o^{\ 2}\ \rho_G\ T_G} \tag{99}$$

The solution to equations (92) and (93) with the boundary conditions given by equation (95) in the region $-(1 + \Delta\tilde{Y}) < \tilde{Y} < (1 + \Delta\tilde{Y})$ is:

$$\tilde{X} = \exp(-\tilde{t}/2K_p) \left\{ (K_D'-1) \cos \frac{\bar{\gamma}\tilde{t}}{2K_p} + \left[\frac{2K_p+\beta(K_D'-1)}{\tilde{\gamma}}\right] \sin \frac{\bar{\gamma}\tilde{t}}{2K_p} \right\} -k_D'\beta \tag{100}$$

$$\tilde{Y} = \hat{Y}_o\left(\frac{\varepsilon+1}{2\ \varepsilon}\right) \exp \left[\frac{(\varepsilon-1)\tilde{t}}{2K_p}\right] + Y_o\ \frac{\varepsilon-1}{2\ \varepsilon} \exp - \left[\frac{(\varepsilon+1)}{2K_p}\ \tilde{t}\right] \tag{101}$$

where $\bar{\gamma} = \left[\dfrac{4\ K_D-\beta}{\beta}\right]^{0.5}$, $\varepsilon = \left[\dfrac{\beta+4\ K_p}{\beta}\right]^{0.5}$, $K_D' = \dfrac{K_p}{K_D}\ \dfrac{d\hat{y}_v}{dX}$

Outside of this region:

$$\tilde{X} - (\tilde{X})_{1+Y_o} = K_p\left[\frac{d\tilde{X}}{dt}\right]_{(1+Y_o)} \left[1 - \exp\left(\frac{{}^{t}(1+\tilde{Y}_o)^{-t}}{K_p}\right)\right] \tag{102}$$

From these solutions target efficiency was calculated as a function of "K_p" and "β" using a digital computer. The maximum values of "K_D" and "K_T" in our range of interest were found to be between 10^{-6} and 4×10^{-3}. These calculations showed that flux forces have practically no effect on the impaction from a jet. The same results were obtained for particle growth. The reason for these results lies in the very short residence time of the particle in the collection region which is measured in 10^{-4} to 10^{-3} seconds as compared to ≈ 0.1 seconds in the bubble and ≈ 0.25 seconds in the spray column.

For impinging jets, flux force/condensation scrubbing would have its major effect where particle growth occurs prior to impingement. Thus, while negligible collection would be caused by phoretic forces, scrubbers incorporating impinging jets as a unit mechanism for particle collection are still to be considered as a possible alternative. A composite scrubber involving condensation and growth in a primary stage and impingement in a secondary stage might be desirable for some applications.

MATHEMATICAL MODEL, LIQUID SHEETS

This section describes the development of a mathematical model for particle collection by liquid sheets. Following the conceptual framework of the Scrubber Handbook, liquid sheets are the basic geometric element involved in the unit mechanism which describes collection in packed columns, wetted wall columns, wetted plates, and similar devices. Included in the treatment are the following effects:

1. Diffusiophoresis
2. Thermophoresis
3. Particle growth by condensation
4. Centrifugal deposition
5. Gravitational settling

Collection by Brownian diffusion is not included because of its small effect on particles in the size range of immediate interest. Turbulent diffusion is also not included because the gas flow in long, straight geometries (such as wetted wall columns and the like) will generally be at Reynolds numbers of only a few thousand. For systems involving short curved geometric elements (such as packed columns) the deposition is dominated by centrifugal (inertial) impaction and turbulence serves mainly to mix the particles in the gas stream.

The first model worked out is for counter-current flow in fairly straight systems such as wetted wall (cylindrical or flat plates) columns. As will be seen, the modification of a few terms can adapt the model to packed beds and similar devices where the contact or surface renewal times for gas and liquid are relatively short. A digital computer was used to solve the simultaneous differential equations for heat and mass transfer and particle growth and collection.

The accompanying sketch illustrates the geometric relationships and the flow directions. Gas enters the bottom of the column at a superficial molal flow rate (wet gas) of "G", gmol/cm²-sec, a temperature of "T_G" °K, water vapor partial pressure of "p" atm, particle concentration of "n_p" particles/cm³, and particle radius of "r_p" cm. Liquid leaves the bottom of the column at a superficial molal flow rate of "L", gmol/cm²-sec and a temperature of "T_L".

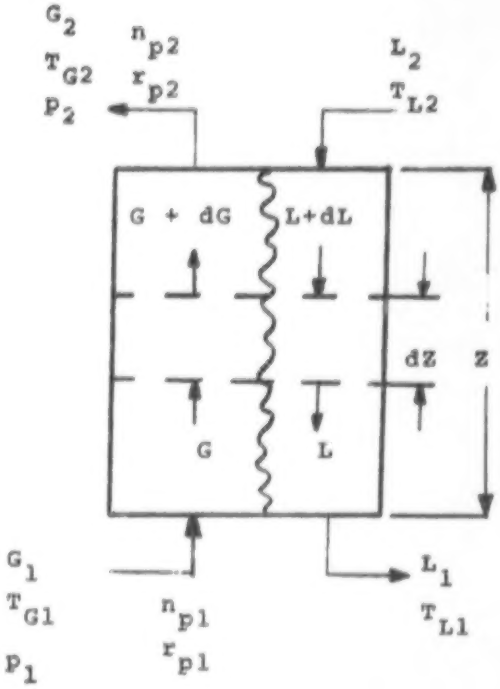

The heat balance about a differential element of the gas-liquid sheet interface is found, as for the case of bubbles, by equating the rate of latent heat evolution for condensation to the rates of heat transfer to the gas plus the rate of heat transfer to the liquid bulk. We obtain:

$$\frac{\hat{k}_G\, L_M}{k_L}\,(p_G - p_i) - \frac{h_G}{h_L}\,(T_i - T_G) - T_i + T_L = 0 \qquad (103)$$

The heat balance about the gas phase in an element of the column involves heat transfer from the liquid sheet and the particles (if there is condensation on the particles), temperature change of the particles, and temperature change of the gas. It can be shown that the product of mass times heat capacity for the particles is a very small percentage (generally less than 1%) of "m C_p" for the gas; so particle heat capacity is neglected, (i.e., the last term on the right of equation (104) is neglected).

$$h_G\ a\ (T_i - T_G)\ dZ + h_p\ a_p\ (T_p - T_G)\ n_p\ \varepsilon\ d_Z = C_p\ d(G\ T_G) + m_p\ C_{pp}\ RT\ d\ (n_p\ G\ T_p) \qquad (104)$$

where:

a = gas/liquid interfacial area per unit volume of scrubber, cm^2/cm^3

ε = volume fraction open space in scrubber

a_p = surface area of particle, cm^2

h_p = heat transfer coefficient, particle to gas cal/cm^2-sec-°K

A heat balance for liquid flowing through the differential element is formed by equating the rate of heat transfer to the temperature change of the liquid.

$$-C_{pL}\ d(L\ T_L) = h_L\ a\ (T_i - T_L)dZ\ (cal/cm^2\ col.\text{-}sec) \qquad (105)$$

The change (decrease) in liquid flow rate as one computes up the column is obtained from a mass balance in which the condensation rate equals the rate of gain (or loss) of liquid flow rate.

$$-dL = \hat{k}_G\ a\ (p_G - p_i)\ dZ\ (g\ mol/cm^2\ col.\text{-}sec) \qquad (106)$$

Note that for co-current flow the signs of equations (105) and (106) would be changed.

The change in gas flow rate is obtained from a mass balance which equates the rates of condensation on particle plus sheets to the rate of loss of water vapor from the gas phase.

$$-d(G\ p_G) = k_G\ a\ (p_G - p_i)\ dZ + k_p\ a_p\ n_p\ \varepsilon\ (p_G - p_p)\ dZ$$

$$(\text{gmol/cm}^2\ \text{col.-sec}) \qquad (107)$$

The rate of growth of particles is computed, as for the case of bubbles, by means of the following equation:

$$r_2^2 - r_1^2 = \frac{2\ D_G\ p(p_G - p_{pi})\ \Delta t}{r\ T_G\ \rho_M\ p_{BM}} \quad (\text{cm}^2) \quad (108)$$

(also 4.3.4-19 in Scrubber Handbook)

Note that equation (108) is solved for the "bulk" value of partial pressure, "p_G". It has been shown earlier in this report that growth can occur in the boundary layer even though "p_G" is below saturation. For the present, we neglect this effect.

Gas phase mass transfer coefficient is taken to be the conventional one for pipe or channel flow:

$$\frac{\hat{k}_G\ d}{D_G}\ RT_G = 0.023\ N_{Re}^{0.83}\ N_{Sc}^{0.44} \qquad (109)$$

If air and water properties are used as for the bubble case, we can reduce equation (109) to (110):

$\mu_G \simeq 6\text{x}10^{-7}\ T\ (\text{g/cm-sec - °K})\ \text{x °K}$

$\rho_G \simeq 0.34/T\ \text{g/cm}^3$

$D_G \simeq 1.2\text{x}10^{-5}\ (T)^{1.75}\ \text{cm}^2/\text{sec}$

$$\hat{k}_G \simeq \frac{0.023\ (u)^{0.83}\ (D_G)^{0.56}}{(\nu_G)^{0.4}\ d^{0.17}\ RT_G} = \frac{3.75\text{x}10^{-3}}{d^{0.17}} = \frac{G}{\varepsilon}^{0.83} \qquad (110)$$

If we assume that the gas phase heat and mass transfer coefficients can be related by means of a penetration theory model, using equal contact times for both coefficients, we find:

$$\frac{h_G}{k_G} = RT_G \frac{\rho_G \; C_{pG} \; k_G}{D_G}^{1/2} \simeq \frac{65.0}{(T_G)^{0.4}} \qquad (111)$$

where: $k_G \simeq 7.3\text{x}10^{-5}$ (cal./cm^2-sec-°K/cm)

The liquid phase heat transfer coefficient is much more difficult to pin down and, indeed, it will be greatly dependent upon the specific fluid flow system used. As an approximation of a representative situation we have taken the heat transfer coefficient predicted for a wetted wall column and adjusted it through a process of comparison with experimental mass transfer coefficients.

Upon review of the experimental data for mass transfer coefficients in wetted wall and packed columns (e.g., Norman, 1961, equation 6.34), it appears that "k_L", and therefore "h_L", for packed columns depend upon liquid rate to the 0.75 power. This reflects the influence of liquid flow rate upon the fraction of packing area which is wetted. The fraction of area wetted varies as liquid rate to the 0.25 power and the transfer rate varies as the 0.5 power, so the total influence of liquid rate depends on the 0.75 power.

For the present purpose of exploring the general characteristics of collection by sheets, we will assume that the liquid rate is high enough and the geometry such that the wetted surface area is constant. Thus an equation such as the following should describe the influence of liquid rate on transfer rate only.

$$h_L \simeq 0.5 \, (v_B)^{1/2} = 0.5 \, \left(\frac{1oL}{a}\right)^{1/2} \qquad (112)$$

where v_B = volumetric liquid flow rate per unit of sheet width, cm^3/sec-cm

Deposition Velocities

In keeping with the previous development for bubbles, the diffusiophoretic and thermophoretic deposition velocities are as given below. It will be recalled that the total particle flux can be computed from the sum of the individual deposition velocities.

$$u_{pD} \simeq 0.83\ RT_G\ \hat{k}_G\ \frac{(p_G - p_i)}{p_{BM}}\ \text{cm/sec} \tag{113}$$

$$u_{pT} \simeq 0.25\ \frac{C'\ \mu_G}{\rho_G\ T_G}\ \frac{dT_G}{dx}\ \text{cm/sec} \tag{114}$$

and, for air/water,

$$u_{pT} \simeq 6.1\text{x}10^{-3}\ C'\ T_G\ h_G\ (T_i - T_G)\ \text{cm/sec} \tag{115}$$

The centrifugal deposition velocity is given by:

$$u_{pC} \simeq \frac{2\ r_p^2\ \rho_p\ C'\ v_G^2}{9\ \mu_G\ R_c}\ (\text{cm/sec}) \tag{116}$$

and for moist air and $\rho_p = 1.0(\text{g/cm}^3)$:

$$u_{pC} \simeq \frac{3.7\text{x}10^5\ r_p^2\ C'\ v_G^2}{T_G\ R_c}\ \text{cm/sec} \tag{117}$$

In the present model we do not include this effect. For curved flows it will be used and "R_c" will be an effective radius of curvature which will depend on the specific geometry.

Gravitational settling for Stokes law is defined by:

$$u_{pG} = \frac{m_p\ C'\ \cos\alpha}{6\pi\ \mu_G\ r_p} \simeq 3.63\text{x}10^8 \left[\frac{C'\ (r_p^3 + r_o^3\ \rho_d)}{r_p\ T_G}\right] \cos\alpha \tag{118}$$

where:

m_p = mass of particle, g

r_o = the original particle radius before growth, cm

ρ_d = the difference between original particle density and density of water, g/cm³

The particle deposition velocity is:

$$u_{ps} = u_{pD} + u_{pT} + u_{pG} + u_{pC} \text{ cm/sec} \qquad (119)$$

Solution

The relationships given above have been solved by a finite difference computation on a digital computer. The results for four computer runs are shown in Table IV and Figures 16 through 19. All of these predictions were made for the case where centrifugal (inertial) and gravitational separation are not active; as would be the case for vertical plane sheets. Column height was taken as 300 cm for runs #1 and #2, and as 100 cm for runs #3 and #4. For all runs the gas flow rate was 0.006 (gmol/cm²-sec) (which corresponds to an air velocity of about 5 ft/sec, depending on temperature), the liquid rate was 0.03 (gmol/cm²-sec), the particle radius was 0.33 (μm), and the gas/liquid interfacial area was 2.0 (cm²/cm³).

The method of solution was to start from the inlet gas and outlet liquid values (i.e., from the bottom of the column) and to compute values of the variables for small increments of length until the top end of the column is reached. Figures 16 through 19 are plots of the several parameters listed below, as a function of distance up the column. Because different column lengths are used, the length coordinate is given as fraction of total length.

T_G and T_L are given in °C; on "temperature scale"

Pt = fractional penetration; on "normalized scale"

$r' = (r_o/r_p)$; on normalized scale

S/2 = 1/2 of saturation ratio; on normalized scale

It can be seen that predicted penetrations for these few conditions are fairly high. Inclusion of centrifugal deposition would give appreciable improvement in penetration because the particle size does increase quickly. This indicates that packed columns would probably be superior to wetted wall configurations. There would also be the beneficial effect on liquid phase heat transfer coefficient if packing were used.

Table IV

RESULTS OF COMPUTER PREDICTIONS OF COLLECTION BY SHEETS

	Inlet Conditions					Outlet Conditions				
Run#	T_G(°C)	T_L(°C)	p_G(atm)	n_p(#/cm³)	Z(cm)	T_G(°C)	T_L(°C)	S ratio	Pt(fr)	r_p (μm)
1	60.	34.7	0.2	3,500	300.	34.8	44.	1.0	0.84	4.54
2	45.	21.8	0.092	3,500	300.	21.9	27.	1.0	0.93	4.1
3	45.	22.5	0.092	3,500	100.	26.1	27.	1.04	0.94	3.96
4	45.	22.4	0.092	10^6	100.	26.4	27.	1.0	0.935	0.85

Note: The above results were computed for the case of vertical, counter-current flow of air and water with no centrifugal deposition. Other common conditions for all runs are as follows:

G = 0.006 (gmol/cm²-sec)
L = 0.03 (gmol/cm²-sec)
r_p = 0.33 (μm)
a = 2.0 (cm² contact area/cm³ column vol.)
S_c = critical saturation ratio for condensation = 1.0

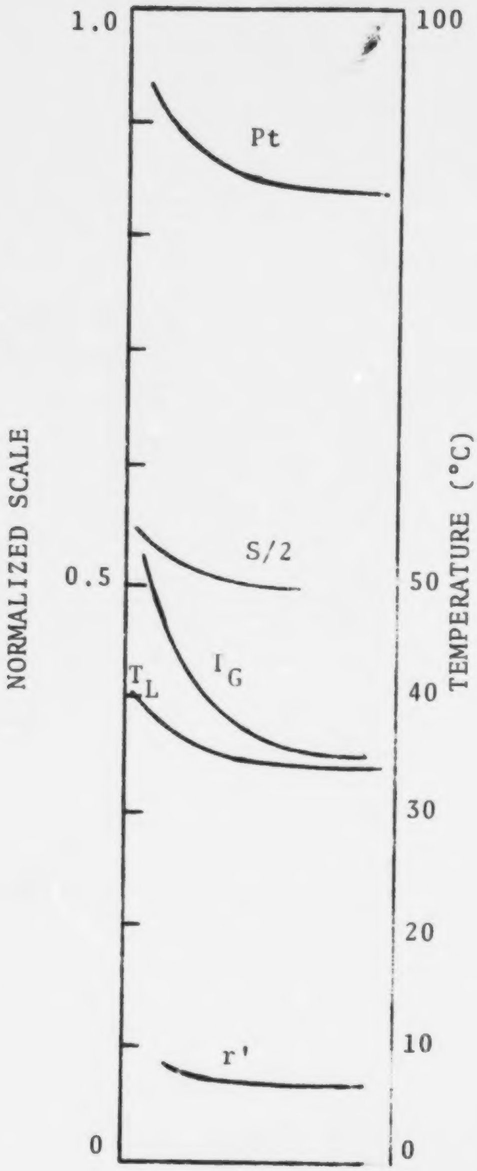

Figure 16

Computed predictions
for sheets, Run #1

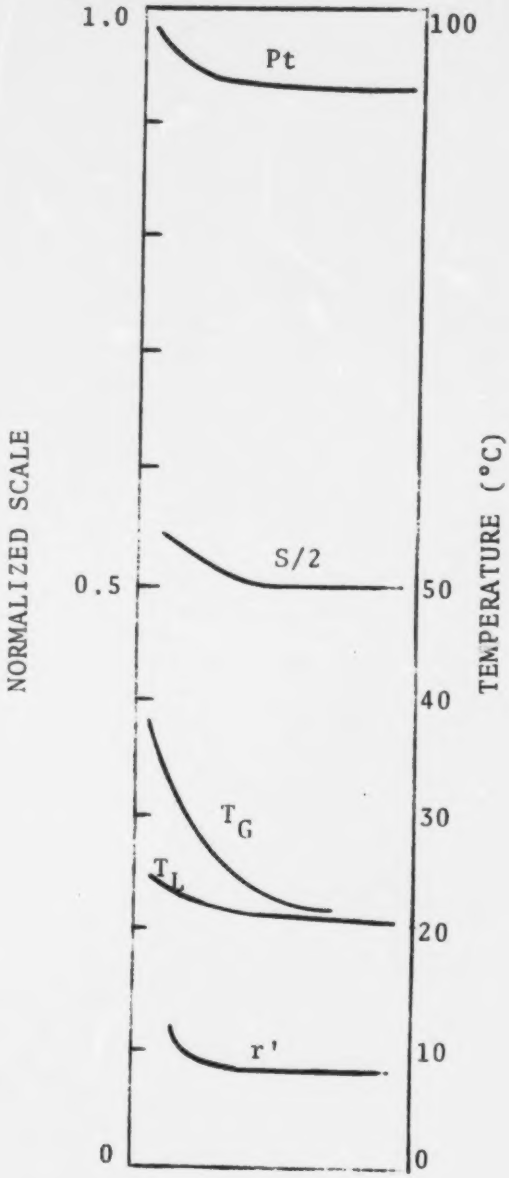

Figure 17

Computed prediction
for sheets, Run #2

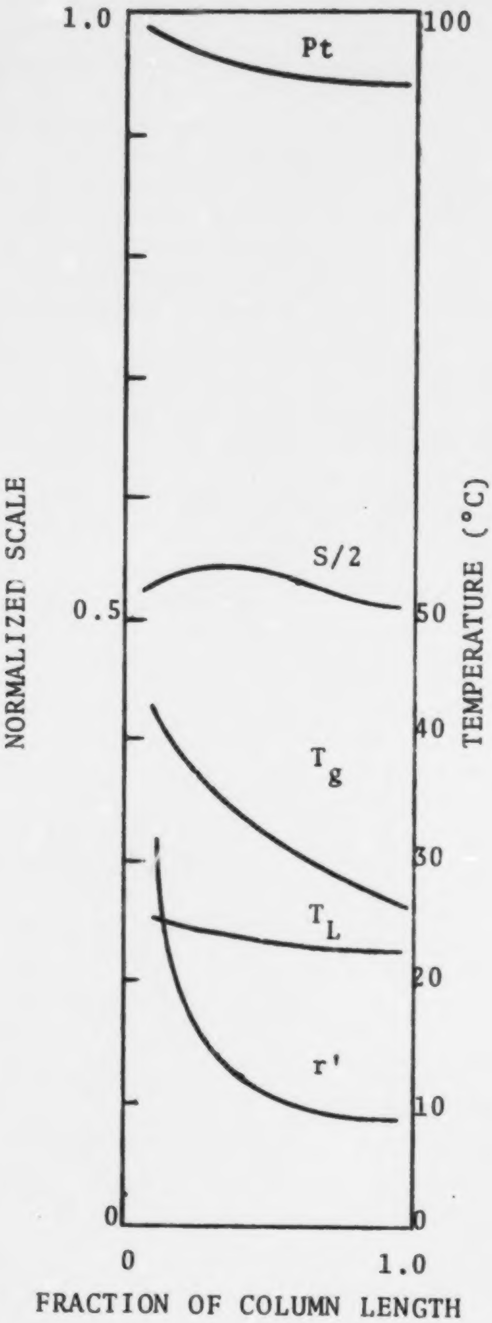

Figure 18
Computed prediction
for sheets, Run #3

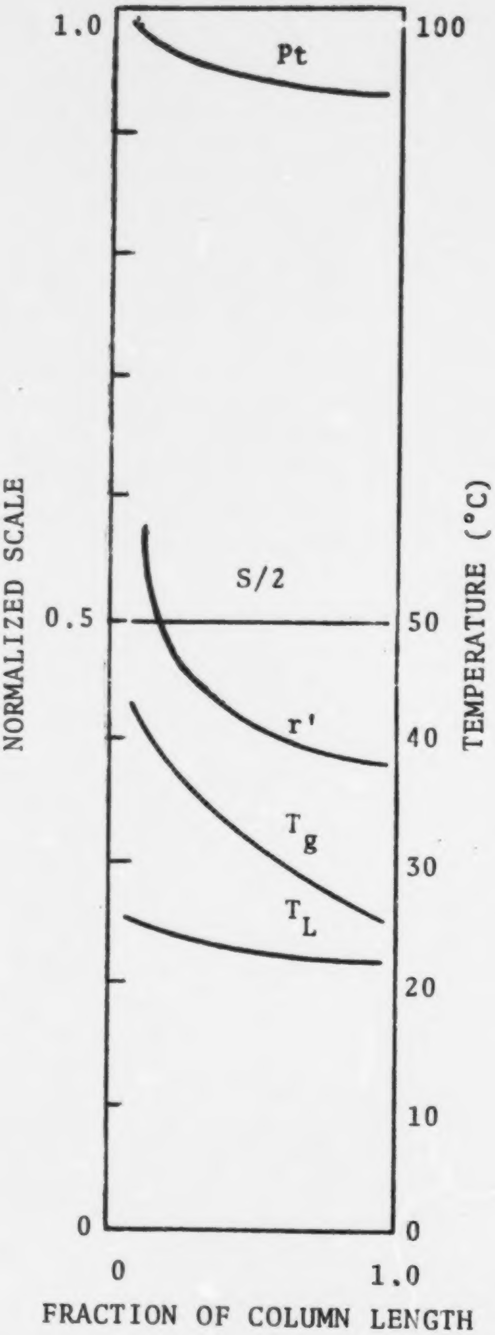

Figure 19
Computed prediction
for sheets, Run #4

As in the case of transfer from bubbles, the effect of high particle concentration (see run #4, Figure 19) is to reduce the water vapor concentration so that diffusiophoretic velocity is lower and particle growth is less than for low particle concentrations. If condensation did not occur on the particles because the critical saturation ratio were not reached, the water vapor concentration would not be depleted and, therefore, the diffusiophoretic velocity would not be dependent on particle concentration.

When condensation does occur, as in the examples shown in Table IV, the particle size may increase sufficiently that collection efficiency by inertial impaction can become significant. In run #4 the particles grew to 1.7 μm diameter even though the inlet concentration was $10^6/cm^3$. Particles this size can be collected at moderate pressure drop.

EXPERIMENTAL

Theoretical considerations had indicated that plate-type scrubbers should be good for FF/C scrubbing on the basis of their assumed heat and mass transfer characteristics. It was also clear that the transfer coefficients were very important in determining particle collection efficiency, so it was important to verify them by experimental measurements. Thus, the kind of experiment needed to provide the crucial test of the preliminary theoretical analysis was defined.

In this section of the report we will describe:

1. Details of the experimental apparatus
2. Experimental procedure
3. Analytical methods
4. Computational methods
5. Results
6. Comparison of experimental results with predictions.

EXPERIMENTAL APPARATUS

A schematic flow diagram of the experimental apparatus is shown in Figure 20. The major components were as follows:

Test Section: The test section consisted of a 10.2 cm diameter glass column. A sieve-plate was installed in it, as the first configuration to be studied for FF/C effects scrubbing.

The plate was made out of 1.6 mm aluminum sheet and had an overall diameter of 10.2 cm. It had 30 perforations of 4.8 mm diameter, adding up to 6.6% free area on the plate. It had two straight weirs, 8.1 cm long and 9.5 mm high, for the liquid inlet and outlet on the plate. As the plate was to be used to study FF/C effects scrubbing, the additional design criteria used were:

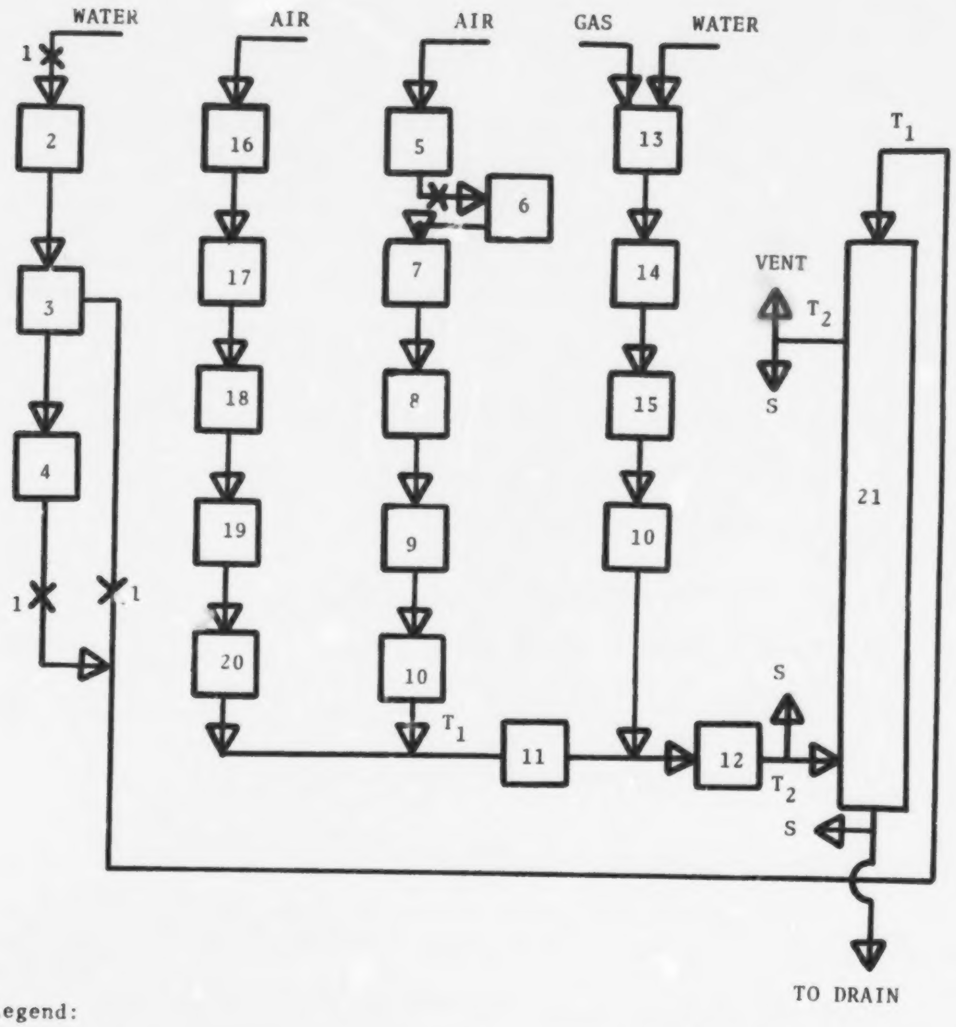
WATER
AIR
AIR
GAS
WATER
1
2
3
4
1
1
16
17
18
19
20
5
6
7
8
9
10
13
14
15
10
T1
VENT
T2
S
21
S
T1
11
12
T2
S
TO DRAIN

Legend:

1. Valves
2. Pressure Regulator
3. Rotameters
4. Water Cooler
5. Air Prefilter
6. Air Blower
7. Air Cooler
8. Venturi-meter
9. Air Heater
10. "Absolute" Filters
11. Particle Charge Neutralizer
12. Gas Mixing Section
13. Boiler
14. Steam Entrainment Separator
15. Pressure Indicator
16. Air Filter
17. Pressure Indicator
18. Collison Atomizer
19. Impactor
20. Evaporation-Condensation Columns
21. Sieve-plate Scrubber

Figure 20 - Experimental apparatus

1. Very low weir height. Since the major portion of the collection is expected to take place during a bubble rise of a few bubble diameters, a large foam height is not needed.

2. Large perforation diameter and low gas velocity in the perforations, since it was desired for experimental purposes to maintain a low collection efficiency during bubble formation.

3. Large weir length, since it will ensure good liquid distribution and thus a constant liquid temperature on the plate.

The operating characteristics of the plate are shown in Figure 21.

The water was introduced from the top to the sieve-plate behind the inlet weir, through a downcomer tube. An outlet downcomer tube located behind the outlet weir removed the water from the plate. A sampling valve was provided in the outlet water flow. The flow rate of water through the test section was measured by a set of rotameters on the inlet line. Water temperature was maintained by distributing the inlet water flow between a cooler and a bypass line before it was introduced in the test section. The inlet and outlet water temperatures were measured by iron-constantan thermocouples located in the respective downcomers.

The air stream, under controlled conditions of temperature, humidity and particle concentration flowed upwards through the perforations in the sieve-plate. The inlet and outlet temperature and humidity were measured by wet and dry bulb thermometers located in the respective lines. Sampling probes for particle concentration and size distribution measurements, together with static pressure taps for measuring the pressure drops, were also provided in the air lines at the inlet and outlet to the test section. A variable height probe was provided in the test section. It could be adjusted to obtain air samples and static pressure readings within the test section, at any height over the sieve-plate. Ample height was provided over the sieve-plate in the test section, to prevent entrainment of water drops in the outlet air stream.

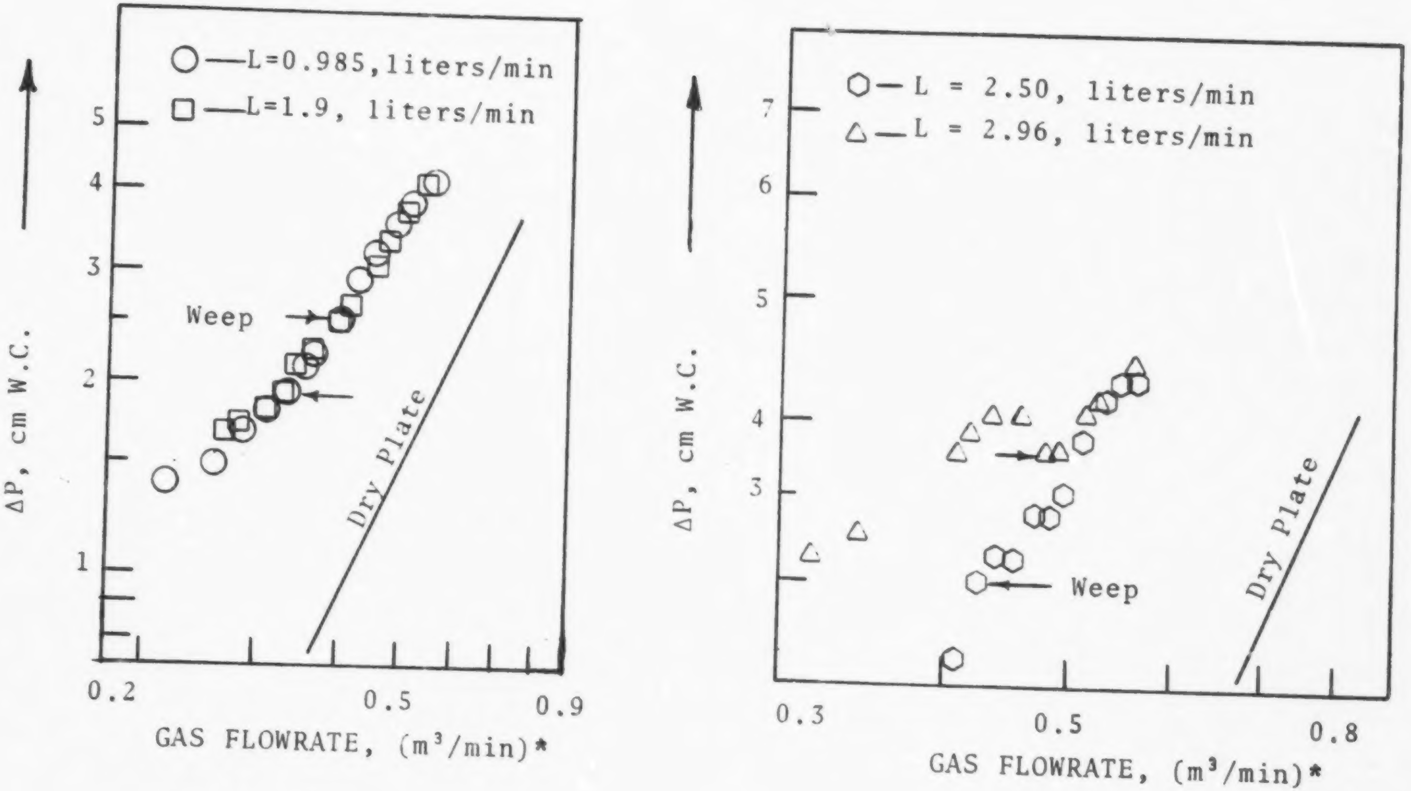

*@ 20°C, 1 atm

Figure 21 - Operating characteristics of the sieve plate.

Air Flow System

A 1/2 HP Rotron "Cyclonair" blower supplied the air flow, which was prefiltered. The air flow-rate was measured by a calibrated venturi meter. A finned-tube heat exchanger in the air line, cooled the air flow by means of ice water to 18°C and a heater using three electrical elements could heat the air if desired. The air was then passed through an "Ultra Aire" absolute filter made by Mine Safety Appliances Company. The filter is rated at 99.97% efficiency of retention for 0.3 μm particles by the manufacturer, and was regularly checked by measuring the particle concentration in the filtered air.

A controlled flow of aerosol from the particle generator was introduced into the air stream. The air stream then passed through a charge-neutralizer utilizing ten Polonium 210 elements, with radioactivity of 500 μc each, mounted on the wall of a 76.2 cm section of 3.8 cm diameter glass pipe. At the maximum air flow-rate of 0.71 (m^3/min) with particle concentration of 10^6 particles/cm^3, the residence time of 0.1 sec in the charge neutralizer is considered sufficient, due to the high energy of disintegration (5.4 Mev) for the Po^{210} alpha particles.

A controlled quantity of steam was then added to the air stream to obtain the desired moisture content in the air. The steam passed through an entrainment separator column packed with bronze wool, and then through an absolute filter similar to the filter used in the air line, before it was introduced into the air stream. The humidified aerosol then entered the sieve-plate column following a mixing section.

Particle Generator

The major components of the particle generator assembly were: (1) a 3-orifice Collison atomizer (CA). (2) an impactor with a cut-off diameter of 2 μm, and (3) an evaporation-condensation (E-C) aerosol generator. The particle generator set-up is shown in Figure 22.

Dibutyl-phthalate (DBP), with 0.01% by weight of anthracene as nucleating agent, was used as aerosol material in the CA. Filtered air at 40 psig was fed to the CA for generating a DBP spray. Particles larger than 2 μm diameter

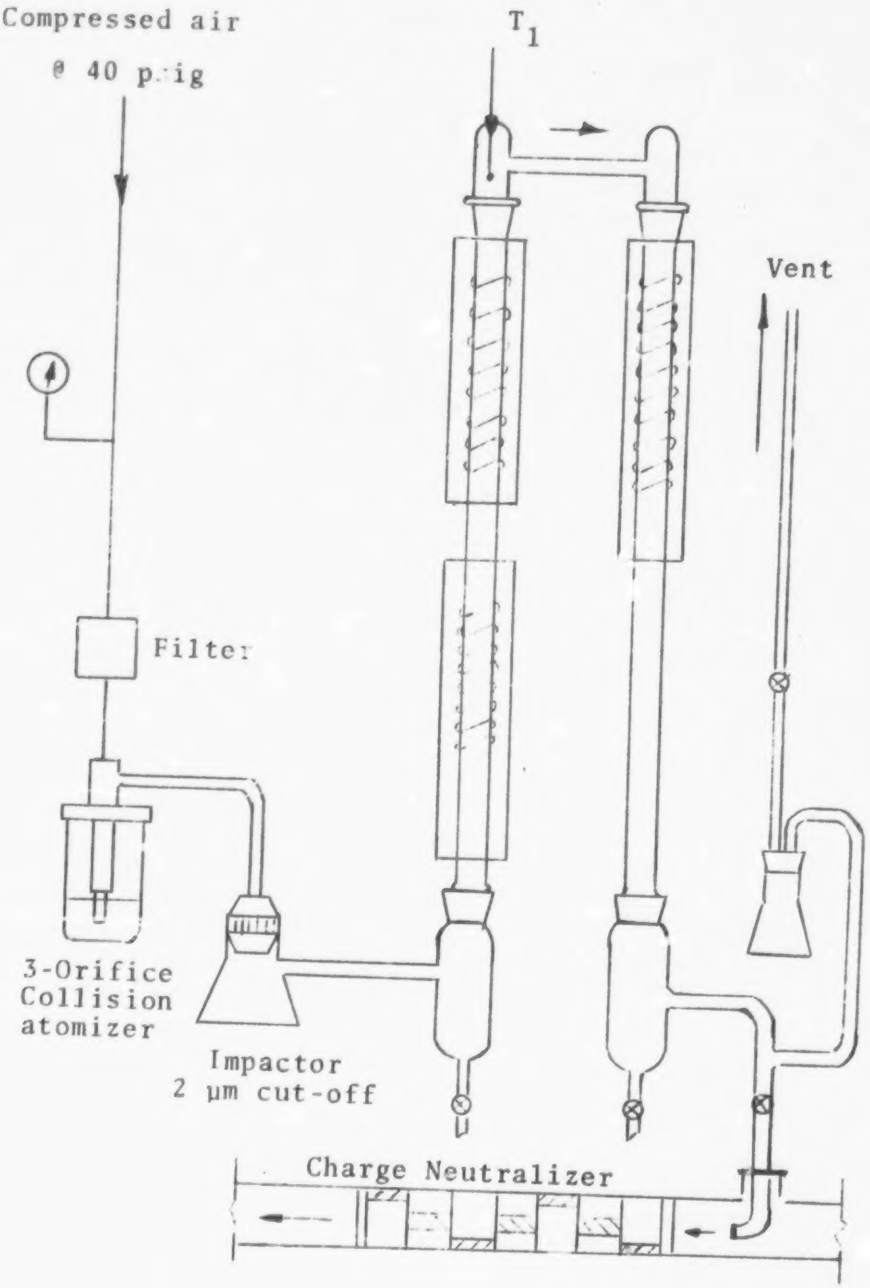
Compressed air
@ 40 psig
T$_1$
Vent
Filter
3-Orifice
Collision
atomizer
Impactor
2 μm cut-off
Charge Neutralizer

Figure 22 - Particle generator assembly

were then removed by the impactor following the CA.

The particles then entered the bottom of the first E-C column, a 2.54 cm O.D. glass tube, 94 cm long with heating tapes wrapped around the tube at top and bottom to serve as evaporation zones. Axial baffles were provided near the entrance to the tube to promote mixing and better heat transfer area in the first evaporating zone. The particles then flowed into the top of the second E-C column. The upper section of the column was a 48 cm long, 2.2 cm O.D. Vigeraux column and the lower section was plain pyrex tubing 30.5 cm long and 2.2 cm O.D. The second E-C column had one evaporation zone located at the top near the entrance to the column.

The particle characteristics were studied for various values of voltages applied to the three heating tapes and various pressures in the compressed air line. The values of 40 psig pressure in the air line and 65V applied to each of the heating tapes were found to give particles with a mass mean diameter, $d_{pg} = 0.7$ μm and a geometric standard deviation, $\sigma_g = 1.215$, measured by the eight stage, non-viable Anderson sampler. As this aerosol was suitable for our purposes, the particle generator was routinely operated at these settings.

Particulate Sampling System

This system consisted of three major components:

(1) Filter sampling system to measure the particle concentration in the inlet and outlet air streams.

(2) The Climet CI-201 particle analyzer to measure the particle concentration and size distribution in the inlet and outlet air streams, and

(3) The eight stage, non-viable Anderson sampler to measure the particle size distribution in the inlet and outlet air streams.

Both the inlet and outlet sampling lines consisted of insulated 6.4 mm aluminum tubing. The sampling probes were located near the center of the air pipes, bent to face the air stream in the direction of flow. Since the particle sizes in the air stream were small (d_{pg} = 0.7 μm, σ_g = 1.215), no consideration need be given for isokinetic sampling. Two lines were drawn from each of the sampling probes, one going to the Climet particle analyzer and the other to the Anderson sampler and the filter sampling systems. The sampling system was so designed, as to keep the sampling lines as short as possible. A schematic diagram of the sampling system is shown in Figure 23.

EXPERIMENTAL PROCEDURE

The experiment was started by bringing the particle generator to the operating conditions. When an aerosol stream containing particles in the range of $0.4\ \mu m \leq d_p \leq 2 \mu m$ is illuminated by a beam of white light, the light scattering by the particles produce angular spectra, known as the higher-order Tyndall spectra. The spectra exhibits different colors depending on the angle of observation. The saturation and brightness of the colors increase with uniformity of particle size. This phenomenon was used to determine whether the particle generator was producing nearly monodisperse aerosol. After an iron-constantan thermocouple located in the E-C column indicated that the temperature had reached a steady state, the aerosol was observed with forward-scattered light from a flashlight until a bright orange color was seen due to the higher order Tyndall Spectra. This normally took 10 to 15 minutes and indicated that the generator was ready.

Before the particles were introduced into the air stream, the air and water flow-rates were brought to the operating values. When a saturated or unsaturated air flow was desired, the temperature of the air was set by either operating the heater or the cooler, the particle concentration was measured in the filtered air using the particle analyzer and then steam was added to reach the operating values of temperature and humidity. Supersaturated air flow was attained by first adding the required amount of steam into heated air flow so that the gas remained unsaturated. The heat was then gradually reduced to reach the desired values of temperature and supersaturation in gas.

After the steady state was reached, which took from thirty to sixty minutes, the flow-rate conditions, foam height, pressure drop across the plate, the inlet and outlet air wet and dry bulb temperatures and the water inlet and outlet temperatures were noted. When the air was

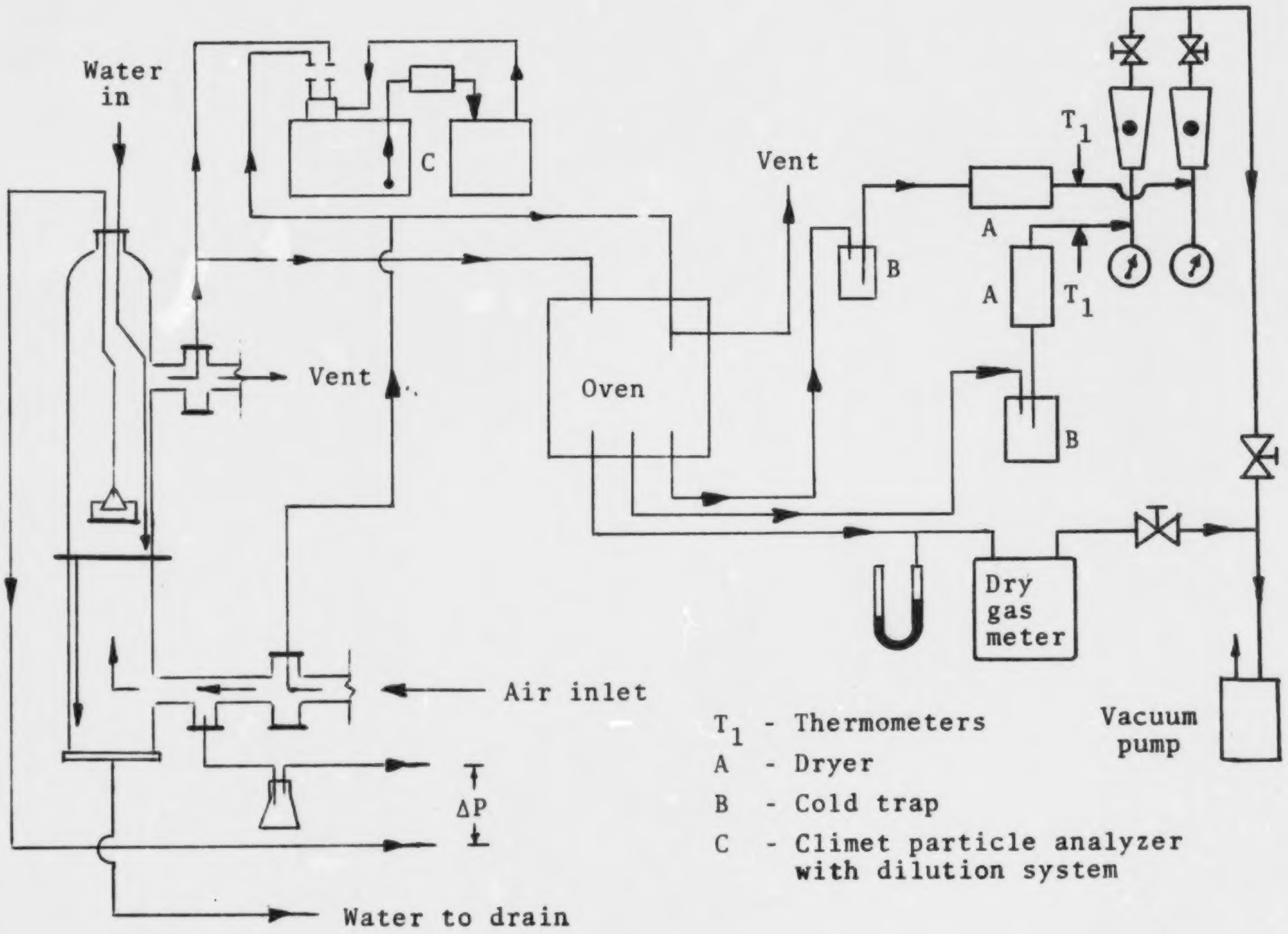
Water in
C
Vent
Vent
Oven
B
A
A
B
T1
T1
Dry gas meter
Air inlet
ΔP
Water to drain
Vacuum pump
T1 - Thermometers
A - Dryer
B - Cold trap
C - Climet particle analyzer with dilution system

Figure 23 - Sampling system.

supersaturated, a sample was drawn from the air line and heated to determine the humidity with wet and dry bulb thermometers. This enabled the determination of the amount of steam lost due to condensation on the walls when the air temperature was reduced.

The particles were then introduced into the air stream. The particle concentration was controlled to obtain approximately 5 mg of sample on the outlet filter in 30 minutes. In the meantime, the Anderson sampler and the filters were prepared and heated in the oven to the inlet gas temperature. The sample lines were heated by drawing air through them. The filter holders were then connected in the respective lines and the sampling lines were checked for possible leakage.

. The inlet and outlet filter sampling was started. The sampling time was approximately 30 minutes and the flow rate was approximately 5.1 litres/min (@ 20°C, 1 atm). All the operating conditions were rechecked while the filter sampling was going on.

Upon completion of the filter sampling, sampling for the particle size distribution in the inlet gas was started using the Anderson sampler. Again, the same precautions were taken against condensation and leakages in the sampling lines as taken earlier for filter sampling. The sampling time was approximately 45 minutes and the flow rate 28.3 (litres/min).

After the sampling using the Anderson sampler was completed, the particle size distribution and concentration in the inlet and outlet air lines were measured using the particle analyzer. This was done by connecting the sampling lines to the particle analyzer and reading the particle concentrations for successively larger particle sizes, using the potentiometer connected to the analyzer.

The inlet valve from the particle generator to the air line was then shut off. The experimental conditions of gas flow rate, etc. were then recorded without the particles, as done earlier, prior to the introduction of the particles.

The filter papers and the Anderson sampler plates were weighed immediately upon the completion of sampling on an analytical balance (Sartorius Model 2443; ±0.05 mg precision).

These were then left to dry in a desiccator and reweighed after at least 20 hours. At this point the run is completed.

The experimental conditions were found to stay very stable, once the steady state was reached. The conditions were checked at the start of each sampling run for the filter sample and the Anderson Sampler. They were rechecked at least once while the sampling was going on and then again at the end of the sampling run. The water and steam flow-rates were significantly affected by variations in the inlet pressures. Pressure regulators and throttle valves on these lines enabled the maintenance of constant flow-rates. The particle generator had been repeatedly tested for consistency in particle size distribution and particle concentration in its output over a period of time. These parameters were found to remain significantly constant at least for a period of up to four hours. For all the experimental runs reported, the temperature conditions for the experiment varied within ±0.5°C during the experimental period.

METHODS OF ANALYSIS AND CALCULATION

As mentioned previously, three sampling methods were used to determine the particle concentration and size distribution. These were: (a) filter sampling, (b) Climet CI-201 particle analyzer and (c) Anderson sampler. Details of each of these methods are given below.

(a) Filter Sampling

47 mm glass fibre filter papers (Type E, made by Gelman Instruments Company) were used in the filter sampling system. The sampling flow-rates were measured by rotameters on each line and were controlled by needle valves. Upstream from the rotameter the line pressures were measured by Dwyer "Magnehelic" pressure gauges and the temperature by iron-constantan thermocouples. Cold traps and dryers were used in the sampling lines to prevent condensation in the rotameters.

The DBP used to generate aerosol was rated by the manufacturer to have a boiling point of 172°C-174°C @ 5mm of Hg. A substantial change in the particle concentration was observed when the gas temperature was changed. This is attributed to the evaporation of some of the aerosol material, DBP. It was decided to maintain the inlet gas temperature below 50°C in order to keep the fraction of DBP in the vapor phase at a low, controllable level. Also, the temperature of both the inlet and outlet filter holders were maintained at the inlet gas temperature, by placing them in an oven. This eliminated any biased effect of gas temperature (due to vaporization) on the particle concentration during the sampling. The inlet and outlet filter sampling were done simultaneously under identical conditions.

The particle mass concentration was calculated as:

$$c_p = \frac{\text{(weight gain on the filter, at inlet gas temperature)}}{\text{(sampling flow-rate, Std. conditions)} \times \text{(sampling time)}} \quad (g/cm^3)$$

where, c_p = particle mass concentration. Note that the particle mass concentration can change with the gas temperature due to the evaporation loss of DBP. The concentration expressed here is at the inlet gas temperature.

The overall penetration (Pt) in the test section was calculated as:

$$Pt = \frac{c_{po}}{c_{pi}}$$

where "c_{po}" and "c_{pi}" are calculated for the same conditions of temperature and pressure.

As the inlet and outlet filter samples were collected with the sample gas heated to the inlet gas temperature in both the lines, and as the line pressures in both the lines were almost same, the maximum difference being less than 12 cm W.G.; "Pt" can be expressed as:

$$Pt = \frac{\text{weight gain on the outlet filter}}{\text{weight gain on the inlet filter}} \qquad (120)$$

At least two samples were taken for each set of conditions to test for reproducibility.

(b) Climet CI-201 Particle Analyzer

The Climet CI-201 particle analyzer operates on the total light-scattering principle, which permits direct characterization of the particles as to their size distribution and concentration. The instrument measures the particle concentrations in the range from 3.5×10^4 to 3.5×10^9 particles/m^3 with the help of the 100/1 dilution system (Model 0294-1). It was modified with a potentiometer so that the counting size threshold could be varied continuously in the range from 0.3 μm to 3 μm diameter instead of being restricted to several fixed sizes. A dryer was placed in the line connecting the particle analyzer to the diluter system to prevent condensation in the optical sensor.

To determine the particle number concentration (n_p, #/cm^3), the potentiometer and the particle size selector switch were set to read the concentration of particles greater than 0.3 μm diameter. Because particle size distribution measured with the Anderson sampler had shown that 100% particles were >0.3 μm, this setting on the instrument indicated the total number of particles per unit sample volume. The inlet and outlet sample lines were connected, in turn, to the instrument and the concentrations were read off the dial.

To determine the particle size distribution, the sample line was connected to the instrument and the potentiometer was set at successively larger values of particle diameters. From these data, the geometric standard deviation (σ_g) and the number mean diameter (d_{pn}) were determined.

(c) The Anderson Sampler

The Anderson Sampler is an eight-stage cascade impactor. The perforations in each stage are designed to provide successively smaller cut-off diameters. Thus, when an aerosol is passed through it, successively smaller diameter particles are collected on the stages and the particle size distribution is determined on a weight basis, by measuring the weight gain on each stage. The cut-off diameters depend on the flow rate through the sampler and a preliminary check of the manufacturer's rated values using an optical microscope was found to be approximately correct. An absolute filter was used after the final stage of the sampler to capture all the particles that escape collection in the sampler.

The flow rate through the sampler was maintained at approximately 28.3 (liters/min) and measured by a calibrated dry gas meter. The sample flow line pressure was measured by a mercury U-tube manometer and the line temperature was measured by an iron-constantan thermocouple before it entered the dry gas meter. As with the filter sampling system, the temperature of the Anderson sampler was maintained at the inlet gas temperature in the oven.

The plates were weighed before and immediately after the sampling, and again after they were dried in a desiccator for over 20 hours, on the Sartorius analytical balance. They were then washed with soap and rinsed successively with de-mineralized water, ethanol and acetone. Then they were placed back in the sampler and the sampler sealed off until the next run.

The geometric standard deviation (σ_g) and the mass mean diameter (d_{pg}) of the aerosol were determined from the weight of particles collected on the plates in different stages with known cut-off diameters The particle mass concentration was also determined as:

$$c_p = \frac{\text{(weight gain on sampler and filter, at inlet gas temp.)}}{\text{(sampling flow-rate, std. conditions)} \times \text{(sampling time)}} \quad (\text{g/cm}^3)$$

This value was then checked against the value determined from filter sampling.

Air Supersaturation

A direct determination of the saturation ratio (S) using the wet and dry bulb thermometers is not possible when the air is supersaturated. Since it was desired to obtain data for different values of $T_{di} < 50°C$, the inlet air was cooled prior to the introduction of steam. When steam was introduced in the air flow, it was found that a part of it condensed in the line. Assuming that the air line was well insulated and there was no heat loss through the pipe, we calculated "S" in the following way:

(a) The air was heated to a temperature higher than T_{di} and steam was introduced at a rate such that the desired $\hat{y}$ was attained, under unsaturated conditions.

(b) The heaters were turned off and the air temperature was allowed to reach a lower steady state value, T_{ds}, keeping the same rate of introduction of steam as in (a).

(c) The mole ratio, and hence S, were calculated from an enthalpy balance. First, the increase in air temperature due to the sensible heat of steam was calculated and then the amount of steam condensed in step (b) was determined. Thus, the partial pressure of vapor, p_G, was determined and S was calculated from:

$$S = \frac{p_G}{\text{Saturated vapor pressure at } T_{ds}}$$

Transfer Coefficients

The transfer coefficients needed for predicting theoretical values of penetration at the experimental conditions are: h_L, k_G, and h_G. The values of these transfer coefficients were determined individually for each run.

The conditions for the gas and liquid flow rates, temperatures and moisture contents were such that the net heat and mass transfer were always from the gas phase to the liquid phase. Under such conditions, the transfer coefficients can be determined using Mickley's method, described by A. S. Foust et al. (1960) and many others. However, the conventional graphical approach is not sufficiently accurate due to the curvature in the enthalpy-temperature saturation curve in this range of gas and liquid conditions.

A computer program was developed to evaluate coefficients for the experimental runs. The approach used was essentially the same as the Mickley's method, except that heat and mass transfer in the gas-phase were used separately instead of being combined into gas-phase enthalpy transfer.

Also, instead of setting the Lewis number;

$$N_{Le} = \frac{k'_{bG}\ \hat{C}_{pm}}{h_{bG}}$$

equal to one, which is not valid when the water vapor concentration is high, the ratio k'_{bG}/h_{bG} was assumed to remain constant for a run. This ratio was calculated from the penetration theory correlation,

$$\frac{\hat{k}_{bG}}{h_{bG}} = \frac{1}{R\ T_G}\left(\frac{D_G}{\rho_G\ C_{pG}\ k_G}\right)^{1/2} \qquad (121)$$

where, k_G = thermal conductivity of gas, $\left(\frac{\text{cal}}{\text{sec-cm-°K}}\right)$

For the experimental conditions, this ratio changes by a maximum of 5.26% (from 0.144 to 0.152 for Run No.'s 7 and 8) for the inlet and exit conditions respectively. Thus, an average value can be used for the ratio during a run, without appreciable error.

After the value of k'_G/h_L is determined from the method discussed above, h_L is computed from a heat balance on the liquid bulk. "k'_{bG}" and "h_{bG}" were then determined from the values of h_L, k'_{bG}/h_L, and k'_{bG}/h'_{bG}.

This approach incorporates the following assumptions:

1. The gas bubbles are spherical and are of a constant diameter throughout the foam.
2. The bubbles are perfectly mixed internally.
3. The foam density is constant throughout the foam layer on the plate.
4. The liquid bulk temperature is constant throughout the foam, and is taken as the average temperature between the liquid inlet and outlet stream.
5. All of the bubble surface area is available for transfer mechanisms and this area lends itself equally for both, heat and mass transfer.
6. The penetration theory adequately predicts the ratio of the gas-phase mass transfer coefficient to the heat transfer coefficient.

Note that the ratio is independent of the surface renewal time.

Accuracy of Measurements

1. Determining Overall Penetration:

The overall penetration, $\overline{Pt}$ was determined as:

$$\overline{Pt} = \frac{\text{weight gain on the outlet filter}}{\text{weight gain on the inlet filter}} \qquad (122)$$

The analytical balance used has a precision of ±0.05 mg.

$$\overline{Pt} = \frac{W_o}{W_i}$$

where, W is the weight gain on the filter.

$$\frac{d\,\overline{Pt}}{\overline{Pt}} = \frac{d\,W_o}{W_o} - \frac{d\,W_i}{W_i}$$

As the absolute values for the error are small compared to the actual weights, we can say that,

$$\frac{\Delta\,\overline{Pt}}{\overline{Pt}} = \frac{\Delta\,W_o}{W_o} - \frac{\Delta\,W_i}{W_i}$$

For calculating maximum error, the error terms are considered to be additive. Thus,

Maximum error, $\overline{Pt} = \dfrac{\Delta\,W_o}{W_o} + \dfrac{\Delta\,W_i}{W_i}$

The precision of the balance is ±0.05 mg.

the maximum values for $\Delta\,W_o = \Delta\,W_i = 0.1$ mg.

Minimum values for $W_o = W_i = 5$ mg.

Maximum error, $\overline{Pt} = \pm\,\dfrac{0.2}{5} = \pm 4\%$.

In the range of experimental conditions, the maximum error in determining $\overline{Pt}$ is ±4%.

2. Determining Particle Characteristics:

The particle characteristics determined were: (a) particle concentration. (b) particle size distribution.

(a) The particle concentrations were measured from the weight gain during filter sampling. The analytical balance used to weigh the filter paper had a precision of ±0.05 mg. Most runs lasted 30 minutes out of which the end effects did not take more than 0.08 minutes, or 0.27% of the sampling time. The rotameters are rated for accuracy in flow measurement at ±5% the maximum error expected in determining the particle mass concentration is ±12.27% for a 5.0 mg sample on the filter.

(b) During the experimentation, the size distribution measured was; $d_{pg} = 0.7$ μm, $\sigma_g = 1.22$ by the Anderson sampler. An analysis of the Anderson sampler performance for determining size distribution of nearly monodisperse aerosols has shown that the "σ_g" value indicated by the sampler would be higher than the actual "σ_g" of the aerosol. The actual "σ_g" value es expected to be between 1.0 and 1.22.

Particle size data taken with the Climet instrument are not included in this report because they were not sufficiently reproducible. Operating problems with the counter and the sample dilution apparatus required that the instrument be sent back to the manufacturer several times for repairs. During the time the instrument was operable the data obtained were not consistent. Therefore, major reliance had to be placed on sizing with the cascade impactor.

3. Air Flow Rate:

The air flow rate was determined by a venturi-meter. The venturi-meter was calibrated using a pitot tube. The maximum error in the flow rate calibration is expected to be ±5% as rated by the manufacturer.

4. Water Flow Rate:

The water flow rate was measured by rotameters in the line. These were calibrated in the laboratory and the maximum error is expected to be 1% of the maximum flow rate.

EXPERIMENTAL RESULTS

The experimental conditions and results are shown in Table V. It was desired to use a high liquid to gas flow-rate ratio (L/G) so as to maintain a low liquid temperature on the sieve plate which permits a high driving force for vapor condensation on the bubble wall. An average (L/G) ratio of 7.7 (ℓ/m^3) was maintained for runs 1 to 6. This was the highest (L/G) value that could be employed without entering the weeping and raining regions of the sieve-plate. The (L/G) ratio was decreased to an average value of 3.53 (ℓ/m^3) for runs 7 and 8.

Two sampling runs were made for each set of experimental conditions. The air was maintained unsaturated for runs 1 and 2. The air temperature was then decreased keeping the humidity unchanged for runs 3 and 4. The effect of increasing the humidity at the original air temperature was studied in runs 5 and 6. Runs 7 and 8 were for a different set of experimental conditions.

Discussion

Collection Mechanisms: The experimental $\bar{P}t$ values are the ratios of outlet to inlet particle mass concentrations as determined from weight gains on sampling filters, as explained earlier. For the experimental conditions, the collection can be attributed to the combined effects of: impaction during bubble formation, diffusiophoresis, thermophoresis, diffusion, and particle growth due to condensation resulting in a higher centrifugal force. Thus, $\bar{P}t$ can be expressed as:

$$\bar{P}t = Pt_F \times Pt_D \times Pt_T \times Pt_{BD} \times Pt_C \qquad (123)$$

For runs 1 to 6, where the flow conditions are approximately identical, the following observations can be made:

1. $\bar{P}t_F$ will be the same for these runs and was calculated at 96%.
2. For these runs, the temperature gradients were not substantially different and were quite small. Thus $\bar{P}t_T$ was high and nearly the same for all the runs.

Table V

EXPERIMENTAL CONDITIONS AND RESULTS

Run No.	Air* Flow-Rate (m^3/min) x 10	Water Flow-Rate (liters/min)	Particle Concentration x10^{-5} (#/cc)	Gas Conditions				Water Temps.		S	$y_i - y_e$	Pt_{exp} (%)	Pt_{theo} (%)	h_{exp} (cm)	h_{theo} (cm)
				Inlet		Exit									
				T_{di} (°C)	y_i	T_{de} (°C)	y_e	T_{Li} (°C)	T_{Lo} (°C)						
1	3.60	2.92	2.3	41	0.059	24	0.031	17.9	19.1	0.73	0.028	89.0	94.0	5.0	7.6
2	3.60	2.92	2.4	41	0.064	25	0.032	17.9	19.1	0.78	0.032	86.6	90.8	5.0	9.2
3	3.66	2.88	[illegible].9	33	0.057	24	0.031	17.9	19.0	1.09	0.026	86.4	88.3	4.7	7.2
4	3.66	2.88	2.3	33	0.059	24	0.031	17.9	19.0	1.12	0.028	82.2	87.0	4.7	7.6
5	3.66	2.62	4.6	41	0.095	28	0.039	17.8	20.0	1.13	0.056	72.9	84.7	4.8	8.4
6	3.66	2.62	4.4	41	0.095	28	0.039	17.8	20.0	1.13	0.056	69.1	84.7	4.8	8.1
7	5.10	2.35	4.7	47	0.111	29	0.042	16.0	21.5	0.93	0.069	84.4	84.8	6.4	10.2
8	5.10	2.46	4.0	42	0.111	29	0.042	16.8	19.0	1.21	0.069	81.9	74.2	7.6	9.7

* @ 20°C, 1 atm.

$$y = \frac{\text{g-mole vapor}}{\text{g-mole dry air}}$$

3. For the particle size used, in the range of 0.5 μm to 1.0 μm, $\overline{Pt}_{BD}$ was insignificant and can be neglected.

4. It is possible that $\overline{Pt}_C$ was nearly the same for all the runs and quite high, as the DBP particles are not highly wettable and would require a saturation ratio larger than perhaps 1.9 in order for water to condense on them. The saturation ratio in the bulk of the gas phase did not go much higher than 1.0.

The results indicate that diffusiophoresis is the major contributor to particle collection efficiency for a single plate. The contributions of the rest of the phenomena to $\overline{Pt}$ will remain approximately the same for all the runs. $\overline{Pt}_D$ depends on the amount of vapor condensed, which can be expressed as $(y_i - y_e)$, or the gmole of vapor condensed per gmole of dry air. Figure 24 is a plot of $\overline{Pt}$ vs. $(y_i - y_e)$ for runs 1 to 6, and also shows $\overline{Pt}_F$ due to impaction during bubble formation, under the experimental conditions.

Comparing $\overline{Pt}_{exp}$ values for runs 1 and 2 with runs 3 and 4, we see that for approximately the same water vapor concentrations, the penetration is lower for the lower gas temperatures. This is also observed by comparing run 7 with run 8. Comparing runs 1 and 2 with runs 5 and 6 shows that the penetration is lower when the water vapor concentration is increased at the same temperature. It is also evident from Table V that the penetration decreases as the saturation ratio, S, increases.

However, further experimental studies under wider ranges of operating conditions are needed before the trend of Pt with any of the parameters can be generalized.

Comparison of results with predictions

The model for collection in a sieve plate scrubber, described earlier was used to predict the theoretical penetration, Pt_{theo}, for the experimental conditions. It was found that the model will satisfactorily predict the

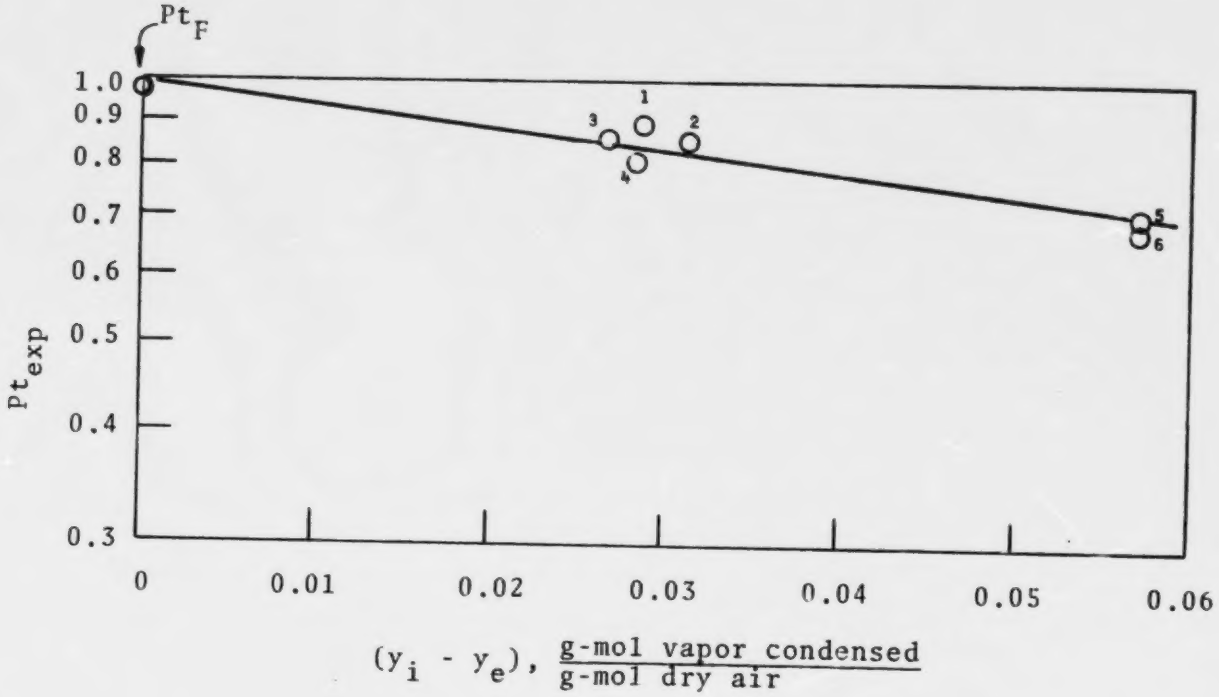

Figure 24 - Particle penetration versus water vapor condensed.

general form and magnitude of experimental results if the proper heat and mass transfer coefficients are used. The heat and mass transfer coefficients, h_L, k'_{bG} and h_{bG}, were determined individually for each run. The calculation procedure is shown in an earlier section and the resulting coefficients are shown in Table VI.

The results for runs 2 to 8 are comparable to the values predicted by the penetration theory for k'_{bG} and h_bG; $1.6\text{x}10^{-4}/p_{BM}$ and $2.2\text{x}10^{-2}/\sqrt{T_G}$ respectively. The values for "h_L" are approximately 10^{-2} times the corresponding value predicted by the penetration theory, 0.31. This indicates that the assumptions regarding the bubble area available for transfer, the bubble diameter, liquid temperature, liquid surface renewal time, and the consistency of the foam density may be in error. The resolution of this question will require additional experimental and computational work.

$\overline{Pt}_{theo}$ values were then calculated for the experimental runs, using the corresponding experimental values of transfer coefficients. The $\overline{Pt}_{theo}$ values, together with the foam height, h_{theo}, indicated by the model to reach the exit gas temperature, are listed in Table V with the corresponding experimental conditions. The difference in h_{exp} and h_{theo} values indicate that the assumptions regarding the bubble diameter area available for transfer and the consistency of the foam density may be in error. These questions could only be resolved by experimentation under highly controlled conditions as indicated earlier.

$\overline{Pt}_{theo}$ is plotted against $\overline{Pt}_{exp}$ on Figure 25. Except for run 8, $\overline{Pt}_{theo}$ was higher than $\overline{Pt}_{exp}$.

To check if the difference between $\overline{Pt}_{theo}$ and $\overline{Pt}_{exp}$ was only due to statistical scatter in the data, the following assumptions were made:

1. $\overline{Pt}_{theo}$ values correctly and uniquely represent the penetration for any set of experimental conditions examined. The experimental conditions do not change during an experimental run. Thus, $\overline{Pt}_{theo}$ represent the mean of $\overline{Pt}_{exp}$ values for any set of experimental conditions.

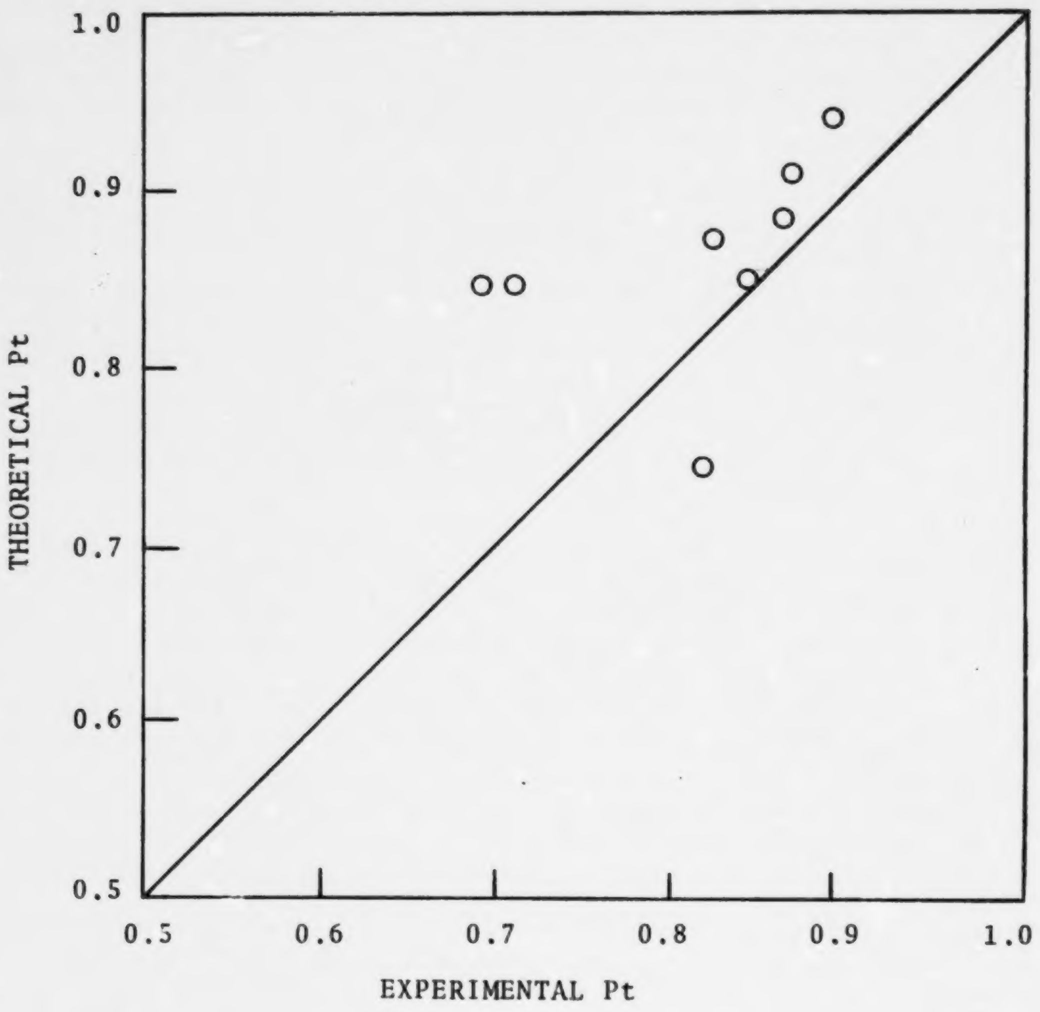

Figure 25 - Theoretical versus experimental penetration.

Table VI

TRANSFER COEFFICIENTS DETERMINED BY MICKLEY'S METHOD

Run No.	$h_L \times 10^3$	$k_{bG} \times 10^4$	$h_{bG}\sqrt{T_G} \times 10^2$
1	1.84	14.72	16.72
2	2.09	2.09	2.48
3	2.56	2.04	2.32
4	2.52	2.02	2.29
5	2.54	2.54	2.95
6	2.54	2.54	2.95
7	3.57	2.50	3.00
8	3.57	2.50	3.00

2. $\overline{Pt}_{exp}$ values are normally distributed about the mean (or $\overline{Pt}_{theo}$) for any set of experimental conditions.

Thus, the standard error between $\overline{Pt}_{theo}$ and $\overline{Pt}_{exp}$ is 6.6%. As this error is higher than the maximum experimental error, 4%, our assumption that $\overline{Pt}_{theo}$ is the true mean of $\overline{Pt}_{exp}$ values is incorrect.

Noting that $\overline{Pt}_{exp}$ values are normally distributed, the probability of obtaining less than two observations on the negative side of the mean, in a sample of eight observations, is 0.035. The low probability indicates that there is a positive bias for $\overline{Pt}_{exp}$ values, when compared to $\overline{Pt}_{theo}$. More experimental data are needed if the statistical relation between $\overline{Pt}_{theo}$ and $\overline{Pt}_{exp}$ is to be studied more rigorously.

Overall, the comparison of experimental data with predictions based on our mathematical model shows that the model is capable of giving useful and realistic results. While additional refinement, as discussed above, is needed, the model can account for what is observed experimentally and gives us a good tool for interpreting what we see and utilizing this knowledge for engineering design of practical equipment.

ECONOMIC FEASIBILITY

The technological feasibility of FF/C scrubbing has been discussed in previous sections and it is clear that fine particles can be collected with high efficiency by this means. Both diffusiophoresis and particle growth by condensation are practically insensitive to particle size and they are the most important factors in FF/C scrubbing. What remains to be shown is whether the cost is low enough. The following section deals with the question of economic feasibility, with the object of determining some broad outlines of the cost picture. Two specific cases of industrial applications for FF/C scrubbing were studied and preliminary process designs and cost estimates are described.

Before getting into the details of case studies it is instructive to consider some general features of FF/C scrubbing. Both the theoretical and experimental results indicate that it should require a minimum of about 0.1 or 0.15 g water condensed/g dry gas in order to grow particles to about 2.0 μm diameter if the concentration is about $10^7/\text{cm}^3$. The experimental data show a penetration of about 70% at a steam condensation of about 0.035 g/g for $n_p \simeq 10^5$ entering one sieve plate.

The computer runs show the effect of steam condensing on the liquid as well as the particles, which raises the steam consumption for a given increase in particle size. These runs indicate that steam condensation of about 0.06 g/g would cause growth to $r_p = 0.85$ μm for $n_p = 10^6/\text{cm}^3$ (see run #4 for sheets, Table IV) and about 0.14 g/g would cause growth to $r_p = 1.4$ μm for $n_p = 10^7/\text{cm}^3$ (see run #17 for plates, Table III). In contrast, we may note that if all the steam condensed on the particles, it would take 0.033 g/g condensed to grow 10^7 particles/cm^3 to $r_p = 1.0$ μm.

For illustrative purposes, we may take 0.15 g/g as representing a low practical steam condensation rate. If steam costs \$1.32/1,000 Kg (\$0.60/1,000 lb), FF/C scrubbing would cost \$0.20/1,000 Kg (\$0.24/1,000 m^3) of dry gas for steam alone. A venturi scrubber which had a performance capability of 80% efficiency on 0.5 μm diameter particles with density of 1.0 g/cm^3 would require a pressure drop of about 450 cm W.C. (see S.H.B. Figure 5.3.6-9). The scrubbing power cost for this pressure drop would be about \$0.24/1,000 m^3 if electricity cost 1.0¢/K.W.H. Thus, the costs for FF/C and high-energy scrubbing are fairly close for this example and will be more favorable for FF/C scrubbing as the collection efficiency requirement becomes more stringent.

It is clear from the above example that FF/C scrubbing might or might not afford to pay for steam, depending on the particle size and concentration, and the required performance. The next question is whether cooling water costs are acceptable. There is a wide range of cooling water costs given in the literature; from about 0.25¢/m^3 to 3.9¢/m^3 (1¢ to 15¢/1,000 gal). Cooling tower depreciation costs are in the vicinity of 0.25¢/m^3 to 0.5¢/m^3, so one might expect costs in this range where water can be recirculated with little loss and no problems.

Cooling water use can be approximated as being 20 times that of steam condensation (in g/min) if a temperature rise of 28°C is assumed for the water in the scrubber. For the steam rate of 0.15 g/g, cooling water would cost \$0.008/1,000 Kg dry gas at 0.25¢/m^3 and \$0.12/1,000 Kg dry gas at 3.9¢/m^3. We may conclude from this that cooling water costs up to about 4¢/m^3 (15¢/1,000 gal) might be generally acceptable, depending on circumstances.

Summing up, we can state as rules of thumb that FF/C scrubbing might generally be economical if the latent heat of vaporization is available without cost and if cooling water is available for less than 4¢/m^3 (15¢/1,000 gal). The factors relating to performance in each case will mitigate these rules and may cause FF/C scrubbing to be more or less desirable economically.

EXAMPLES

Two specific cases were chosen for evaluation because they met the criteria of involving an expensive process for fine particulate removal and a hot gas. A basic oxygen furnace and a Kraft pulping liquor recovery furnace were the sources studied.

The economic analyses presented here are based on our present technical understanding of the FF/C scrubber and are limited by the status of this understanding as represented in this report. Heat and mass transfer coefficient and the critical saturation values required for nucleation were either based on experimental data or calculated and checked against similar coefficients for similar cases.

The capital and especially the operating costs of the FF/C scrubber vary according to geographical location, availability of cold water and climatic conditions. Our estimations are based on the availability of water at 20°C.

The calculations were made for large industrial plants and this assumes that one could satisfactorily scale-up processes which have been studied only in the laboratory. Accepted scale-up methods were used to extrapolate the laboratory results to the industrial scale.

BASIC OXYGEN FURNACE EMISSION CONTROL

In recent years the use of the Basic Oxygen Furnace (B.O.F.) is increasing among the various steelmaking processes. The major reason for its wide acceptance is its short cycle which lasts about 50 minutes. The Basic Oxygen Furnaces vary in size from less than 50 ton/heat to over 400 ton/heat with 200-250 ton/heat being a common size. During about twenty minutes of each cycle oxygen is blown into the bath and that is when the flue gas reaches a temperature of over 1,480°C. The reason for this high temperature lies in the high CO content of the flue gas.

Because of the low fuel value and hazardous properties of CO, in most U.S. plants air is permitted to leak into the systems at the hood inlet in order to burn the CO to CO_2. In most foreign countries the CO is used either for its heat value or for chemical synthesis. This is done in one of two ways: 1. The gases containing the CO are cleaned and then transferred for further use. 2. The CO is burned to CO_2 as in most U.S. processes but the heat recovered in a waste heat boiler.

The gas stream leaving the B.O.F. during the first part of the cycle contain less dust, mainly kish, and is at a lower temperature. During the period when oxygen is blown the flue gas is hot and its dust load is as high as 45-90 grams per standard cubic meter of dry gas. The dust consists mainly of iron oxides, slag and other metallic oxide fumes.

Present Control Methods

Venturi scrubbers and electrostatic precipitators are presently used to control B.O.F. emission. Both have their advantages and disadvantages and one is not preferred over the other. When electrostatic precipitators are used the hot gases are first cooled to 320°C in an evaporation chamber or a spark box. The evaporation chamber is followed by a drop-out box where the larger dust particles settle. In the spark box excess water is sprayed and the large dust particles settle together with the excess water and are removed from the system. The dirty gases now at 320°C enter the electrostatic precipitator, are drawn by the fan and sent out through the stack.

When high energy venturi scrubbers are used to clean the gas, the gas is also first cooled by water injection. Concurrently the large particles are removed from the gas and the water sludge is drained. The gas then enters a venturi scrubber followed by an entrainment separator. In most cases the gas is further cooled in a cooling section to increase its density and as a result the fan efficiency. The cold gases enter the fan that emit them through a stack to the atmosphere.

Background Data

Information regarding the B.O.F. process, dust load and particle size distribution were collected from the following sources: Battelle report to NAPCA on the Iron and Steel Industry (1969), an article by H. C. Henschen (1968), M.R.I. report on particulate emissions (1971) and SRI Manual of Electrostatic Precipitators Technology (1970).

The dust load coming out of the B.O.F. ranges from 45-90 grams/standard dry cubic meter of gas. Most air pollution control agencies require that the dust concentration in the outlet gas not exceed 0.115 gram/standard dry cubic meter of gas (which is practically invisible). Thus a collection efficiency of 99.74% to 99.87% is required. The dust particle size distribution is reported by M.R.I. to have a mass median diameter of 0.095 μm and a geometric standard deviation of $\sigma_g = 2.3$. The dust composition and properties were also taken from the M.R.I. report.

For design purposes we shall consider a shop which consists of two 250 ton vessels, one of which is assumed to be in operation while the other is assumed to be shut down for relining. Such a shop makes about 30 heats of steel a day or one every 48 minutes. During about 20 minutes of each cycle oxygen is blown into the bath at a rate of 710.0 m^3/min (25,000 CFM). About 3.75 ton of dust, mostly oxides of iron, are discharged from the vessel during the blowing period. During the majority of the blowing period the gas discharging from the furnace mouth is at ≈1,500°C and contains 90% CO and 10% CO_2. Upon combustion with the theoretical quantity of air a temperature in excess of 2,000°C can be developed at the furnace mouth. For calculation purposes we assumed the gas temperature when entering quenchers to be constant at ≈1,500°C during the hot part of the cycle. (We shall consider later the beginning and end of the cycle when the gas temperature is lower.) At this temperature the gas flow rate is 29,400 actual cubic meter per minute (1.04×10^6 ACFM).

Steam addition is beneficial for efficient operation of the FF/C scrubber if it can increase the saturation ratio above 1.0. For this example we will assume that it can be done.

An alternative approach would be to saturate the gas by direct contact with water sprays and dispense with the steam generation and storage apparatus. This may be superior economically and it might also be that the specific nature of the particulates makes it impossible to sustain a saturation ratio higher than 1.0 so that the indirect generation of steam for addition to the gas would have no benefit.

The sensible heat of the flue gases will be utilized in three ways: a. A steam production in a waste heat boiler. b. Air reheat at the tail end of the process to prevent steam plume and give the gas additional buoyancy. c. Gas saturation with water vapor by spraying water into the gas in a saturation chamber.

From these operating conditions and with the use of material and energy balances the process flowsheet illustrated schematically in Figure 26 was calculated. The calculation method we have developed for a FF/C spray tower scrubber could now be used to calculate the scrubber performance. Particle growth was calculated based on a critical supersaturation of one.

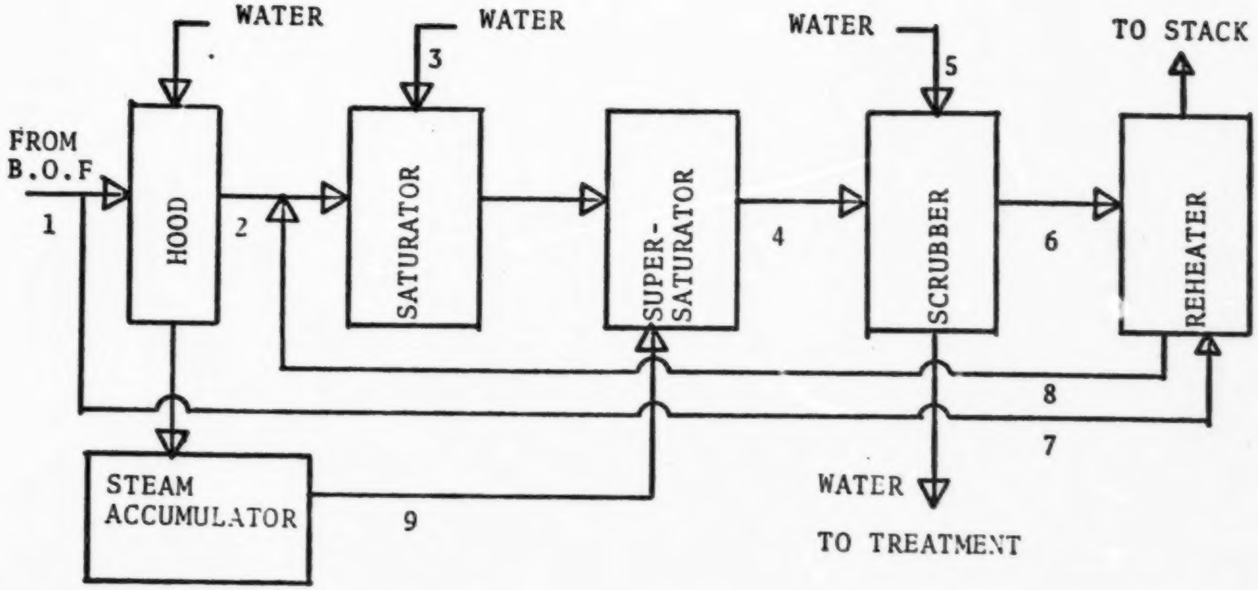
WATER
WATER
WATER
TO STACK
FROM B.O.F
1
HOOD
2
3
SATURATOR
SUPER-SATURATOR
4
5
SCRUBBER
6
REHEATER
8
7
STEAM ACCUMULATOR
9
WATER
TO TREATMENT

Stream #	1	2	3	4	5	6	7	8	9
Am³/min	29,000	12,600	0.8	9,550	6.6	7,500	760	190	
T °C	1,500	315	54	54		47	1,500	150	116

Figure 26 - Flow scheme for B.O.F. gas cleaning.

A heat balance shows that enough steam is produced during the high temperature part of the cycle to supply the needs of the whole cycle. Steam accumulators are required to store the excess steam which is generated during the hot period. The clean, cool gas now enters the fan which transfers it through a reheater and a stack to the atmosphere. The reheater was calculated based on the TVA experiments that warming the flue gases by 50°F is enough to prevent visible steam condensation when the ambient temperature ranges between 50°F and 80°F.

Since the purpose of this study is to show how FF/C scrubber compares with other control equipment a common ground for comparison was sought. No attempt was made to optimize the system and the only changes made were those necessary for the FF/C scrubber to work adequately.

Capital cost information came from the following sources: Battelle report (1969), Swindell and Dressler study (1969), A.P.T. Scrubber Handbook (1972), Cost Engineering in the Process Industries (1960) and Modern Cost Engineering Techniques (1970). The method used to calculate the capital costs is the one described in: "Data Techniques for Preliminary Capital Cost Estimating" by K. M. Guthrie, Modern Cost Engineering Techniques. The method is based on calculating the F.O.B. equipment cost and the multiplying by various factors for materials, labor, indirect costs, contingency, and fee. The capital cost was then adjusted to a common time base. The Chemical Engineering Plant Cost Index was used to account for cost changes with time.

Cost of FF/C System

Equipment for the system shown schematically in Figure 27 and discussed above was selected and sized for the purpose of cost estimation. A summary of the results of this process design and cost estimation are as follows:

Capital Cost:	
Tubular Membrane Hood (estimated from the cost of waste heat boilers)	$690,000
Steam Accumulators, 3 vessels, 1.0 m dia. x 25.0 m long	513,000
Saturator 4.6m dia x 30.0m long	53,000
Spray Tower (3.0 m high)	218,000
Reheater (300 m^2 area)	96,000
Blower (1,300 HP)	100,000
Subtotal	$1,670,000
Piping @ 9% of total	150,000
Total	$1,820,000
Annual Operating Costs:	
Maintenance @4% of capital cost	$ 73,000
Capital expenses and depreciation @20% of capital cost	364,000
Plant O.H. @ $0.10/ACFM-year	50,000
Power @$0.011/hw-hr	104,000
Water: 247 gpm @ $.40/Mgal	47,500
2000 gpm @ $.15/Mgal	144,000
Labor: 8000 hrs @ $5/hr	40,000
TOTAL	$ 822,500

There is no charge for steam in the operating costs since the gas sensible heat is used for steam production. The water and boiler costs are included in their proper places.

TABLE VII

B.O.F. CONTROL SYSTEM COSTS

Item	M.R.I. Report	Swindell-Dressler Report	S.R.I. Report
Electrostatic Precipitator			
Capital Cost	$4,900,000	$4,150,000	$5,000,000
Annual Cost	1,660,000	1,520,000	—
Fabric Filter			
Capital Cost	4,500,000	3,200,000	—
Annual Cost	1,260,000	1,160,000	
High Energy Scrubber			
Capital Cost	6,000,000	3,800,000	—
Annual Cost	2,360,000	1,850,000	—

FF/C Scrubber Costs by A.P.T., Inc.

Capital Cost	$1,820,000
Annual Cost	$ 822,500

For comparison, the costs presented by Midwest Research Institute, Swindell-Dressler and Southern Research Institute are given in Table VII. The costs quoted can be reduced by various manipulations, such as assuming two B.O.F. furnaces operating at staggered intervals, etc. However, to obtain a comparison between the three alternatives the same conditions were assumed for all three control equipments, which would not necessarily lead to the lowest conceivable costs.

KRAFT RECOVERY FURNACE CONTROL

Characteristic air-pollution problems of the pulp industry are associated with the release of malodorous sulfur compounds and particulate matter. Pulp is made by either the sulfate (kraft), sulfite, semichemical, soda, or by a mechanical process. Most of the pulp produced in the United States is made by the kraft process. In the following we shall examine the economics of using a FF/C scrubber to control the fine particles emitted from the recovery furnace in the kraft process.

The chemical pulping process known as Kraft pulping, employs a cooking liquor whose main ingredients are sodium sulfide and sodium hydroxide in solution.

The spent cooking liquor is black from the lignin, waste fibers, and dissolved sulfide salts--hence called "black liquor". Vitally important to the economics of the kraft process is the recovery and recycle of inorganic chemicals in the black liquor. To accomplish chemical recovery, black liquor is concentrated by evaporation and burned in recovery furnaces. Most of the organic and inorganic sulfur is reduced in the lower oxygen-poor region of the furnace to form an ash or smelt of molten chemicals, primarily sodium sulfide and carbonate.

Recovery furnaces also produce valuable process steam from the heat of the burning black liquor. Hot gases from the combustion zone relinquish most of their heat energy in passing over boiler tubes and heat economizers. Steam may be used elsewhere in the pulp-making process or sent to turbines for electrical power generation. Additional utilization of the furnace heat is accomplished by the use of a direct contact evaporator. Such an evaporator utilizes the heat of the flue gases to further evaporate black liquor just prior to its firing in the recovery furnace.

Direct contact evaporation has one serious drawback, however, from an air-pollution standpoint--the stripping of hydrogen sulfide which occurs when acidic flue gases contact the black liquor. Following the direct contact evaporator, furnace gases pass through collectors (such as electrostatic precipitators and scrubbers) to remove particulate matter consisting of sodium salts and carbon particles. Exhaust gases containing the remaining particulates, plus the malodorous sulfur compounds, then pass to the atmosphere.

When the black liquor is burned in the furnace, an appreciable quantity of particulate is liberated. Chemical content of the solids entrained in the recovery furnace flue gases is a function of furnace operating conditions and feed liquor composition. Usually Na_2SO_4, Na_2CO_3, and NaCl in the fume can vary greatly from mill to mill. For example, NaCl is present in measurable quantities when logs have been stored in salt water before chipping; inland mills have less NaCl passing through the recovery system. The SRI Manual of Electrostatic Precipitator Technology (1972) presents size distribution data obtained from electron microscope pictures. The mass median particle diameter is 1.94 μm and the geometric standard deviation is 2.06.

All the particles emitted from the recovery furnace are soluble and do not require supersaturation for growth. They will even grow when the saturation ratio is less than 1.0 (≈80% of the particles are Na_2SO_4 which will start growing at a relative humidity of ≈90%).

To use a condensation scrubber advantageously, the size of the waste heat boiler is increased and the exit temperature of the flue gases is reduced to ≈120°C. The gases then flow through a waste heat recovery venturi evaporator and into the condensation scrubber system as shown in Figure 27. A surface condenser (heat exchanger) was selected to condense most of the water vapor from the gas stream leaving the cyclone separator following the venturi evaporator. The purpose of this condenser is to isolate the condensate liquid which contains dissolved salts so that it can be recycled to the process without requiring concentration and so that the cooling water can be kept clean. An alternative approach would be to use a direct contact condenser and circulate the condenser coolant liquid through the tubes of an evaporative type cooler.

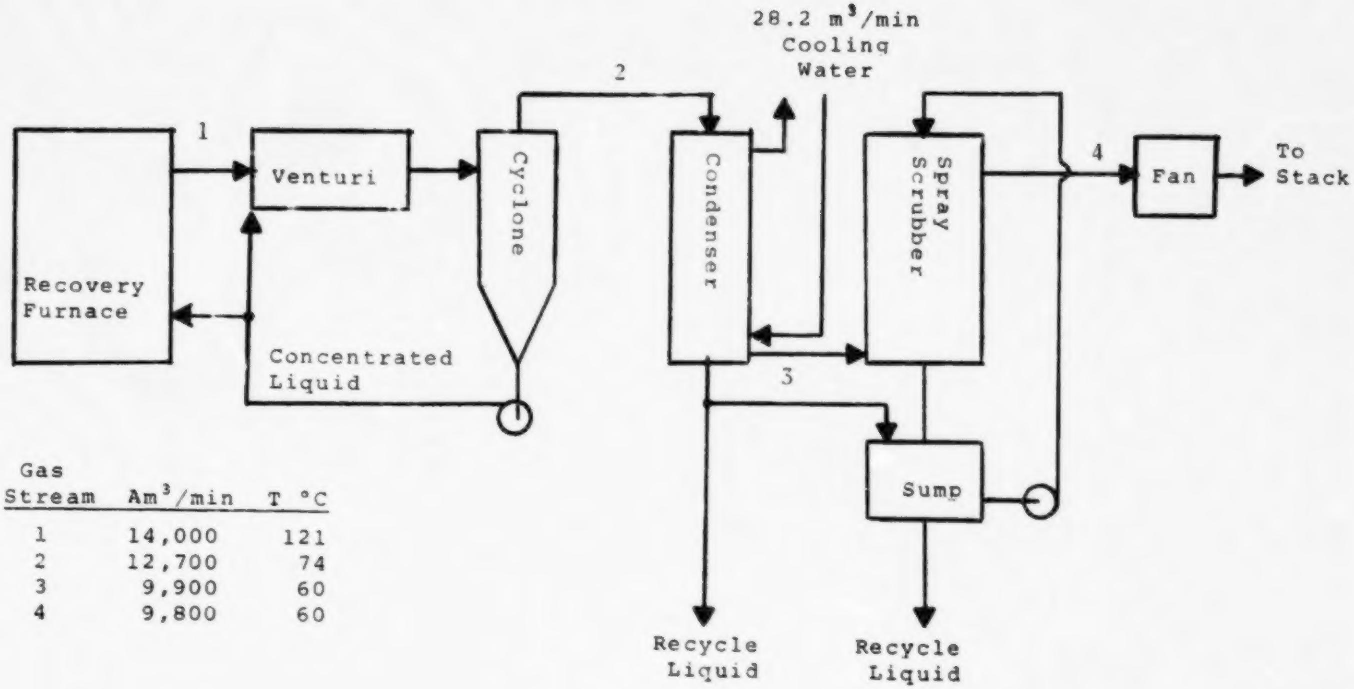
Recovery Furnace
1
Venturi
Cyclone
Concentrated Liquid
2
Condenser
28.2 m³/min Cooling Water
3
Recycle Liquid
Spray Scrubber
Sump
Recycle Liquid
4
Fan
To Stack

Gas Stream	Am^3/min	T °C
1	14,000	121
2	12,700	74
3	9,900	60
4	9,800	60

Figure 27 - Flowsheet for FF/C scrubber on Kraft liquor recovery furnace.

Spray scrubber liquid would recirculate at nearly constant temperature and with makeup liquid flow rate being equal to the rate of blow-down liquid flow back to the process. Particle collection efficiency in the spray scrubber would be 95% for the design shown; in order to be comparable to one of the alternatives given by Hendrickson et al. (see below). Because the major collection mechanism active in the scrubber would be inertial impaction of the grown particles, the scrubber penetration could be decreased by increasing liquid rate or contact length, or by appropriately changing other factors. It would be possible to decrease penetration from 5.0% to 0.25% by doubling scrubber length, for example.

Much information regarding emission control in the wood pulping industry is found in the report "Control of Atmospheric Emissions in the Wood Pulping Industry", E. R. Hendrickson et al., (1970). In that study, they presented the economics for several processes for upgrading the performance of existing Kraft furnace air pollution control systems. Costs for two of these processes will be compared with costs for the FF/C scrubbing system described above. Inlet gas flow rates, temperatures, particulate loadings and other pulping process conditions are the same for the FF/C system and the two alternatives listed below:

1. Increase the collection efficiency of an existing system by converting an existing venturi scrubber to a low efficiency (about 50%) venturi/cyclone evaporator and adding a 99% efficiency electrostatic precipitator.

2. Make the same change as in No. 1, except add a 97% efficiency second stage venturi rather than the electrostatic precipitator.

The FF/C system is also based on the change to a venturi/cyclone evaporator. Costs for the FF/C system were computed to be as follows:

Capital Investment

Condenser (7,500 m^2 area)	$400,000
Spray Scrubber (4m high, concrete lined)	160,000
Pumps (4x7.5 m^3/min)	40,000
Stack (piping costs are included above)	11,600
Total	$611,000

Annual Costs

Capital cost and depreciation	$121,500
Cooling water @ 1.25¢/m^3	180,000
Maintenance @4% of capital	24,400
Labor (8,000 hr)	44,000
Sub-total	$369,900

Credits

Chemicals recycled	$310,000
Power saved on scrubber fan @1¢/KWH	36,000
Sub-total	$346,000
Total net cost	$ 24,000

Costs for the three alternatives cited here were estimated as shown below:

Alternative	Capital Investment	Annual Cost
1. Add electrostatic precipitator for 99.5% overall	$1,930,000	$420,000
2. Add second stage venturi	710,000	32,000
3. Add FF/C system for 97% overall	611,000	24,000

It can be seen that within the accuracy of this kind of estimate the venturi and the FF/C add-on systems are about even. If high efficiency were required, however, the FF/C system could decidedly surpass either of the other two systems because the major additional expense required would be for another scrubber increment. Thus the additional capital investment would be about $160,000 and the additional annual operating cost would be perhaps $40,000.

FUTURE RESEARCH RECOMMENDATION

The primary objective of investigating the feasibility of FF/C scrubbing has been achieved with a clearly affirmative result. It has been shown in the present program that FF/C scrubbing can remove fine particles at high efficiency and that, within some limitations, it is more economical than other means of particle collection. Mathematical modeling of the many simultaneous phenomena taking place in an FF/C scrubber has been accomplished for some important unit mechanisms, although several coefficients remain to be fitted to experimental data.

In accordance with the original objective of selecting and performing a brief exploratory experiment of significant nature, our experimental work extended over a narrow range of conditions. Within this range the agreement between theoretical predictions and experimental results for particle collection is fairly good, once the heat and mass transfer coefficients are evaluated from experimental data. However, despite the good agreement, theoretical predictions of collection efficiency for plates are consistently higher than the experimental results. This, along with the discrepancy between computed and predicted liquid phase heat transfer coefficients, indicates that the mathematical model for bubbles should be revised.

To achieve the objective of building a working FF/C scrubber, development work will be required in three main areas:

1. Complete the experimental evaluations and development of the theoretical models for bubbles, sheets, and drops.

2. Define and develop an optimal FF/C scrubber, based on the improved design methods.

3. Build a pilot plant scale unit of the proposed optimum FF/C scrubber. Test the pilot unit in the laboratory and under actual operating conditions in the field.

The rest of this section will be devoted to a detailed discussion of these three topics.

EVALUATION OF THEORETICAL MODELS

Our present model for bubbles (i.e., plate type devices), when compared to experimental results, presents two major questions:

A. Why is the computed liquid phase heat transfer coefficient so low in comparison to the predicted coefficient?

B. Why is the predicted particle penetration higher than the experimental?

Possible explanations to these questions may be:

1. Incorrect estimate of the heat and mass transfer area.

2. Low estimate of liquid surface temperature, if co-current flow of liquid with rising bubbles is significant.

3. Unusual sieve plate design and operating conditions have caused a significant departure from customary behavior.

4. Different bubble shape and gas dynamics cause different transfer rates and particle deposition by centrifugal force.

5. Measurement problems may introduce errors.

In order to resolve the questions raised up to this point, it will be necessary to perform experiments which provide the following features:

1. Particles used for tests should have a range of surface properties and high enough vapor pressure that gas temperature of 80°C will cause negligible vaporization.

2. Wettable particles should be used in some runs so that the effect of growth can be clearly identified. These runs should be at relatively low saturations, such as were used for D.B.P. aerosol in the runs reported here.

3. Large water vapor concentration gradients should be used under conditions such that saturation is low enough to avoid condensation on particles. This could be achieved through the use of high gas and liquid temperatures with non-wettable particles.

4. Sieve plates with more customary dimensions as for mass transfer, should be used and operated at usual gas velocities.

5. Packed columns should be used to validate the "liquid sheets" model. The more defineable transfer surface area and liquid renewal time for packings as compared to plates will enable a less equivocal interpretation of particle penetration and transport rate data.

We consider this extension of the work on bubbles and sheets important since it will test the assumptions made in deriving the theoretical model. Once they are either proven or modified so as to be valid, the concepts from these models can be used to derive unit mechanism equations for other geometries.

DEFINE AND DEVELOP AN OPTIMAL FF/C SCRUBBER

To design an efficient and economical FF/C scrubber one should attempt to optimize the geometric configurations, the method by which the desired saturation ratio is achieved and the combination of collectors to achieve various stages of particle separation.

In the work done to date, various unit mechanism equations were derived. The next step is to integrate these equations so that they describe a scrubber. For example, the unit mechanism equation for the collection of particles by drops can be integrated into a venturi type design, a spray column, an ejector venturi, part of a wet cyclone, an impingement and entrainment scrubber or a moving bed scrubber. Collection by sheets can be integrated into packed bed scrubbers, baffle and secondary flow scrubbers or similar designs. Similarly, the bubble model is the basis for various plate type devices. Devices which combine several unit mechanisms can also be explored through mathematical modeling. Only after this is done can we say which device best utilizes the FF/C effects and is most efficient and economical.

It follows from our present models that saturation and particle growth are very important. The economics of the scrubber may depend in the final analysis, on our ability to obtain the required saturation ratio in a large enough fraction of the aerosol, to permit nucleation and growth of almost all the particles.

Several ways to achieve the required degree of saturation have been described previously. All possible ways should be checked for each device until the method most suitable is found. It is quite probable that no single method would be best in all cases and different methods will better suit different aerosols. Approaches such as the alteration of particle wettability by means of a pretreatment in which there is some absorption of a surface conditioning should be explored.

Once a scrubber geometry most suitable for particle collection and the formation of the desired saturation ratio has been defined, it becomes a straight-forward matter to build the scrubber. This scrubber should then be tested in the laboratory under controlled conditions in order to determine whether theoretical predictions and experimental findings agree. It could be expected that during these tests further modifications will make the scrubber a more efficient one.

FIELD TESTS OF PILOT SCALE FF/C SCRUBBER

The efficiency and economics of FF/C scrubbers are much more sensitive to the properties of the dust being removed and to the presence of small condensation nuclei than most other scrubbers. For this reason field tests on various dusts emanating from different sources are necessary. A good way to obtain these results is to build a mobile FF/C scrubber and test it on various industrial sources. These field tests will give us valuable information on the behavior and economics of FF/C scrubbers when the dust is neither uniform nor monodisperse. Further, the effects of trace components, process variations, and other practical complications will become known.

An important adjunct of the field tests should be the development and proving-out of analytical methods for the definition of all significant properties of the source. For example, it is of special importance that we be able to measure the particle number concentration, the critical saturation ratio, and the number of condensation nuclei; in addition to the usual size distribution, etc. The ultimate aim should be to eliminate the need for pilot testing in order to determine FF/C scrubbing feasibility.

Another round of process design and economic evaluation should be performed after the pilot study information has been obtained and assimilated. The accuracy of cost estimates is highly dependent on the amount of process detail available and on the specificity of equipment definition. Items such as cooling towers, water treatment, and large (and cheap) heat exchangers are very significant in the FF/C process economics and should be studied in detail.

It should be noted that the program reported here did not stop with the termination of the contract period of performance. Additional work to answer some of the questions discussed here has been funded under another contract.

REFERENCES

Abraham, F. F. A Re-Examination of Homogeneous Nucleation Theory: Thermodynamic Aspects. J Atmospheric Sci. 25:47-53, 1968

Air Pollution Manual. Part 2. American Industrial Hygiene Association. 1968.

Amelin, A. G. Theory of Fog Condensation. Second Edition. Jerusalem, Israel Program for Scientific Translations, 1967. 235 p.

Barnes, T. M., and H. W. Lownie Jr. A Cost Analysis of Air Pollution Controls in the Integrated Iron and Steel Industry. Battelle Memorial Institute. Columbus, Ohio. Contract No. PH-22-68-65. May 1969. 259 p.

Brock, J. R. On the Theory of Thermal Forces Acting on Aerosol Particles. J Coll Sci. 17:768-780, 1962.

Brown, G. G. and Associates. Unit Operations. New York, John Wiley & Sons, Inc., 1950.

Calvert, S., J. Goldshmid, D. Leith, and D. Mehta. Scrubber Handbook. A.P.T., Inc. Riverside, California. EPA Contract No. CPA-70-95. August 1972.

Chilton, C. H. Cost Engineering in the Process Industries. New York, McGraw-Hill, 1960. 475 p.

Davies, J. T. Turbulence Phenomena. New York and London, Academic Press, 1972. 412 p.

Davis, R. J. and J. Truitt. Using Condensing Steam for Air Cleaning. Instruments and Control Systems. p 68-70, November 1972.

Demshin, V. Ya., and G. V. Ermakov. Investigation of the Performance of Dust Removal Apparatus of the Foam Type with Preliminary Condensation of Water Vapor on the Dust Particles. Zhurnal Prikladnoi Khimii. 38(3): 691-693, March 1965.

Derjaguin, B. V., and Y. I. Yalamov. Theory of Thermophoresis of Large Aerosol Particles. J Coll Sci. 20: 555-570, 1965.

Derjaguin, B.V., Y. I. Yalamov. Theory of Thermophoresis of Large Aerosol Particles. J Coll Interface Sci. 22:117-225, 1966.

Derjaguin, B.V., A. I. Storozhilova, and Y. I. Rabinovich. Experimental Verification of the Theory of Thermophoresis of Aerosol Particles. J Coll Interface Sci. 21:35-58, 1966.

Derjaguin, B.V., and S. P. Bakanov. Dokl Akad Nauk SSSP (Phys Chem, USSR). 147:139, 1967.

Epstein, P.S. Zur Theorie des Radiometers. Z Phys 54:537, 1929.

Fletcher, N. H. Size Effect in Heterogeneous Nucleation. J Chem Phys. 29:572-576, 1958.

Fletcher, N. H. The Physics of Rain Clouds. London, Cambridge University Press, 1962. 389p.

Foust, A. S., L. A. Wenzel, C. W. Clump, L. Maus, and L. B. Andersen. Principles of Unit Operations. New York, John Wiley & Sons, Inc., 1960. 578p.

Fuchs, N. A. Evaporation and Droplet Growth in Gaseous Media. New York, Pergamon Press, 1959. 72p.

Fuchs, N. A. The Mechanics of Aerosols. New York, Pergamon Press, 1964. 408p.

Goldsmith, P., and F. G. May. Diffusiophoresis and Thermophoresis in Water Vapor Systems. In: Aerosol Science, Davies, C.N. (ed.). New York, Academic Press, 1966. p.163-194.

Hales, J. M., T. W. Horst, and L. C. Schwendiman. Aerosol Transport in a Condensing-Steam Boundary Layer. Battelle Northwest, Richland, Washington. Publication Number BNWL-1125. June 1970. 63p.

Hales, J. M., and L. C. Schwendiman. Phoretic Transport of Aerosols in Laminar Boundary Layers. Battelle Northwest, Richland, Washington. Publication Number BNWL-SA-3734. February 1971. 14p.

Hales, J. M., L. C. Schwendiman, and T. W. Horst. Battelle Northwest, Richland, Washington. Publication Number BNWL-SA-3592. 1971.

Handbook of Emissions, Effluents and Control Practices for Stationary Particulate Pollution Source. Midwest Research Institute. Report to NAPCA, Contract No. CPA-22-69-104. 1970.

Hendrickson, E. R., J. E. Robertson, and J. B. Koogler. Control of Atmospheric Emissions in the Wood Pulp Industry. Environmental Engineering, Inc. Gainesville, Florida. Contract No. PHS-CPA-22-69-18. March 1970. 269 p.

Henschen, H. C. Wet Vs. Dry Gas Cleaning in the Steel Industry. Air Poll Control Assoc J 18:338-342, 1968.

Herne, H. The Classical Computation of the Aerodynamic Capture of Particles by Spheres. Intern J of Air and Water Poll. 3:26-34, 1960.

Hidy, G. M., and J. R. Brock. The Dynamics of Aerocolloidal Systems. New York, Pergamon Press, 1970, 379 p.

Horst, T. W. A Review of Particle Transport in a Condensing Steam Environment. Battelle Northwest, Richland, Washington. Publication Number BNWL-848. June 1968. 45p.

Howell, W. E. The Growth of Cloud Drops in Uniformly Cooled Air. J of Met., 6:134, 1949.

Junge, D. Die Konstitution des Atmospharischen Aerosols. Ann Met (Beiheft). 1952.

Kinzer, G. D., and R. Gunn. The Evaporation Temperature and Thermal Relaxation Time of Free Falling Water Drops. J of Met. 8:71-82, 1951.

Klauss, P. R., P. L. Sieffert, and J. F. Skelly. Costs and Performance of Control Systems and Control Equipment. Swindell-Dressler Company. Appendix C for A Cost Analysis of Air Pollution Controls in the Integrated Iron and Steel Industry. Battelle Memorial Institute. Columbus, Ohio. Contract No. PH-22-68-65. May 1969. 122p.

Lancaster, B. W., and W. Strauss. A Study of Steam Injection Into Wet Scrubbers. Ind Eng Chem Fundamentals. 10(3):362-369, March 1971.

Langmuir, J., and K. Blodgett. A Mathematical Investigation of Water Droplet Trajectories. Amer. A.F. Tech. Report 5418. 1946.

Lapple, C. W., and H. J. Kamack. Performance of Wet Dust Scrubbers. Chem Eng Prog. 51(3):110-121, March 1955.

Litvinov, A. T. Vestnik tekhnicheskoy i ekonomicheskoy informatsii. 5:26-29, 1964.

Litvinov, A. T. Khimicheskayer promyshlennost. 8:64-69. 1964.

Litvinov, A. T. Stal'. 7:667-669, 1965.

Litvinov, A. T. Influence of Condensation on the Effectiveness of Capture of Fine Particles During Cleaning of Gases by the Wet Method. Zhurnal Prikladnoi Khimii. 40(2):353-361, February 1967.

Litvinov, A. T. Fine Gas Scrubbing to Remove Highly Dispersed Hydrophobic Particles Using the Condensation Effect. Stal'. 2:184-186, 1972.

Mashita, T. Industrial Public Nuisance. 7:573, 1971.

Mason, B. J. The Physics of Clouds. Oxford 1957.

Matsuzaki, K. Japanese patent Number Sho 41-41184, 1970.

Maxwell, J. Collected Scientific Papers. Cambridge 1890.

Mercer, T. T., and H. Y. Chow. Impaction from Rectangular Jets. J Coll Interface Sci. 27:75-83, 1968.

Control Techniques for Particulate Air Pollutants. NAPCA Publication No. AP-51, Washington, D.C. 1969.

Norman, W. S. Absorption, Distillation and Cooling Towers. New York, John Wiley & Sons, Inc., 1961. 477p.

Nuzhnyi, V. M., Yu. I. Shimanskii, and G. K. Ivanitskii. Some Aspects of the Diffusion Theory of Evaporation of Drops of Volatile Liquids. Coll. J. USSR. 27:494-498, 1965.

Oglesby, Jr. S., and G. B. Nichols. A Manual of Electrostatic Precipitator Technology. Part II. Southern Research Institute. 1970.

Popper, H. Modern Cost Engineering Techniques. New York, McGraw-Hill. 1970.

Prokhorov, P. S., and L. F. Leonov. Investigation of Long Range Diffusion Forces Between Water Droplets and Non-Volatile Particles. Diss Faraday Soc. 30:124-129, 1960.

Ranz, W. E., and J. B. Wong. Impaction of Dust and Smoke Particles on Surface and Body Collectors. Ind Eng Chem 44:1371-1380, 1952.

Rozen, A. M., and V. M. Kostin. Collection of Finely Dispersed Aerosols in Plate Columns by Condensation Enlargement. Inter Chem Eng. 7:464-467, July 1967.

Schadt, C. F., and R. D. Cadle. Thermal Forces on Aerosol Particles. J Phys Chem. 65:1689-1694, 1961.

Schauer, P. J. Removal of Submicron Aerosol Particles from Moving Gas Stream. Ind Eng Chem. 43(7):1532-1538, July 1951.

Schlichting, H. Boundary Layer Theory. New York, McGraw-Hill, 1960.

Schmitt, K. H. Untersuchungen on Schwebstoffteilehen in Temperaturfeld. Z. Naturforsch 14a:870-881, 1959.

Schmitt, K. H., and L. Waldmann. Untersuchungen on Schwebstoffteilchen im Diffundierenden Gasen. Z. Naturforsch 15a:843-851, 1960.

Semrau, K. T., C. W. Marynowski, K. E. Lunde, and C. E. Lapple. Influence of Power Input on Efficiency of Dust Scrubber. Ind Eng Chem. 50(11):1615-1620, November 1958.

Sparks, L. E., and M. J. Pilat. Effect of Diffusiophoresis on Particle Collection by Wet Scrubbers. Atmospheric Environment. 4:1-10, 1970.

Taheri, M., and S. Calvert. Removal of Small Particles From Air by Foam in a Sieve-Plate Column. J Air Poll Control Assoc. 18:240-245, 1968.

Terebenin, A. N., and A. P. Bykov. Zhurnal Prikladnoi Khimii (USSR). 45:1012, 1972.

Varga, Jr. J., and H. W. Lownie, Jr. A System Analysis of the Integrated Iron and Steel Industry. Report No. PB 184557. 1969.

Volmer, M. Kinetik der Phasenbilding. Dresden and Leipzig: Steinkopff. 1939.

Waldmann, L., and K. H. Schmitt. Thermophoresis and Diffusiophoresis of Aerosols. In: Aerosol Science, Davies, C. N. (ed.). New York, Academic Press, 1966. p 137-161.

Whitaker, S. Forced Convection Heat Transfer Correlations for Flow in Pipes, Past Flat Plates, Single Cylinders, Single Spheres and for Flow in Packed Beds and Tube Bundles. AIChE J. 18:361-371, 1972.

GLOSSARY

a - constant defined by equation (12)

a_b - specific surface area of bubble, cm^{-1}

A_p - area of plate, cm^2

b - constant defined by equation (13)

B - dimensionless parameter defined by equation 4-38

c - mass concentration Kg/m^3 or g/cm^3

c_A - molar concentration, $gmol/cm^3$

C' - Cunningham correction factor, dimensionless

C_p - specific heat, kcal/kg-°C or cal/g-°C

C_t - temperature jump coefficient, = 2.3, dimensionless

C_m - isothermal slip coefficient, = 1.25, dimensionless

d - diameter, m or cm

D - diffusivity, cm^2/sec

D_p - particle diffusivity for Brownian diffusion, cm^2/sec

F - fraction of the total condensing vapor which condense on the drops.

F_x - flux force in "x" direction, dynes

F_ℓ - foam density, ratio of clear liquid height to total foam height.

G - gas flow rate, $gmol/cm^2$-sec

G_F - dimensionless quantity defined by equation (14), (18) or (24)

h - heat transfer coefficient, cal/sec-cm^2-°C

I - integral defined by equation 4-40

i - Van't Hoff factor

J - dimensionless parameter defined by equation 4-45

k_A - thermal conductivity of substance A, cal/sec-cm-°C

k' - mass transfer coefficient, gmol/cm^2-sec-atm

K_D - diffusiophoresis constant defined by equation (94)

K_G - overall gas phase transfer coefficient gmol/sec-atm-cm^2

K_p - inertia parameter defined by equation (24)

K_{pB} - particle flux coefficient for Brownian diffusion, cm/sec

K_T - thermophoresis constant defined by equation (99)

L - liquid mass flowrate, kg/sec or g/sec

L_M - latent heat of vaporization cal/g

m - mass, kg or g

m - moles of solute in a drop, gmol/drop

M - molecular weight, kg/kgmol or g/gmol

n - particle number concentration, no./cm^3

N - mass flux, kg/m^2-sec or g/cm^2-sec

N - particle flux, no./cm^2-sec or g/cm^2-sec

N_{pB} - particle flux due to Brownian diffusion, no./cm^2-sec

p - partial pressure of solute, mbar or atm

p_{BM} - mean partial pressure of non-transferring gas, atm

Pt - penetration (one minus efficiency), fraction or percent

Pt_c, Pt_n, and Pt_T are defined in equations (42), (43) and (44)

q - mass vapor condensed per mass particles, g/g

Q - volumetric flow rate, m^3/sec, cm^3/sec or ℓ/sec

Q - heat transferred per unit cross-section area of column, cal/cm^2

r - radius, cm or μm

r'_p - dimensionless particle radius in equation (91)

R - ideal gas law constant

R_c - effective radius of curvature

s - distance from jet nozzle to plate, cm

S - saturation ratio, atm/atm

t - time, sec

T - temperature, °K (or °C, where specified)

T' - dimensionless temperature in equation (89)

u - velocity, m/sec or cm/sec

v - velocity, cm/sec

v_B - liquid flow rate per unit width, cm^3/sec-cm

V - volume, m^3 or cm^3

W - jet width, cm

W - weight gain on filter

x - distance in "x" direction, cm

$\tilde{X}$ - dimensionless distance in "x" direction

y - mole fraction, gmol/gmol

Y - distance in "Y" direction

z_p - height of foam, cm

Z - distance in "Z" direction

Z' - thermophoretic parameter

Dimensionless Numbers

$N_{FD} \equiv \frac{u_F}{v_o}$, Flux deposition number

$N_{Nu} \equiv \frac{h'd_y}{k_G}$, Nusselt number

$N_{Sc} \equiv \mu_G / \rho_G D_G$, Schmidt number

$N_{Pr} \equiv C_p \mu/k$, Prandtl number

$N_{Pe} \equiv du/D$, Peclet number

$N_{Re} \equiv \rho du/\mu$, Reynolds number

$N_{Kn} \equiv \lambda/r_p$, Knudsen number

Greek

α - contact angle of a drop on a solid surface, degrees

α - fraction of particle mass increase as predicted theoretically, used in equation (40)

β - dimensionless jet spacing = 2 s/w

δ - boundary layer thickness, cm or μm

ε - volume fraction voids in scrubber

Θ - contact time, sec

η - efficiency due to a unit mechanism, fraction or percent

λ - mean free path of gas molecules, cm or μm

ρ - density, kg/m^3 or g/cm^3

σ_g - geometric standard deviation

σ_{12} - diffusion slip factor in equation 6, dimensionless

τ - relaxation time, sec

μ - viscosity, g/cm-sec

ν - kinematic viscosity = μ/ρ, cm^2/sec

Subscripts

b - bubble

BD - Brownian diffusion

C - centrifugal

d - drop

D - diffusiophoretic

d - difference

e - exit

exp - experimental

f - foam

F - impaction during bubble formation
F - flux force
G - gas phase

i - interface

i - in

i - increment

L - liquid phase

m - mixture

M - molal quantity

p - particle

pa - aerodynamic

pB - particle, Brownian diffusion

pD - particle, diffusiophoresis

pn - particle, number mean

pT - particle, thermophoresis

pI - particle, inertial

s - surface

s - sum of

t - terminal velocity

tg - tangential

theo - theoretical

T - turbulent layer

T - thermophoretic

v - vapor

x - in the "x" direction

y - in the "y" direction

o - original condition

∞ - for plane surface

Superscripts

* - in equilibrium

^ - film

~ - dimensionless quantity

— - overall or average